UAB
Universitat Autònoma de Barcelona

Molecular design of bivalent ligands for GPCRs

Marc Gómez Autet

Molecular design of bivalent ligands for GPCRs

Marc Gómez Autet

Supervisor
Leonardo Pardo

Laboratory of Computational Medicine
Biostatistics Unit, Faculty of Medicine

UAB
Universitat Autònoma
de Barcelona

Doctorate program in Bioinformatics
2024

Contents

Chapter 1

Introduction

1.1. G Protein-Coupled Receptors

Cell functioning in multicellular organisms relies heavily on the reception of signals that come from outside of the cellular membrane. The main part of this task is carried out by membrane receptors, among which G protein-coupled receptors (GPCRs) stand as the largest family (≈800 genes) of transmembrane proteins encoded in the human genome (3-4% of the human proteome) [1]. Members of this family include receptors for a wide variety of extracellular molecules that range from photons or ions to neurotransmitters, hormones, odorants, and others. Indeed, GPCRs are expressed in most of the body's tissues and are stimulated by these ligands to trigger second-messenger cascades which are key for cell signaling and virtually all aspects of human physiology, including vision, taste, odor sensing and neurotransmission [1]. As such, they are involved in many human diseases and represent the pharmaceutical target of approximately 34% of all drugs approved by the US Food and Drug Administration (FDA) [2].

In 1994, GPCRs were first phylogenetically classified into the known A-F classification system, of which D and E are not found in vertebrates [3]. However, Fredriksson and colleagues demonstrated, one decade later, that most human GPCRs can be categorized into five main families: Glutamate (class C, 22 receptors), Rhodopsin

(class A, >700 receptors including ≈400 olfactory receptors), Adhesion (class B2, 33 receptors), Frizzled (class F, 11 receptors), and Secretin (class B1, 41 receptors) [4]. This classification system is referred to by the acronym GRAFS. Within these five classes, class A stands out as the largest and most therapeutically targeted family [5] and it will be the focus of this thesis. Despite interacting with a huge diversity of ligands, all GPCRs share a transmembrane domain with a common structural architecture defined by a bundle of 7 transmembrane (TM) α-helical segments connected by three extracellular loops (ECLs) and three intracellular loops (ICLs) (Figure 1.1).

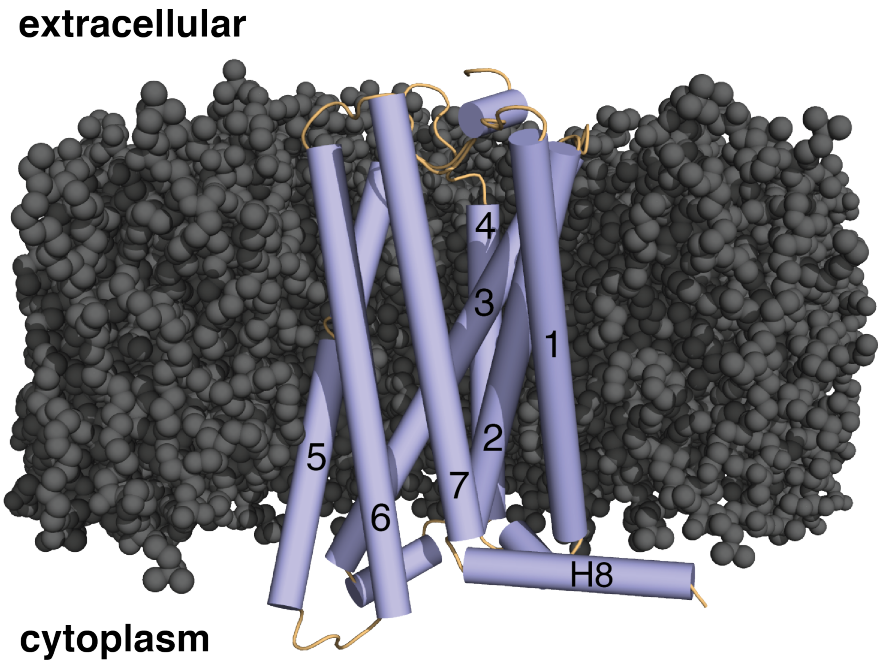

Figure 1.1: GPCR embedded in a lipid bilayer. GPCRs share an architecture with seven transmembrane helices (numbers) which alternatively span from the extracellular side (N-terminal) to the cytoplasm (C-terminal) joined by protein loops. Helical segments are depicted in blue cylinders whereas unstructured protein segments are in thin orange cylinders. Grey spheres represent membrane lipids.

Advances in crystallography and cryogenic electron microscopy (cryo-EM) of GPCRs have shed light on the ligand binding and the molecular mechanisms of signal transduction. The most common feature of GPCR activation entails a reorganization of the cytoplasmic side of the receptor thanks to a large outward movement of transmembrane helix 6 (TM6) (Figures 1.2 and 1.3D) and smaller rearrangements of other helices [6]. This process leads to and exposition of an intracellular pocket which can effectively engage the signaling proteins: G proteins, G protein–coupled receptor kinases (GRKs) or β-arrestins (Figures 1.2 and 1.3D). GPCRs are highly dynamic systems that exist in a wide range of functionally distinct states and, in absence of any external stimulus (i.e., an endogenous ligand), they can transition among multiple conformation states (ie., inactive, intermediate, active) which explains part of their basal activity [7] (Figure 1.3). Then, when a ligand binds to a GPCR, it can modify the fraction of time the receptor spends in each of its conformational states, resulting in modulation of intracellular signaling responses [8].

In class A GPCRs, the endogenous ligands bind in a conserved pocked within the transmembrane domain of the receptor known as the orthosteric binding side (Figure 1.4B). Orthosteric ligands can be categorized into four groups based on their intrinsic efficacy: full agonists induce maximal signaling responses; partial agonists fail to induce full receptor activity even at saturating concentrations; neutral antagonists hinder the binding of other ligands without affecting the signal activity; and inverse agonists decrease basal activity (Figure 1.3) [7]. Additionally, GPCRs can be modulated allosterically by molecules that bind to allosteric pockets which are distinct from the orthosteric binding site (Figure 1.4). It is important to note that not all these non-orthosteric sites are truly allosteric[1], but since the majority appear to be, "allosteric" has become synonymous with "non-orthosteric" for GPCRs. Depending on their ability to increase, decrease, or cause no effect on the action of the orthosteric ligand, al-

[1]Allosterism is defined as "the process by which the binding or/and function of an endogenous or exogenous ligand at one location (the orthosteric site) is influenced by the binding of another ligand or protein at a topographically distinc site (the allosteric site).

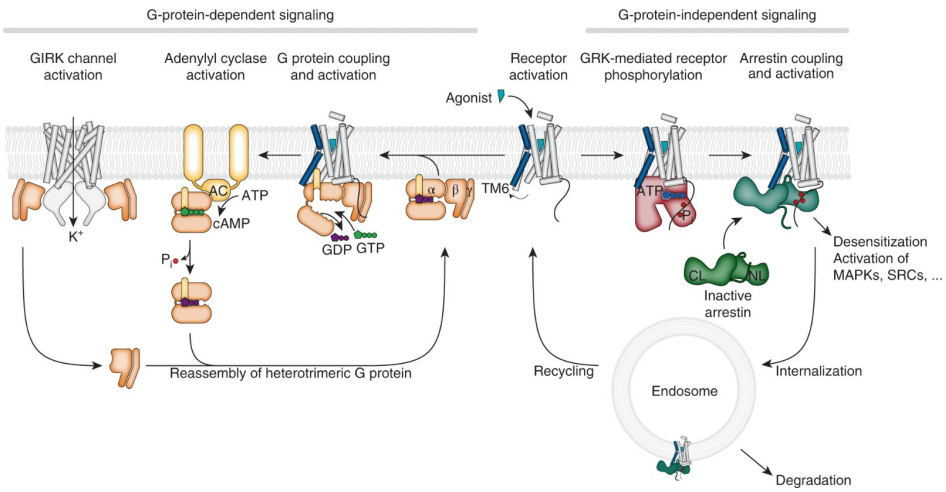

Figure 1.2: GPCR receptor signaling. Agonist binding to the receptor triggers the outward movement of TM6, opening an intracellular cavity that allows the binding to a diverse set of signaling proteins. Coupling of heterotrimeric G protein to the receptor (G-protein-dependent signaling, left) triggers an exchange of GDP to GTP, through a large-scale opening of the α-helical domain from the Ras domain in the α-subunit, resulting in dissociation of the α and βγ subunits [9, 10]. The GTP-bound state of the α-subunit activates Adenylyl cyclase (AC) which converts ATP into cAMP. βγ subunits interact with GIRKs to make them permeable to K_+ ions. On the other side, activation of GPCRs also leads to phosphorylation by GRKs and coupling to arrestins (G-protein-independent signaling, right) which eventually triggers endosome mediated internalization of the receptor, leading to its recycling or degradation. Taken from [11].

losteric modulators have been categorized as positive (PAM), negative (NAM) or silent (SAM), respectively (Figure 1.4A) [12]. In addition to pure PAMs and NAMs that do not modify receptor activity in the absence of orthosteric ligands, other allosteric ligands possess intrinsic efficacy and either increase or decrease GPCR-mediated signaling (allosteric agonists and antagonists, respectively). This group also includes agonist-PAMs (agoPAMs) which show both intrinsic agonist efficacy and the ability to increase the potency and/or efficacy of orthosteric agonists.

Although classical pharmacology only discussed GPCR allosterism in terms of intramolecular interactions between orthosteric and

allosteric sites, there is mounting evidence that also intermolecular receptor-receptor interactions can alter the recognition, pharmacology and signaling of GPCRs. A receptor heteromer is considered "a macromelcular complex composed of at least two (functional) receptor units (protomers) with biochemical properties that are demonstrably different from those of its individual components" [13]. Despite the initial skepticism and discussion [14, 15], it is now increasingly accepted that GPCRs form homomers (between same types of protomers) and heteromers (between different types of protomers) [16]. These oligomers are in some cases the predominant species [17] and constitute primary functional signaling units [13].

Drug discovery programs targeting GPCRs have led to numerous successful therapeutic agents, but the design of molecules that bind GPCRs has been challenging. Indeed, available drugs usually aim for the orthosteric binding site [18] and target only 108 unique GPCRs that are $<$15% of the $\approx$800 genes [19]. The main reason has been the complexity of finding molecules with enough efficacy, to modulate receptor signaling; and with high selectivity for a specific GPCR subtype, to prevent off-target side effects. This, combined with the complexity that class A GPCR oligomerization brought to the table, has heightened interest in finding novel alternatives to overcome the main limitations of monovalent drugs.

1.2. Multivalent ligands and GPCRs

Historically, efforts to develop ligands targeting GPCRs have primarily focused on monovalent agonists and antagonists that interact with the orthosteric binding site to either mimic or block the action of the endogenous ligand [12, 22]. The main issue with the targeting of the orthosteric binding site is its high evolutionary conservation between closely related receptors to maintain protein function, which makes it difficult for drug discovery programs to develop selective compounds and avoid off-target side effects [7]. The five receptor subtypes (M_1R-M_5R) of the muscarinic acetylcholine receptor family, for instance, show high sequence similarity in their orthosteric binding

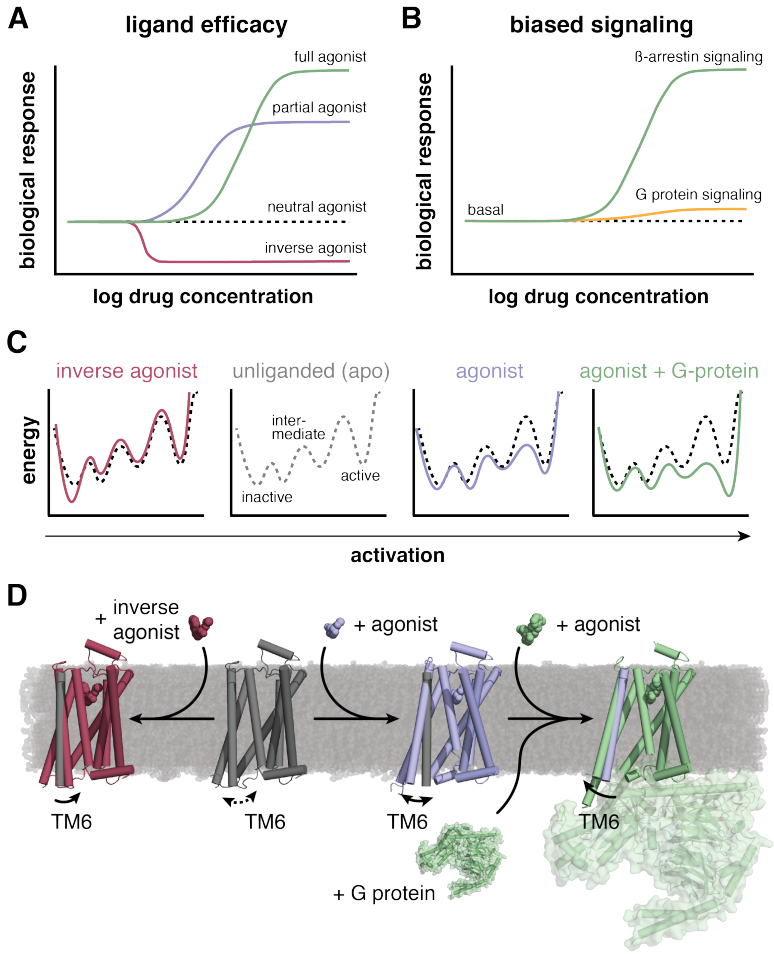

Figure 1.3: Dynamic properties of GPCRs. (A) Efficacy of each type of ligand. Full agonist and partial agonist induce maximal and submaximal responses, respectively. Neutral agonist does not alter basal activity, while inverse agonist inhibits it. Adapted from [20]. (B) Biological response of a ß-arrestin biased ligand, as an example of biased ligands, which preferentially activate one specific signaling pathway. Adapted from [20]. (C) Scheme of the conformational energy landscape of GPCR activation accompanied by (D) a representation of the hallmarks of GPCR activation, TM6 outward movement. In apo receptor the TM6 is highly dynamic, mainly populating inactive-like conformations. The inactive conformation is stabilized by inverse agonists while agonist binding promotes outward movement of TM6. Fully stabilized active conformation of TM6 is only achieved in presence of both agonist and G-protein. Adapted from [21].

site. This made it challenging to develop subtype selective synthetic M_1R agonists for the treatment of Alzheimer's disease without causing gastrointestinal and cardiovascular side effects caused by non-specific binding in the peripheral M_2R and M_3R subtypes [22]. Despite a specific M_1R partial agonist with low adverse effects was later published with promising results [23], numerous projects involving orthosteric drug discovery show a slow pace or have been discontinued for similar reasons [7]. Other associated complexities in the discovery of orthosteric drugs are that these sites can be too shallow to accommodate certain molecules, that the endogenous ligand can be difficult to replace because of its high affinity; and that mutation-caused drug resistances occur rather frequently [24]. Indeed, even when desired selectivity is achieved, some studies using orthosteric ligands have reported on-target side effects caused by the uniform activation of multiple signaling cascades of GPCRs or the disturbance of spatial and temporal patterns in comparison to the endogenous agonists [7].

Allosteric monovalent ligands emerged as a promising alternative approach for developing highly selective ligands for GPCRs which promised to offer several key advantages as therapeutic drugs over orthosteric ligands. Importantly, allosteric ligands bind to sites that are often less conserved than orthosteric sites, which are under more evolutionary pressure [25]. This allows the optimization of highly selective compounds for some GPCR subtypes that were inaccessible for traditional approaches and the decrease in off-target side effects. Structural determination of GPCRs in different functional states and in the presence of allosteric modulators have revealed not only the allosteric ligand-receptor interactions but also the existence of multiple allosteric sites which are distributed across the entire GPCR surface [7] (Figure 1.4B). In fact, Hedderich and colleagues performed a computation analysis leading to the discovery of novel "orphan" (i.e., as-of-yet untargeted) pockets and reaffirmed that almost the entire surface of the receptor structure is indeed potentially druggable [26]. Another advantage of pure allosteric ligands over orthosteric ligands is that their effects are saturable, i.e., once the allosteric pocket is fully occupied with ligand no additional effects are being observed [7], which decreases the likelihood of on-target side effects due to over-

dosing. Furthermore, pure allosteric modulators lack intrinsic activity (as they only exert an effect when the endogenous agonist is present) so they conserve the natural spatio-temporal patterns of endogenous ligands, which avoids excessive receptor activation and rapid desensitization –reducing the development of drug tolerance [7, 25]. Finally, allosteric drugs can be also used as an alternative when classical orthosteric drugs face mutation-caused drug resistances or when the target receptors are poorly druggable by small-molecule orthosteric ligands (e.g. peptide receptors with wide and deep orthosteric binding pockets) [7]. Although allosteric ligands are often more selective for their targets and allosterically modulating the actions of endogenous ligands provides substantial therapeutics benefits, the increasing effort on these drugs has faced some obstacles. Indeed, according to the Allosteric Database (ASD, http://mdl.shsmu.edu.cn/ASD), there are only four allosteric drugs targeting GPCRs (Cinacalcet, Ticagrelor, Ivermectin, and ATx-201) approved by the FDA. The primary issue with these monovalent ligands is that the mechanism in which these molecules affect signaling is not as direct as the one for orthosteric drugs, so they are usually less potent [18, 24]. Also, there is no reason why mutations would not appear in these sites under drug selection pressure as it occurs with orthosteric drugs [24].

Hence, it appears challenging to simultaneously enhance both potency and selectivity in drug design when targeting only one site. Novel approaches to overcome this problem that go beyond orthosteric and allosteric drugs include the discovery of multivalent ligands [28–30]. A multivalent ligand is a molecule endowed with two or more binding sites capable of interacting with multiple targets simultaneously (Figure 1.5). Portoghese and colleagues, introduced for first time in 1982 the concept of a bivalent ligand directed toward opioid receptors [31]. These molecules were characterized by possessing two pharmacophores interconnected by a "connecting chain" which in this thesis will be referred to as "linker" –it has also often been named "spacer". In that original idea, both pharmacophores were identical and targeted the orthosteric binding site. It must be noted that these compounds were designed prior to unveiling of the 3D structure of any GPCR and before the concept of a GPCR oligomer as a functional

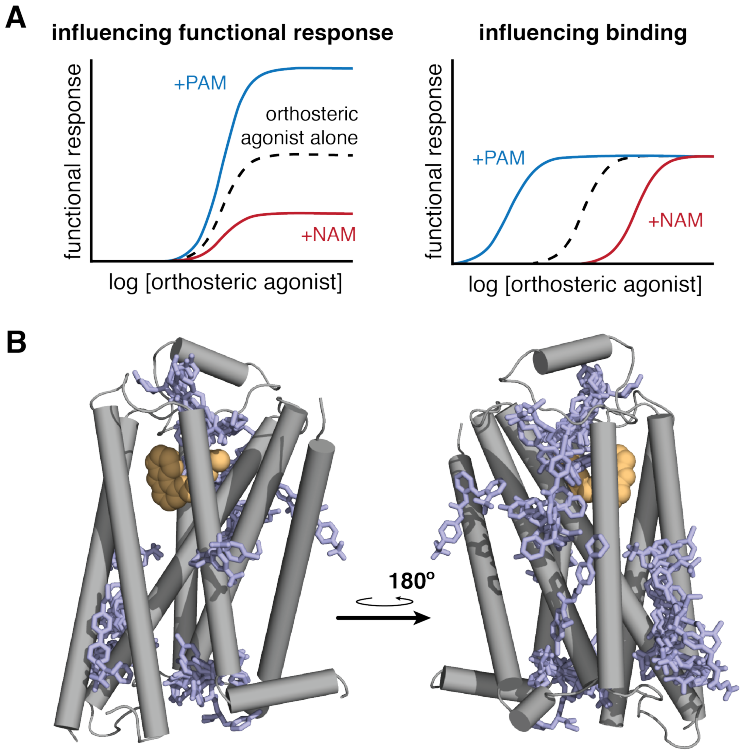

Figure 1.4: GPCR allosteric modulation. (A) Functional responses of allosteric modulators. Adapted from [27]. (B) Allosteric ligands found in solved Class A GPCR structures. Orthosteric ligand is depicted in orange spheres whereas allosteric ligands are in blue sticks.

unit. Indeed, it was originally hypothesized that bivalent ligands would exhibit increased potency over the monovalent analogue by enhancing the local concentration of pharmacophores and by bridging two neighboring GPCRs by the orthosteric binding sites [32]. Importantly, the authors observed that the increase in potency and efficacy was dependent on the length of the linker [31], which could serve as a molecular ruler to guess the distance between these two sites when bound by the bivalent ligand. Furthermore, the authors identified in subsequent studies that, for certain bivalents with rigid linkers, both termini of the bivalent ligand were not binding to vicinal receptors but rather the same receptor with high selectivity –reviewed in [32]. From this moment on, we will refer to this type of multivalent ligands as "bitopic ligands" to differentiate them from the term "bivalent ligands", which will be reserved for compounds that target two different receptors. Certainly, the conceptual framework has evolved since the work conducted by Portoghese and colleagues –we now have much more information about GPCR 3D structure and oligomerization–, yet the application of multivalent molecules (i.e. bivalent and bitopic ligands) to adjust affinities and efficacies remains relevant [32]. In reverse of the chronological order of their discovery, we will begin by discussing bitopic ligands, as they target the GPCR receptor as a monomeric entity; before introducing bivalent ligands, which target higher order complexes.

1.2.1. Bitopic ligands and GPCRs

The bitopic ligands are multivalent ligands (i.e., single molecules with two pharmacophores linked by linker) that simultaneously bind the orthosteric site as well as an allosteric site of the same receptor (Figure 1.5C) –technically, a bitopic ligand can also target two allosteric sites of a receptor, but as no such cases are presented in this thesis, this will be overlooked. Being a single molecule differs this strategy from the named orthosteric-allosteric therapy which consists in co-administrating the two drugs [33]. By simultaneously binding the core functional region (i.e., the orthosteric binding site) as well as a less conserved region (i.e., an allosteric binding site), bitopic ligands

achieve a balance between potency and selectivity [24]. Portoghese and colleagues employed the "message–address" concept introduced by Schwyzer [34] to describe the functioning of these compounds [35, 36] wherein the "message" is the primary pharmacophore, that binds the orthosteric binding site; whereas the "address" is de secondary pharmacophore, that confers additional interactions which can improve affinity and selectivity for a GPCR subtype. Also, they are more prone to avoid drug resistance thanks to the reduced likelihood of mutations occurring at both sites [24].

As poor structural information was available, the binding modes of bivalent ligands were not well characterized in the early research. A considerable part of the bitopic molecules were found by serendipity by finding that a randomly designed bivalent ligand was, in fact, bitopic [24] –usually because of their limited sizes. These molecules, as the ones originally designed by Portoghese and collegues, were synthesized symmetrically with identical orthosteric pharmacophores for both ends –i.e., the "message" and the "address" were indistinguishable from each other. In order to comprehend how a molecule with two orthosteric pharmacophores may function as a bitopic ligand, it is important to understand the mechanism by which an orthosteric ligand enters the receptor orthosteric site. Indeed, one of the most classical allosteric pockets of GPCRs is the namely extracellular cavity, metastable binding site, or vestibule –the latter being the term we will use in this thesis. This area is found in the entry pathway toward the orthosteric site, and it has been involved in the recognition of the orthosteric ligand [9, 37]. Upon binding of a suitable ligand to the vestibule, the receptor undergoes a conformational change that allows it to move further into the receptor to engage the orthosteric binding site [38]. Therefore, bivalent ligands made of two orthosteric pharmacophores could simultaneously bind both sites and act as a bitopic ligand. However, the current and growing knowledge in GPCR architecture and the discovery of both, new allosteric binding sites and allosteric drugs, facilitates the rational discovery of novel bitopic ligands with symmetrical (homobivalent) or asymmetrical (heterobivalent) ends. It is now easier for us to hypothesize its binding modes and, therefore, chose with better precision the suit-

able pharmacophores, linker sizes and the experiments to prove their mode of action. While the most notable strengths of bitopic ligands are the previously discussed enhancements in affinity and selectivity for a GPCR subtype, these molecules also draw interest due to other advantages and peculiarities over monovalent ligands and can be designed with different aims –reviewed in [24].

A win in potency and selectivity. Potency and selectivity are key attributes in drug evaluation. On one side, the potency reflects the drug effect at a certain concentration, and it is usually measured by the concentration of half maximum effect (i.e., IC_{50} and EC_{50}) or the equilibrium constant of drug disossciation (K_d). On the other side, the selectivity describes the relative potency of a drug for the interested target in comparison to other targets –especially to receptors within the same subfamily. Orthosteric drugs are usually highly potent because of their direct inhibition or activation mechanisms, but they have restricted selectivity due to high conservation of residues in orthosteric sites [7, 24]. In contrast, allosteric drugs typically exhibit better selectivity thanks to their binding to less conservated allosteric sites, while their indirect mechanism allows less potency [7, 24]. Notably, bitopic ligands have shown better selectivity than the orthosteric synthon and a better potency than the allosteric synthon by combining both molecules in a single compound [24].

Overcoming mutation-caused drug resistance. One of the causes of drug resistance –which is a major concern in clinical therapy– is residue mutation in the binding sites of target proteins [24, 39]. Such mutations can disrupt key interactions between residues of the binding site and the drug which could reduce potency. Both orthosteric and allosteric single-sited targeting strategies encounter drug resistance with almost the same probability [24]. However, bitopic ligands reduce this probability as it is much less likely for mutations to appear simultaneously at both orthosteric and allosteric sites. Indeed, as long as one pharmacophore could bind the target protein, the other one would be positioned in close proximity for binding thanks to the linker design [24, 40].

Using bitopic ligands as molecular rulers. The definition of conformation clusters of proteins is key for the understanding of their biological functions and the design of targeted drugs [24]. An ensemble of bitopic ligands with different linker lengths, for instance, can be used to measure the distance between two sites. Indeed, each of the distances would further be an index of conformational changes. Then, if we plot the length of the linker with the potency of each bitopic ligand, each of the local maxima could represent a dominant conformation of the protein [24]. In contrast, other experimental techniques to evaluate molecular distances, such as fluorescence resonance energy transfer (FRET) experiments, require the fusion of fluorescent groups which can bias the conformation ensemble.

Discovery of function biased modulators. In contrast with the endogenous agonist –which is unbiased by definition– and most of the orthosteric drugs for GPCRs, a biased ligand favors certain receptor conformations which traduce into selecting one of the signaling pathways –the canonical G protein or the ß-arrestin pathway– over the other [7]. Indeed, this type of ligands can be used to selectively activate the signaling pathway with beneficial therapeutic effects while attenuating those that produce on-target side effects [7, 24]. As an extension of allosteric modulators, bitopic ligands could also be used to bias the signal with the advantage of not requiring the natural ligand for the activation [24].

Others. The use of these compounds is still undergoing significant development, so new ways of exploiting their strengths continue to emerge. Thus far, additional applications have been the design of partial agonists and highly sensitive fluorescent tracers [24].

1.2.2. Bivalent ligands and oligomers of GPCRs

Recent studies propose GPCR oligomers, in form of homomers or heteromers, as the "actual targets" of molecules that bind to the orthosteric binding site [41]. Indeed, they are sometimes the predominant species [17] and constitute primary signaling units [13]. GPCR

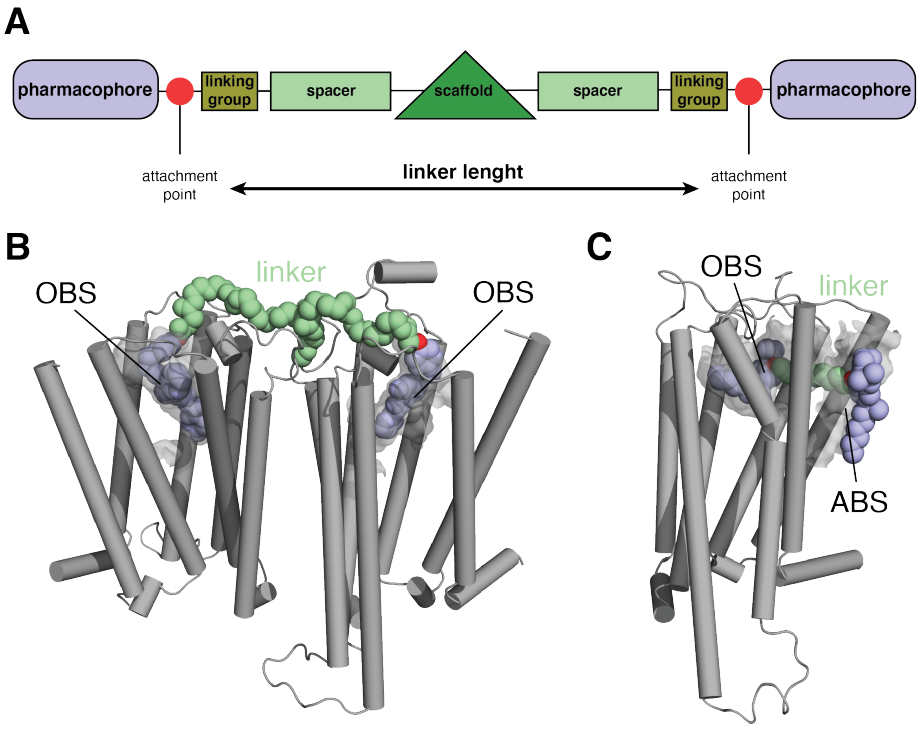

Figure 1.5: (A) Building blocks of a bivalent ligand and binding modes of a (B) bivalent ligand and a (C) bitopic ligand, respectively. While bivalent ligands can bind two sites of two different protomers of a dimer (in this case the OBS), the term "bitopic ligand" is reserved to those bivalent ligands which bind two sites of the same receptor (usually the OBS and one ABS). OBS, orthosteric binding site; ABS, allosteric binding site.

oligomerization can significantly impact the regulation of receptor signaling and pharmacology [42]. Although the large number of GPCRs ($\simeq$ 800, $\simeq$ 300 for non-sensory) might suggest a heightened likelihood of casual and non-functional oligomers, it has been shown that the intermolecular interactions between GPCRs are, in fact, highly specific –namely not all GPCRs interact with each other, only few of them. To date, no specific rules have been established to predict whether two given GPCRs will form heterodimers. An online tool (http://www.gpcr-hetnet.com/) provides information on both experimentally determined interactions within the GPCR superfamily and non-interacting GPCRs that can serve as negative controls [43].

The concept of GPCR oligomerization is highly controversial. Specifically, there has been an intense debate regarding the existence and functional relevance of Class A dimers [44]. Bivalent ligands are valuable tools to interrogate GPCR dimers and demonstrate their existence even in native tissue. Importantly, they can be used to study a specific GPCR dimer behavior without any receptor modification bias [45]. As exposed for bitopic ligands, bivalent ligands used as experimental tools could serve as molecular rulers to assess distance between two protomers of an oligomer or highly sensitive fluorescent tracers for specific dimers. Moreover, although limited by problematic molecular properties –e.g., high molecular weight and lipophilicity–, such compounds may also evolve to useful pharmacological agents [45].

The pharmacologic interest in GPCR oligomers is especially derived from the fact that they are likely to have a restricted tissue distribution and/or to be up- or downregulated in specific tissues under pathological conditions [16, 42, 46]. A major focus has been on the generation of oligomer-selective tools that target oligomers in native tissues [42]. These include antibodies that selectively recognize an epitope in the oligomer [47] or/and the development of high-affinity bivalent ligands (fluorophore-coupled or not) that selectively target the dimer. Bivalent ligands would be the paradigm of dimer-selective drugs [48] able to modulate receptor function within a particular GPCR dimer with lesser secondary effects, key to design a new generation of GPCR drugs.

In the same manner as with the bitopic ligands, bivalent ligands with an optimally designed linker are expected to demonstrate greater potency than the derived from the sum of its two monovalent pharmacophores, and high selectivity of drug action towards a certain dimeric subtype [32, 45]. This synergistic effect is based on the assumption that in the scenario where the bivalent ligand is univalently bound, the pathway to bivalent binding is expected to be favored over the univalent binding of a second ligand [45]. Furthermore, it has been observed that these compounds can also exhibit biased signaling [45], which can be used in drug design to reduce on-target side effects.

Finally, there is also evidence suggesting that GPCRs could form higher order pre-coupled complexes in the membrane involving not only tetramers of GPCRs –heterodimers in which each of its protomers form part of an homodimer–, but also signaling proteins such as G proteins and the adenylyl cyclase (AC) [49]. The existence of such formations opens the door to the complex design of multivalent ligands with more than two pharmacophores to selectively target these macro complexes.

Bibliography

[1] K. L. Pierce, R. T. Premont, R. J. Lefkowitz, "Seven-transmembrane receptors", *Nature reviews. Molecular cell biology* **2002**, *3*, 639–650.

[2] P. Kolb, T. Kenakin, S. P. Alexander, M. Bermudez, L. M. Bohn, C. S. Breinholt, M. Bouvier, S. J. Hill, E. Kostenis, K. A. Martemyanov, R. R. Neubig, H. O. Onaran, S. Rajagopal, B. L. Roth, J. Selent, A. K. Shukla, M. E. Sommer, D. E. Gloriam, "Community guidelines for GPCR ligand bias: IUPHAR review 32", *British journal of pharmacology* **2022**, *179*, 3651–3674.

[3] L. F. Kolakowski, "GCRDb: a G-protein-coupled receptor database.", *Receptors & Channels* **1994**, *2*, 1–7.

[4] R. Fredriksson, M. C. Lagerström, L. G. Lundin, H. B. Schiöth, "The G-protein-coupled receptors in the human genome form five main families. Phylogenetic analysis, paralogon groups, and fingerprints", *Molecular pharmacology* **2003**, *63*, 1256–1272.

[5] D. Yang, Q. Zhou, V. Labroska, S. Qin, S. Darbalaei, Y. Wu, E. Yuliantie, L. Xie, H. Tao, J. Cheng, Q. Liu, S. Zhao, W. Shui, Y. Jiang, M. W. Wang, "G protein-coupled receptors: structure- and function-based drug discovery", *Signal Transduction and Targeted Therapy 2020 6:1* **2021**, *6*, 1–27.

[6] W. I. Weis, B. K. Kobilka, "The Molecular Basis of G Protein-Coupled Receptor Activation", *Annual review of biochemistry* **2018**, *87*, 897–919.

[7] M. Persechino, J. B. Hedderich, P. Kolb, D. Hilger, "Allosteric modulation of GPCRs: From structural insights to in silico drug discovery", *Pharmacology & therapeutics* **2022**, *237*.

[8] N. J. Smith, G. Milligan, "Allostery at G protein-coupled receptor homo- and heteromers: uncharted pharmacological landscapes", *Pharmacological reviews* **2010**, *62*, 701–725.

[9] R. O. Dror, A. C. Pan, D. H. Arlow, D. W. Borhani, P. Maragakis, Y. Shan, H. Xu, D. E. Shaw, "Pathway and mechanism of drug binding to G-protein-coupled receptors", *Proceedings of the National Academy of Sciences of the United States of America* **2011**, *108*, 13118–13123.

[10] C. Galés, J. J. V. Durm, S. Schaak, S. Pontier, Y. Percherancier, M. Audet, H. Paris, M. Bouvier, "Probing the activation-promoted structural rearrangements in preassembled receptor-G protein complexes", *Nature structural & molecular biology* **2006**, *13*, 778–786.

[11] D. Hilger, M. Masureel, B. K. Kobilka, "Structure and dynamics of GPCR signaling complexes", *Nature structural & molecular biology* **2018**, *25*, 4–12.

[12] A. Christopoulos, "Advances in G protein-coupled receptor allostery: from function to structure", *Molecular pharmacology* **2014**, *86*, 463–478.

[13] S. Ferré, R. Baler, M. Bouvier, M. G. Caron, L. A. Devi, T. Durroux, K. Fuxe, S. R. George, J. A. Javitch, M. J. Lohse, K. Mackie, G. Milligan, K. D. Pfleger, J. P. Pin, N. D. Volkow, M. Waldhoer, A. S. Woods, R. Franco, "Building a new conceptual framework for receptor heteromers", *Nature chemical biology* **2009**, *5*, 131–134.

[14] M. Bouvier, T. E. Hébert, "CrossTalk proposal: Weighing the evidence for Class A GPCR dimers, the evidence favours dimers", *The Journal of physiology* **2014**, *592*, 2439–2441.

[15] N. A. Lambert, J. A. Javitch, "CrossTalk opposing view: Weighing the evidence for class A GPCR dimers, the jury is still out", *The Journal of physiology* **2014**, *592*, 2443–2445.

[16] S. Ferré, V. Casadó, L. A. Devi, M. Filizola, R. Jockers, M. J. Lohse, G. Milligan, J. P. Pin, X. Guitart, "G protein-coupled receptor oligomerization revisited: functional and pharmacological perspectives", *Pharmacological reviews* **2014**, *66*, 413–434.

[17] K. Herrick-Davis, E. Grinde, A. Cowan, J. E. Mazurkiewicz, "Fluorescence correlation spectroscopy analysis of serotonin, adrenergic, muscarinic, and dopamine receptor dimerization: the oligomer number puzzle", *Molecular pharmacology* **2013**, *84*, 630–642.

[18] D. Wacker, R. C. Stevens, B. L. Roth, "How Ligands Illuminate GPCR Molecular Pharmacology", *Cell* **2017**, *170*, 414–427.

[19] A. S. Hauser, M. M. Attwood, M. Rask-Andersen, H. B. Schiöth, D. E. Gloriam, "Trends in GPCR drug discovery: new agents, targets and indications", *Nature reviews. Drug discovery* **2017**, *16*, 829–842.

[20] D. Hilger, "The role of structural dynamics in GPCR-mediated signaling", *The FEBS journal* **2021**, *288*, 2461–2489.

[21] M. Casiraghi, "Biophysical investigations of class A GPCRs", *Biochimie* **2023**, *205*, 86–94.

[22] C. C. Felder, P. J. Goldsmith, K. Jackson, H. E. Sanger, D. A. Evans, A. J. Mogg, L. M. Broad, "Current status of muscarinic M1 and M4 receptors as drug targets for neurodegenerative diseases", *Neuropharmacology* **2018**, *136*, 449–458.

[23] A. J. Brown, S. J. Bradley, F. H. Marshall, G. A. Brown, K. A. Bennett, J. Brown, J. E. Cansfield, D. M. Cross, C. de Graaf, B. D. Hudson, L. Dwomoh, J. M. Dias, J. C. Errey, E. Hurrell, J. Liptrot, G. Mattedi, C. Molloy, P. J. Nathan, K. Okrasa, G. Osborne, J. C. Patel, M. Pickworth, N. Robertson, S. Shahabi, C. Bundgaard, K. Phillips, L. M. Broad, A. V. Goonawardena, S. R. Morairty, M. Browning, F. Perini, G. R. Dawson, J. F. Deakin, R. T. Smith, P. M. Sexton, J. Warneck, M. Vinson, T. Tasker, B. G. Tehan, B. Teobald, A. Christopoulos, C. J. Langmead, A. Jazayeri, R. M. Cooke, P. Rucktooa, M. S. Congreve, M. Weir, A. B. Tobin, "From structure to clinic: Design of a muscarinic M1 receptor agonist with potential to treatment of Alzheimer's disease", *Cell* **2021**, *184*, 5886–5901.e22.

[24] J. Zha, J. He, C. Wu, M. Zhang, X. Liu, J. Zhang, "Designing drugs and chemical probes with the dualsteric approach", *Chemical Society reviews* **2023**, *52*, 8651–8677.

[25] C. Zhu, X. Lan, Z. Wei, J. Yu, J. Zhang, "Allosteric modulation of G protein-coupled receptors as a novel therapeutic strategy in neuropathic pain", *Acta Pharmaceutica Sinica B* **2024**, *14*, 67–86.

[26] J. B. Hedderich, M. Persechino, K. Becker, F. M. Heydenreich, T. Gutermuth, M. Bouvier, M. Bünemann, P. Kolb, "The pocketome of G-protein-coupled receptors reveals previously untargeted allosteric sites", *Nature communications* **2022**, *13*.

[27] S. Brogi, A. Tafi, L. Désaubry, C. G. Nebigil, "Discovery of GPCR ligands for probing signal transduction pathways", *Frontiers in pharmacology* **2014**, *5*.

[28] J. R. Lane, P. M. Sexton, A. Christopoulos, "Bridging the gap: bitopic ligands of G-protein-coupled receptors", *Trends in pharmacological sciences* **2013**, *34*, 59–66.

[29] K. Mohr, J. Schmitz, R. Schrage, C. Tränkle, U. Holzgrabe, "Molecular alliance-from orthosteric and allosteric ligands to dualsteric/bitopic agonists at G protein coupled receptors", *Angewandte Chemie* **2013**, *52*, 508–516.

[30] S. J. Bradley, A. B. Tobin, "Design of Next-Generation G Protein-Coupled Receptor Drugs: Linking Novel Pharmacology and In Vivo Animal Models", *Annual review of pharmacology and toxicology* **2016**, *56*, 535–559.

[31] M. Erez, A. E. Takemori, P. S. Portoghese, "Narcotic antagonistic potency of bivalent ligands which contain beta-naltrexamine. Evidence for bridging between proximal recognition sites", *Journal of medicinal chemistry* **1982**, *25*, 847–849.

[32] A. H. Newman, F. O. Battiti, A. Bonifazi, "2016 Philip S. Portoghese Medicinal Chemistry Lectureship: Designing Bivalent or Bitopic Molecules for G-Protein Coupled Receptors. The Whole Is Greater Than the Sum of Its Parts", *Journal of medicinal chemistry* **2020**, *63*, 1779–1797.

[33] D. Ni, Y. Li, Y. Qiu, J. Pu, S. Lu, J. Zhang, "Combining Allosteric and Orthosteric Drugs to Overcome Drug Resistance", *Trends in pharmacological sciences* **2020**, *41*, 336–348.

[34] R. Schwyzer, "ACTH: a short introductory review", *Annals of the New York Academy of Sciences* **1977**, *297*, 3–26.

[35] P. S. Portoghese, H. Nagase, A. E. Takemori, "Only one pharmacophore is required for the kappa opioid antagonist selectivity of norbinaltorphimine", *Journal of medicinal chemistry* **1988**, *31*, 1344–1347.

[36] P. S. Portoghese, "Bivalent ligands and the message-address concept in the design of selective opioid receptor antagonists", *Trends in pharmacological sciences* **1989**, *10*, 230–235.

[37] A. González, T. Perez-Acle, L. Pardo, X. Deupi, "Molecular basis of ligand dissociation in β-adrenergic receptors", *PloS one* **2011**, *6*.

[38] P. Fronik, B. I. Gaiser, D. S. Pedersen, "Bitopic Ligands and Metastable Binding Sites: Opportunities for G Protein-Coupled Receptor (GPCR) Medicinal Chemistry", *Journal of medicinal chemistry* **2017**, *60*, 4126–4134.

[39] R. Pisa, T. M. Kapoor, "Chemical strategies to overcome resistance against targeted anticancer therapeutics", *Nature chemical biology* **2020**, *16*, 817–825.

[40] V. S. Rodrik-Outmezguine, M. Okaniwa, Z. Yao, C. J. Novotny, C. McWhirter, A. Banaji, H. Won, W. Wong, M. Berger, E. D. Stanchina, D. G. Barratt, S. Cosulich, T. Klinowska, N. Rosen, K. M. Shokat, "Overcoming mTOR resistance mutations with a new-generation mTOR inhibitor", *Nature* **2016**, *534*, 272–276.

[41] R. Franco, V. Casadó, A. Cortés, C. Ferrada, J. Mallol, A. Woods, C. Lluis, E. I. Canela, S. Ferré, "Basic concepts in G-protein-coupled receptor homo- and heterodimerization", *TheScientificWorldJournal* **2007**, *7*, 48–57.

[42] I. Gomes, M. A. Ayoub, W. Fujita, W. C. Jaeger, K. D. Pfleger, L. A. Devi, "G Protein-Coupled Receptor Heteromers", *Annual review of pharmacology and toxicology* **2016**, *56*, 403–425.

[43] D. O. Borroto-Escuela, I. Brito, W. Romero-Fernandez, M. D. Palma, J. Oflijan, K. Skieterska, J. Duchou, K. V. Craenenbroeck, D. Suárez-Boomgaard, A. Rivera, D. Guidolin, L. F. Agnati, K. Fuxe, "The G protein-coupled receptor heterodimer network (GPCR-HetNet) and its hub components", *International journal of molecular sciences* **2014**, *15*, 8570–8590.

[44] J. H. Felce, S. J. Davis, D. Klenerman, "Single-Molecule Analysis of G Protein-Coupled Receptor Stoichiometry: Approaches and Limitations", *Trends in pharmacological sciences* **2018**, *39*, 96–108.

[45] M. Qian, Z. Sun, X. Chen, S. V. Calenbergh, "Study of G protein-coupled receptors dimerization: From bivalent ligands to drug-like small molecules", *Bioorganic chemistry* **2023**, *140*.

[46] A. Cortés, E. Moreno, M. Rodríguez-Ruiz, E. I. Canela, V. Casadó, "Targeting the dopamine D3 receptor: an overview of drug design strategies", *Expert opinion on drug discovery* **2016**, *11*, 641–664.

[47] A. Gupta, J. Mulder, I. Gomes, R. Rozenfeld, I. Bushlin, E. Ong, M. Lim, E. Maillet, M. Junek, C. M. Cahill, T. Harkany, L. A. Devi, "Increased abundance of opioid receptor heteromers after chronic morphine administration", *Science signaling* **2010**, *3*.

[48] V. Casadó-Anguera, A. Cortés, V. Casadó, E. Moreno, "Targeting the receptor-based interactome of the dopamine D1 receptor: looking for heteromer-selective drugs", *Expert opinion on drug discovery* **2019**, *14*, 1297–1312.

[49] G. Navarro, A. Cordomí, V. Casadó-Anguera, E. Moreno, N. S. Cai, A. Cortés, E. I. Canela, C. W. Dessauer, V. Casadó, L. Pardo, C. Lluís, S. Ferré, "Evidence for functional pre-coupled complexes of receptor heteromers and adenylyl cyclase", *Nature communications* **2018**, *9*.

Chapter 2

Objectives

Despite the proven success of GPCRs as drug targets, useful ligands do not exist for most of them, due to the high evolutionary conservation of the orthosteric binding site between closely related receptors. This makes difficult, for drug discovery programs, to develop selective compounds and avoid off-target side effects. Novel approaches to modulate GPCRs, overcoming this problem, involve the discovery of bitopic ligands that bind the orthosteric site as well as a less conserved site at the entrance of the binding site, or bivalent/multivalent ligands that target physiologically relevant GPCR (homo/hetero)-oligomers. Thus, the global objective of this thesis is to understand the molecular basis to selectively target GPCRs, using complementary computational and experimental (performed by others, see below) techniques. The objectives are:

2.1 Implementing a computational framework to guide the design and evaluation of bitopic and bivalent ligands.

Bitopic and bivalent ligands are single chemical entities composed of two pharmacophore units, covalently linked by an appropriate spacer, that bind the orthosteric site as well as a less conserved site within the same receptor unit or bridge two receptor units. The spacer length is a key factor in the design of these type of ligands. Thus,

we want to develop and implement an overall computational methodology to model, simulate, and analyze these ligands and predict the proper spacer length for achieving affinity and selectivity.

2.2 Designing bitopic ligands of the cannabinoid receptor 2 to increase selectivity.

We want to design and evaluate bitopic ligands for the cannabinoid receptor 2 (CB_2R) with increased selectivity over the cannabinoid receptor 1 (CB_1R). These compounds have symmetrical pharmacophore units that can simultaneously bind the orthosteric site and a complementary, membrane-facing, site between TMs 1 and 7 (*Case Study 1*). It has been shown that this type of ligands, with a precise linker size, can modulate the dynamics of receptor homodimerization. We want to understand the mechanism by which modulation of CB_2R homodimerization, through a specific TM interface, promoted by the ligand, provides unique pharmacological properties, such as increased potency in G_i binding and enhanced β-arrestin recruitment (*Case Study 2*).

2.3 Designing heterobivalent ligands for a GPCR heterodimer.

The spacer length of heterobivalent ligands is a key factor and depends on the heterodimer interface, the surface of the extracellular domains of the heterodimer, and the position and orientation of the attachment points of the spacer to the pharmacophore moieties. The designed compounds must be capable of simultaneous binding of the pharmacophoric units to the orthosteric binding sites of the heterodimer. We have used as model heteromers the complexes between dopamine D_1-histamine H_3 receptors (D_1R-H_3R) (*Case Study 3*) and adenosine A_{2A}-dopamine D_2 receptors ($A_{2A}R$-D_2R) (*Case Study 4*).

2.4 Designing heterotetravalent ligands for a GPCR heterotetramer.

Of special functional significance are those heteromers constituted by one homodimer coupled to a G_s protein and another different homodimer coupled to a G_i protein, a GPCR heterotetramer. Thus, we aim to rationally design and evaluate heterotetravalent ligands for the $A_{2A}R$-D_2R receptor heterotetramer that is capable of simultaneous binding to the orthosteric binding site of the four protomers (*Case Study 5*).

This research has been performed by combining structural bioinformatics, molecular dynamics and data-mining of structure and sequence databases with experimental results from site-directed mutagenesis, functional assays and biophysical techniques. It is important to note that chemical synthesis, chemical biology, and in vitro evaluation has been performed by others listed in the original publications.

Chapter 3

Methods

The unveiling of the structural information of GPCRs has played a major role in drug development by being source of the mechanistic understanding of their activation mechanism. However, there is still receptor structures, key structural parts of many receptors –usually extracellular and/or intracellular domains and N- and/or C-terminus-, ligand binding modes, and oligomerization interfaces of the systems of interest which are unknown and must be modelled by computational techniques. Also, as GPCRs are dynamic proteins with high flexibility which allows their existence in multiple conformations, a single structure is usually not enough to decipher the role of certain factors, such as ligand stability, and the exploration of their molecular dynamics is required. Below we describe the methods, both computational and experimental (performed by collaborators), employed in the thesis to rationally design multivalent ligands and characterize the ligand-receptor-effector systems of interest.

3.1. Homology modeling

Homology modeling is a technique that predicts the unknown structure of a *target* receptor using the known structure of a homologous *template* receptor. It is based on the principle that proteins with similar sequences (>30%) maintain a similar structure [1]. Pro-

vided with a sequence alignment and the *template* structure files (one or more), the MODELLER software [2, 3] calculates a model of the *target* protein containing all non-hydrogen atoms. MODELLER implements the comparative protein modeling of the *target* protein by satisfaction of spatial restraints derived from the alignment and expressed as probability density functions for the features restrained [4]. Among other additional tasks, MODELLER can also *de novo* model missing loops [5]. In 2021, AlphaFold2 was introduced as an artificial-intelligence based alternative trained on pairs of available sequence-structure data to predict protein structure, demonstrating outstanding performance [6]. GPCRs exist and are resolved in multiple conformations, so it is important to highlight that AlphaFold is biased towards the active state. This is due to an actual bias in the structures available, as the active or active-like GPCR structures represent around the 60% (https://gpcrdb.org/structure/statistics).

Each receptor studied in this thesis had at least one resolved structure. However, MODELLER was mainly used to model the unresolved parts of the receptors and intracellular partners and mutate the mutations of the resolved structure to the native sequence. This includes, for instance, the modelling of the inactive D_1R or the s18s19 loop of the ß-arrestin. The stability of the predicted models was assessed by molecular dynamics (MD) simulations.

3.2. Modeling a GPCR dimer

The modeling of GPCR dimers was needed for those studies involving multivalent ligands targeting a GPCR oligomer. As mentioned in the Introduction, oligomerization among GPCRs is highly specific and the interaction interfaces between the receptors are very challenging to predict *in silico*. However, several methods have been proposed with relative success to computationally predict the interfaces for GPCR oligomerization, which include sequence-based methods, protein-protein docking and MD simulations [7]. On the experimental side, synthetic peptides with the sequence of a particular TM helix of a receptor, fused to cell-penetrating peptides [8, 9], are

used to disrupt biomolecular fluorescence complementation (BiFC) signals (see section *3.5 Experimental methods*) and have been key to predict contacts between the TM domains of interacting GPCRs. Other experimental data can also help rationalize the interfaces of GPCR dimers. For instance, cross-antagonism between two dimerizing GPCRs occurs when an agonist or an antagonist of one of the protomers inhibits the affinity or efficacy of an agonist of the other molecularly distinct protomer [10]. This has been attributed to the formation of a high surface complementary between TM helices 5 and 6 of the two protomers, via a four-helix bundle [11] that blocks the opening of the intracellular cavity for G protein binding at the other protomer [10]. Thus, a TM5/6 interface can be predicted for GPCR dimers that show cross-antagonism. Finally, orthosteric and allosteric GPCR mutants can also be used to predict the binding mode of the bivalent ligand which, together with the linker length, can sometimes provide us with enough restraints to model the dimer interface.

After identifying the interface, the available GPCR structural data can be used to model the dimeric complex. Although only the apelin receptor dimer has been disclosed in the Class A GPCRs family by cryo-EM [12], there are also crystallographic structures of GPCRs that contain possible (homo)dimers. Whether theses interfaces are feasible or experimental artifacts due to crystal packing is still controversial [13]. Nevertheless, these structures represent real interactions with accurate structural information and can still be used as templates.

According to the experimental findings, every dimer studied in this thesis displayed a symmetrical disposition (i.e., involves the same TM helices for both protomers) and involved either helices TM1 and TM7 (TM1/7 interface); TM5 and TM6 (TM5/6 interface); TM6 alone (TM6 interface); or TM4 and TM5 (TM4/5). The templates for the modeling of each one of the interfaces have been extracted from crystal structures (Figure 3.1), except for the TM6 interface which was modelled using the protein-protein docking software HADDOCK 2.2 [14] as previously reported [15, 16]. Indeed, for interfaces TM4/5 and TM5/6 the potential for oligomeric interaction is studied in the original publication [11, 17].

Generally, the protocol used in this thesis for modeling dimers after the interface was known has been as follows: (i) aligning the receptors of interest with the template, (ii) removing any significant clashes or structural hindrances by visual inspection, (iii) energy minimization, and (iv) performing MD simulations to assess the stability of the complex. In addition, for the modelling of the adenosine $A_{A2}A$–dopamine D_2 tetramer we first modelled the homodimeric parts, and then we aligned the internal protomers to a template with the heterodimeric interface. Figure 3.1 shows the dimers studied in this thesis and the template structures used for the modeling of each interface.

3.3. Designing a multivalent ligand

The design of multivalent ligands begins with the selection of the pharmacophores. This choice is based on (i) the receptor, in the case of bitopic ligands, or receptors, in the case of bivalent o tetravalent ligands, that will be targeted; (ii) the orthosteric or allosteric site of the receptor where each of the pharmacophores will bind, and (iii) the desired pharmacological properties. Next, each of the pharmacophores are docked to their corresponding binding sites of the monomer, dimer o tetramer model.

The aim of ligand-protein docking is to predict the primary binding mode (or modes) of a ligand within a protein of known three-dimensional structure. Usually, available GPCR structures bound to orthosteric and/or allosteric ligands can serve as references to dock a similar ligand of interest. Additionally, specialized software capable of generating docking solutions and employing scoring functions to evaluate their energetic feasibility can be used for this purpose [19]. AutoDock [20] and the docking facility in the Molecular Operating Environment (MOE) (Chemical Computing Group Inc., Montreal, Quebec, Canada) software have been used to generate docking solutions. The top scoring ones were visually inspected and those conformations which were compatible with the binding site and the physiological context were studied with MD simulations.

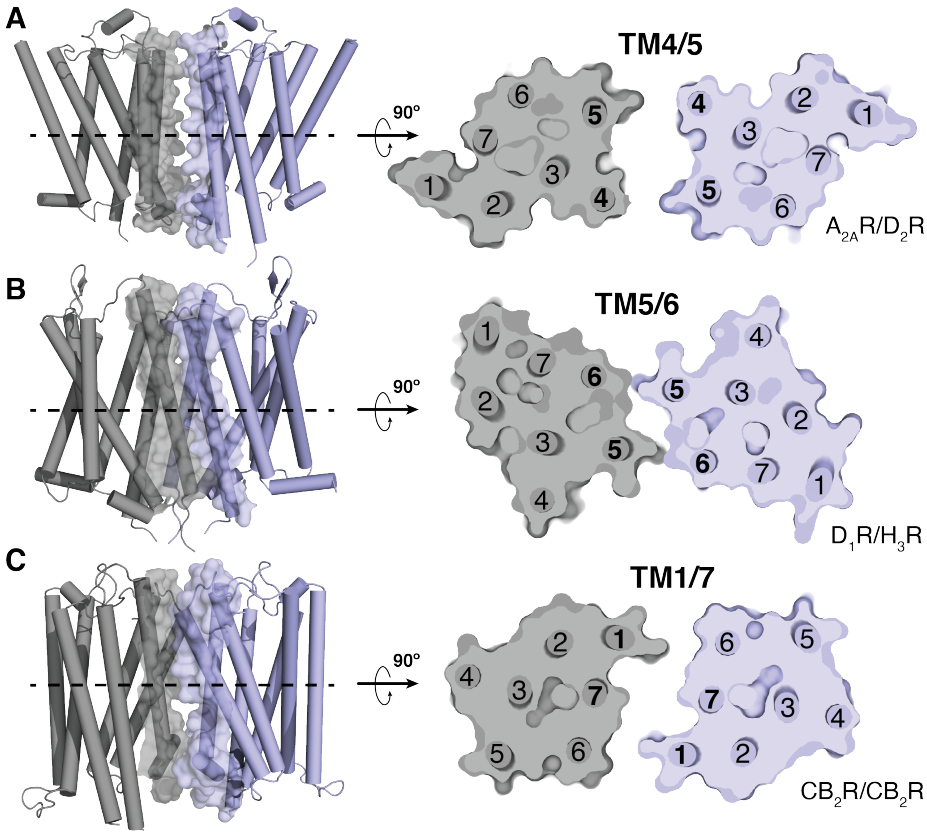

Figure 3.1: Crystal structures used as templates for the modeling of the dimeric interfaces studied in this thesis. Representations of (A) the TM4/5, (B) the TM5/6 and (C) the TM1/7 interfaces as observed in the crystal structures of (A) the β_1 adrenergic receptor in a dimeric state (β_1AR) (PDB id: 4GPO) [17]; (B) the μ-opioid receptor (MOR) bound to a morphinan antagonist (PDB id: 4DKL) [11]; and (C) the 5-HT_{2C} serotonin receptor (5-HT_{2C}) in complex with ritanserin (PDB id: 6BQH) [18]. The dimeric structures are presented in two orientations: sideview from the membrane plane (left) and a slice of the transverse plane viewed from the extracellular site (right). Next to the sliced view are indicated the homo- and heterodimers build using each of the structures as templates.

Once the binding poses of the pharmacophores are modelled, an attachment point from which the linker will be derived is selected for each of them (Figure 3.2). The attachment point is chosen based on the orientation towards the extracellular side, chemical accessibility, and maintenance of the affinity, selectivity, and biological activity of the pharmacophore structure [21, 22]. Subsequently, the distance between the attachment points, which will be covered by the linker, is estimated. To do so, we used the approach developed by Perez-Benito et al. [23], who created a computational tool with this purpose for the MOE software. The tool assesses the preferred linker length by calculating the shortest path between two attachment points and adjusting linker moieties of different lengths to the van der Waals surface of the receptor (or receptors).

Finally, the components of the linker also play an important role in the synthesis and pharmacological properties of the multivalent ligand. The linker can consist of up to three building blocks (Figure 3.2): (i) the scaffold, which permits at least the attachment of two different pharmacophore-containing chains –additional attachment of pharmacophore-containing chains or a reporter molecule, can be used to study higher order oligomers or for imaging studies, respectively–; (ii) the spacer, which is usually composed of alkyl or polyethylene glycol (PEG) units and can be tuned to modify the length of the linker; and (iii) the linker moieties that connect the pharmacophores with the spacer, facilitating their incorporation to the bivalent system.

Additionally, once designed and modelled into the respective GPCR monomer or oligomer complex, all the multivalent ligands were evaluated using molecular dynamics simulations (Figure 3.2).

3.4. MD simulations

Protein structures are very valuable per se, but they only retain information about a snapshot, thus lacking most of the dynamic context. Molecular dynamics (MD) simulations have been used with great success to study structure-function relationships of GPCRs by capturing the characteristic flexibility and dynamism of these systems

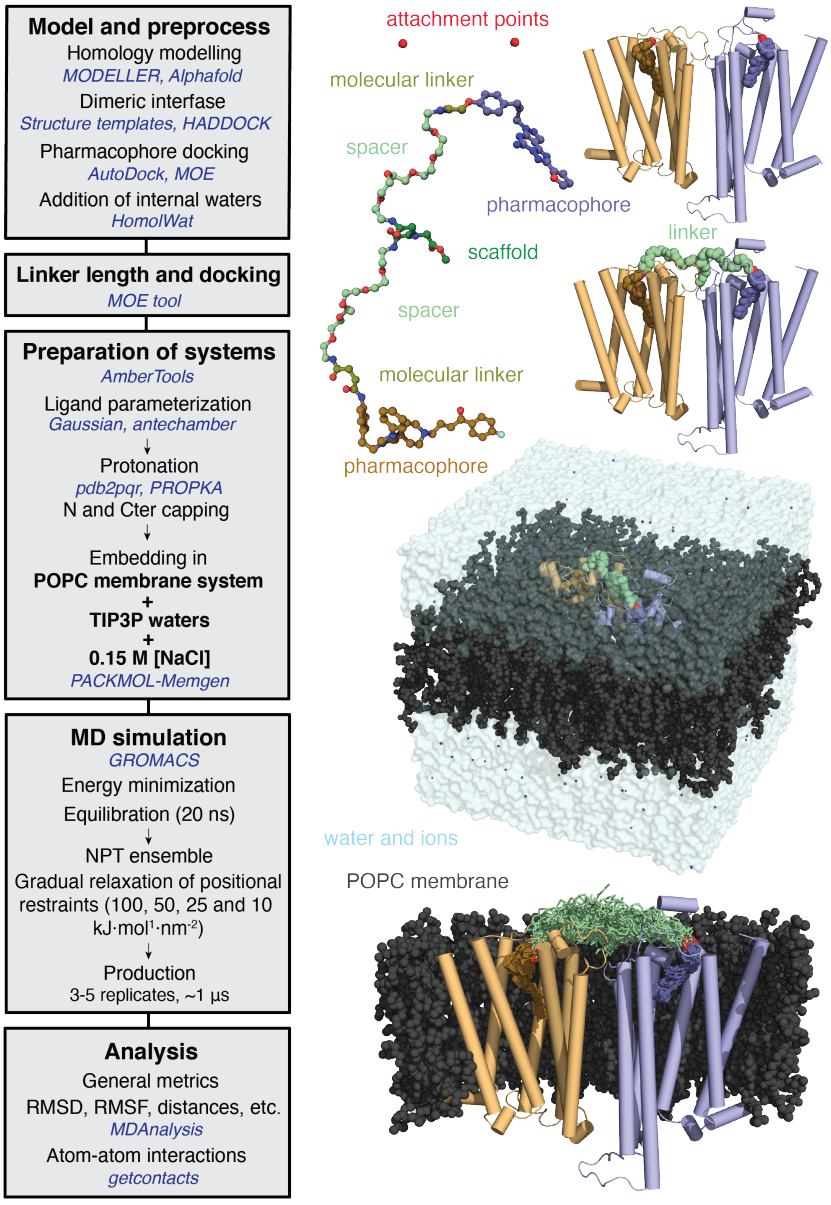

Figure 3.2: Workflow of the unbiased all-atom MD simulations protocol for a multivalent ligand. The software used in each step is depicted in blue italics.

[24]. This deterministic method produces a dynamical trajectory by iteratively solving the classical equations of motion on a group of particles (atoms) interacting by a simple harmonic force.

In this model, the potential energy of the system is simplified as a function of the position of the atoms (coordinates) mathematically expressed by means of a "force field". There are real experimental parameters behind each force field which are built on either quantum mechanics calculations or by fitting different sets of experimental data. These parameters define each type of particle with a set of features that determine their movement in the simulation. The definition of the potential energy in standard force fields is described as a sum of potentials of the intra- and intermolecular interactions in the system. Thus, a typical force field function is usually divided in bonded ($V^{bonds} + V^{angles} + V^{dihedrals} + V^{improper}$) and non-bonded ($V^{van\ der\ Waals} + V^{electrostatics}$) terms. Despite several force fields of varying levels of complexity exist, the MD simulations of this thesis were conducted within an all-atom level of description (i.e., where each particle represents one atom) using the amber14sb library [25] for protein and ions, a GROMACS adaptation of lipid14 [26] for lipids, TIP3P [27] for water, and the general Amber force field (GAFF2) [28] with HF/6-31G*-derived restrained electrostatic potential (RESP) atomic charges for ligands [29].

MD simulations require a preparation of an initial input with the 3D coordinates of all the atoms in the biomolecular system of interest. Thus, once the protein complex bound to a ligand was fully modelled (see above), protonation states were assigned with the PDB 2PQR tool [30] using PROPKA to predict the pKa values of ionizable groups in the proteins at pH 6.5 [31], disulfide bonds between cysteines were built using the tleap module of Ambertools19, and highly conserved internal water molecules were added using HomolWat [32]. The final systems for MD were built using PACKMOL-Memgen software [33] which embeds the protein-ligand-internal water complex into a lipid bilayer box containing a 1-palmitoyl-2-oleoyl-sn-glycero-3-phosphatidylcholine (POPC) membrane, water molecules and monoatomic Na^+ and Cl^- ions (0.15 M) (as represented in Figure 3.2).

The simulation box is subjected to certain thermodynamic conditions that are defined by the macroscopic ensembles. The most common ensembles are the NVT or canonical ensemble (constant number of atoms N, volume V and temperature T) and the NPT or isothermal-isobaric ensemble (constant number of atoms N, pressure P and temperature T). To maintain temperature and pressure values, systems are coupled to thermostats and barostats. Pressure control is more complex in membrane simulations compared to temperature control, primarily due to the presence of the water-membrane interface and the fluctuations of the area per lipid [34]. Hence, NPT is the method of choice when simulating systems with a lipid bilayer. The pressure coupling in these systems must be different on the X and Y axis (coupled together) from the Z axis –namely semi-isotropic or anisotropic coupling. Also, periodic boundary conditions (PBC) are used to avoid problems with boundary effects caused by the finite size of the simulation box.

Before the production phase, each molecular system (box) was subjected to 1000 cycles of energy minimization, followed by 23 ns of a six step NPT equilibration phase (10 ns + 5 ns + 2 ns + 2 ns + 2 ns + 2 ns) to ensure the stability of the thermodynamic properties (i.e., temperature, pressure, volume, density, and number of atoms), the hydration of the receptor cavities and the lipid packing around the protein. During the equilibration steps the position restraints were gradually relaxed. In the first step, only the hydrogen atoms were able to move freely, while in the second step, the restraints on the protein loops were released. For the subsequent 4 steps, the restraints on the ligand and the α-carbon atoms of the protein were gradually relaxed from 1000, 400, 25 to 10 kJ mol^{-1} nm^{-2}. At the same time, the phosphate group of the POPC molecules was also restrained and gradually released only in the Z axis to mitigate artifacts in the membrane.

After equilibration, unrestrained MD simulations (several replicas between 0.5-1 µs) were produced at a constant temperature of 300 K, using separate v-rescale thermostats for the receptor, ligands, membrane, and solvent molecules. A time step of 2.0 fs was used for the integration of equations of motion –as it cannot be longer than the faster process in the system (heavy atom bond vibration)

[35]. All bonds and angles were kept frozen using the LINCS algorithms. Lennard-Jones interactions were computed using a cutoff of 10 Å, and the electrostatic interactions were treated using PME with the same real-space cutoff under periodic boundary conditions. The GROMACS MD software [36] was used to run all the simulations presented in this thesis. Figure 3.2 shows a schematic workflow of the MD protocol.

The analysis of the obtained MD trajectories was performed by monitoring interatomic distances, angles, dihedrals, and root-mean square deviation (RMSD) or fluctuation (RMSF). RMSD is measured between the positions of the selection of interest (e.g., Cαatoms) at frame n and n-1, thus, a time evolution can be computed. RMSF instead measures the average displacement of each element in the selection (e.g., each Cαatom) to its average position along the simulation. Both quantities are usually indicative of stability in the trajectory. All these variables were studied using the python package MDAnalysis [37, 38]. The analysis of non-covalent interactions was performed with the python package getcontacts (https://getcontacts.github.io/).

3.5. Experimental methods

All computational studies conducted in this thesis have been carried out in close collaboration with experimental laboratories. This collaboration not only provided crucial information for the design of the multivalent ligands, such as the interaction interfaces of GPCR dimers which dictate the linker length, but also allowed for the synthesis of the compounds and experimental validation of the computational models through affinity, selectivity, protein-protein interaction, and functional assays. Below, the key techniques used to validate the computational analysis will be outlined.

3.5.1. Study of affinity and potency of ligands

Receptor-ligand binding assays emerged as one of the first *in vitro* methods used to study receptor function and they remain vital in

both basic GPCR research and drug discovery [39]. Although these studies usually cannot differentiate between agonists and antagonists or inverse agonists [40], they can provide quantitative information about receptor expression and receptor affinity for almost any ligand. This makes binding assays essential for basic GPCR research and drug discovery.

GPCR radioligand binding assays involve incubating a preparation of the receptor with a radiolabeled ligand to allow them to bind to each other, followed by quantifying the amount of receptor-bound label. The simplest binding assays involve the interaction between the receptor, R, and the radioligand, L^*, to give the complex RL^* according to the reaction:

$$R + L^* \rightleftharpoons RL^*$$

The association rate constant, k_{on}, defines the probability that the encounter between R and L^* will result in the formation of the RL^* complex. Taking this into account, the rate of formation of RL* is given by $k_{on} \cdot [R] \cdot [L^*]$, where [R] and $[L^*]$ are the concentrations of unbounded receptor and radioligand, respectively. Similarly, the rate of breakdown of the RL^* complex is the product between the dissociation rate constant, k_{off}, and $[RL^*]$. When the reaction is at equilibrium the association and dissociation rates are equal (i.e., $k_{on} \cdot [R] \cdot [L^*] = k_{off} \cdot [RL^*]$), which rearranges to $k_{on} / k_{off} = [RL^*] / [R] \cdot [L^*]$. The k_{on} / k_{off} ratio is also known as the equilibrium affinity constant, K_a, whereas the equilibrium dissociation constant, K_d, is the inverse of K_a (i.e, k_{off} / k_{on} or $[R] \cdot [L^*] / [RL^*]$ at equilibrium). Importantly, the K_d is also the concentration of free ligand (in moles/liter) when 50% of the receptor molecules are occupied by ligand. Thus, higher ligand affinities are directly related with lower K_d values, as they result in half-maximal occupation of receptor at lower ligand concentrations.

One of the considerations regarding this technique is the binding of the radioligands to nonreceptor sites, such as cell membranes or other proteins, which is named nonspecific binding (NSB). The total binding measured in the experiment is the sum of specific and nonspecific radioligand binding, so it must be corrected to determine the "specific binding" to the receptor. Usually, the NSB is measured by

adding and excess of an unlabeled competitive ligand, which inhibits the binding of the radioligand to the receptor without disrupting the interactions with nonreceptor components of the assay. Then, the measured NSB is subtracted from the total binding to calculate the specific binding.

The affinity and potency of the compounds presented in this thesis were evaluated through an indirect binding assay, specifically, a radioligand competition binding assay. For this slightly different approach, fixed concentrations of the receptor and the radioligand are mixed with varying concentrations of the unlabeled ligand of interest, A, which shares the same (e.g., orthosteric) binding site as the radioligand. This results in competition between the formation of the unlabeled ligand-receptor complex, RA, and the labeled complex, RL^*, according to the reaction:

$$RA \rightleftharpoons A + R + L^* \rightleftharpoons RL^*$$

For this approach, the radioligand binding in the absence of unlabeled ligand, is the maximum binding in the assay (B0) and increasing concentrations of unlabeled ligand progressively inhibit radioligand binding. Typically, a semilogarithmic plot of bound radioligand against the $\log_{10}$ concentration of unlabeled ligand results in an inverse sigmoid curve with a maximum equal to B0 and a minim equal to NSB (Figure 3.3). The ligand concentration that inhibits binding of the radioligand by 50% (IC_{50}) may then be used to estimate the affinity of the unlabeled ligand. Indeed, when the radioligand concentration is low ($<$0.1 K_d of the radioligand), the IC_{50} value is essentially equal to the equilibrium dissociation constant of the unlabeled ligand (K_i) [39].

3.5.2. Study of protein-protein interactions

In the 1960s, Osamu Shimomura discovered in a type of jellyfish the first fluorescent protein (which emits light when stimulated with light) and the first bioluminescent protein (which emits light when stimulated with a reagent) [41]. The former is the widely used Green Fluorescent Protein (GFP), while the latter was an aequorin, which

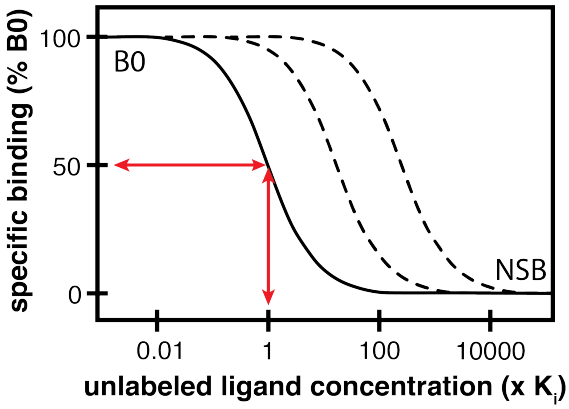

Figure 3.3: Indirect receptor-radioligand binding curves in the presence of a competitive unlabeled ligand. The schematic shows specific binding as a function of the starting concentration of unlabeled ligand. The solid line curve shows binding in the presence of a low concentration of radioligand ($\leq$0.1 K_d), where the IC_{50} (red arrows) is equal to the K_i if there is no ligand depletion. The dashed curves show the parallel rightward shift that occurs with increased radioligand concentration, which increases IC_{50}. NSB, nonspecific binding. Adapted from [39].

only produces blue light when stimulated by calcium. Interestingly, GFP only glowed green when it was near to a stimulated aequorin, which also represented the first characterization of resonance energy transfer [41]. These discoveries inspired the development of the techniques used in this thesis for the study of protein-protein interactions.

Ghosh and colleagues engineered, in 2000, a method to study heteromerization by splitting the GFP into two and fusing each half to two subunits of an anti-parallel leucine zipper [42]. The approach is based on the premise that when the two protomers interact, the two GFP halves will be close enough to hybridize and reconstitute a functional fluorescent protein. Thus, if the heteromerization occurs, the reconstituted GFP will emit detectable green light upon stimulation. This technique was termed Biomolecular Fluorescent Complementation (BiFC) [43]. The same concept can be applied to study GPCR dimerization dynamics by fusing the split GFP fragments with the receptors (Figure 3.4A). Specifically, the Yellow Fluorescent Protein

(YFP) was used instead of the GFP in the experiments of this thesis.

In the studies shown in this thesis, the BiFC technique has also been used in combination of the namely synthetic transmembrane helix peptides (TMPs). The TMPs contain the sequence corresponding to a given GPCR TM helix and the sequence of the protein transduction domain from the human immunodeficiency virus TAT protein [44] (Figure 3.4B). The latter is a strong positively charged which drives the insertion of the entire peptide in the membrane, with the TAT sequence being located in the intracellular area. In this approach of the technique, the BiFP fluorescence signal is measured both in the presence and absence of TMPs. If co-transfecting a specific TMP results in a decrease of the observed signal, one can assume that the peptide is competing with the interaction interface between the receptors and, therefore, that the corresponding TM to the sequence of that TMP is involved in the dimerization interface (Figure 3.4C). This also ensures that the BiFC signal is driven by specific GPCR interactions, as some studies have reported cases where the fusion of the fluorescent protein might be forcing the interaction between the fusion partners [43, 45]. Previous publications have demonstrated the destabilizing effects in previous publications not included in this thesis [14–16, 18]. In the studies shown in this thesis that involved a GPCR oligomer, the BiFC approach used in combination of the TMPs has been used to identify the interfaces, which guided the computational modelling of the systems.

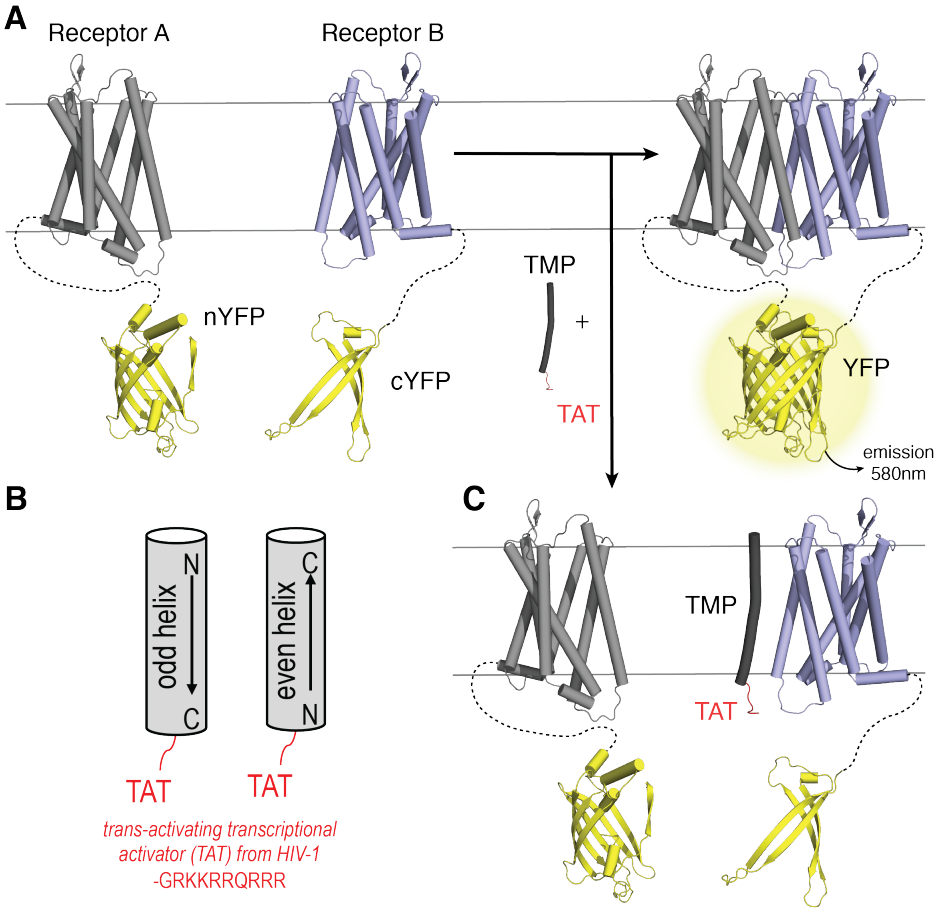

Figure 3.4: Bimolecular fluorescence complementation (BiFC) combined with transmembrane helix peptides (TMPs). (A) Graphical representation of the complementation. (B) TMPs are designed so that the TAT sequence is always facing the cytosol. Thus, TMPs with the sequences of the TMs 1, 3, 5 and 7 are synthesized with the TAT sequence fused at the C-terminus, and TMs 2, 4 and 6 at the N-terminus. (C) TMPs can compete with the interaction interface of the two receptors studied.

Bibliography

[1] B. Rost, "Twilight zone of protein sequence alignments", *Protein engineering* **1999**, *12*, 85–94.

[2] N. Eswar, B. Webb, M. A. Marti-Renom, M. Madhusudhan, D. Eramian, M.-y. Shen, U. Pieper, A. Sali, "Comparative protein structure modeling using Modeller", *Current protocols in bioinformatics* **2006**, *Chapter 5*.

[3] M. A. Martí-Renom, A. C. Stuart, A. Fiser, R. Sánchez, F. Melo, A. Šali, "Comparative protein structure modeling of genes and genomes", *Annual review of biophysics and biomolecular structure* **2000**, *29*, 291–325.

[4] A. Šali, T. L. Blundell, "Comparative protein modelling by satisfaction of spatial restraints", *Journal of molecular biology* **1993**, *234*, 779–815.

[5] A. Fiser, R. K. G. Do, A. Šali, "Modeling of loops in protein structures", *Protein science* **2000**, *9*, 1753–1773.

[6] J. Jumper, R. Evans, A. Pritzel, T. Green, M. Figurnov, O. Ronneberger, K. Tunyasuvunakool, R. Bates, A. Žídek, A. Potapenko, A. Bridgland, C. Meyer, S. A. Kohl, A. J. Ballard, A. Cowie, B. Romera-Paredes, S. Nikolov, R. Jain, J. Adler, T. Back, S. Petersen, D. Reiman, E. Clancy, M. Zielinski, M. Steinegger, M. Pacholska, T. Berghammer, S. Bodenstein, D. Silver, O. Vinyals, A. W. Senior, K. Kavukcuoglu, P. Kohli, D. Hassabis, "Highly accurate protein structure prediction with AlphaFold", *Nature* **2021**, *596*, 583–589.

[7] C. A. Barreto, S. J. Baptista, A. J. Preto, P. Matos-Filipe, J. Mourão, R. Melo, I. Moreira, "Prediction and targeting of GPCR oligomer interfaces", *Progress in Molecular Biology and Translational Science* **2020**, *169*, 105–149.

[8] F. Milletti, "Cell-penetrating peptides: classes, origin, and current landscape", *Drug discovery today* **2012**, *17*, 850–860.

[9] G. Guidotti, L. Brambilla, D. Rossi, "Cell-Penetrating Peptides: From Basic Research to Clinics", *Trends in pharmacological sciences* **2017**, *38*, 406–424.

[10] S. Ferré, F. Ciruela, C. W. Dessauer, J. González-Maeso, T. E. Hébert, R. Jockers, D. E. Logothetis, L. Pardo, "G protein-coupled receptor-effector macromolecular membrane assemblies (GEMMAs)", *Pharmacology & therapeutics* **2022**, *231*.

[11] A. Manglik, A. C. Kruse, T. S. Kobilka, F. S. Thian, J. M. Mathiesen, R. K. Sunahara, L. Pardo, W. I. Weis, B. K. Kobilka, S. Granier, "Crystal structure of the μ-opioid receptor bound to a morphinan antagonist", *Nature* **2012**, *485*, 321–326.

[12] Y. Yue, L. Liu, L. J. Wu, Y. Wu, L. Wang, F. Li, J. Liu, G. W. Han, B. Chen, X. Lin, R. L. Brouillette, É. Breault, J. M. Longpré, S. Shi, H. Lei, P. Sarret, R. C. Stevens, M. A. Hanson, F. Xu, "Structural insight into apelin receptor-G protein stoichiometry", *Nature structural & molecular biology* **2022**, *29*, 688–697.

[13] R. E. Stenkamp, "Identifying G protein-coupled receptor dimers from crystal packings", *Acta crystallographica. Section D Structural biology* **2018**, *74*, 655–670.

[14] S. J. D. Vries, M. V. Dijk, A. M. Bonvin, "The HADDOCK web server for data-driven biomolecular docking", *Nature protocols* **2010**, *5*, 883–897.

[15] G. Navarro, A. Cordomí, V. Casadó-Anguera, E. Moreno, N. S. Cai, A. Cortés, E. I. Canela, C. W. Dessauer, V. Casadó, L. Pardo, C. Lluís, S. Ferré, "Evidence for functional pre-coupled complexes of receptor heteromers and adenylyl cyclase", *Nature communications* **2018**, *9*.

[16] D. Pulido, V. Casadó-Anguera, L. Pérez-Benito, E. Moreno, A. Cordomí, L. López, A. Cortés, S. Ferré, L. Pardo, V. Casadó, M. Royo, "Design of a True Bivalent Ligand with Picomolar Binding Affinity for a G Protein-Coupled Receptor Homodimer", *Journal of medicinal chemistry* **2018**, *61*, 9335–9346.

[17] J. Huang, S. Chen, J. J. Zhang, X. Y. Huang, "Crystal structure of oligomeric β1-adrenergic G protein-coupled receptors in ligand-free basal state", *Nature structural & molecular biology* **2013**, *20*, 419–425.

[18] Y. Peng, J. D. McCorvy, K. Harpsøe, K. Lansu, S. Yuan, P. Popov, L. Qu, M. Pu, T. Che, L. F. Nikolajsen, X. P. Huang, Y. Wu, L. Shen, W. E. Bjørn-Yoshimoto, K. Ding, D. Wacker, G. W. Han, J. Cheng, V. Katritch, A. A. Jensen, M. A. Hanson, S. Zhao, D. E. Gloriam, B. L. Roth, R. C. Stevens, Z. J. Liu, "5-HT2C Receptor Structures Reveal the Structural Basis of GPCR Polypharmacology", *Cell* **2018**, *172*, 719–730.e14.

[19] G. L. Szwabowski, D. L. Baker, A. L. Parrill, "Application of computational methods for class A GPCR Ligand discovery", *Journal of molecular graphics & modelling* **2023**, *121*.

[20] J. Eberhardt, D. Santos-Martins, A. F. Tillack, S. Forli, "AutoDock Vina 1.2.0: New Docking Methods, Expanded Force Field, and Python Bindings", *Journal of chemical information and modeling* **2021**, *61*, 3891–3898.

[21] C. Hiller, J. Kühhorn, P. Gmeiner, "Class A G-protein-coupled receptor (GPCR) dimers and bivalent ligands", *Journal of medicinal chemistry* **2013**, *56*, 6542–6559.

[22] J. Shonberg, P. J. Scammells, B. Capuano, "Design strategies for bivalent ligands targeting GPCRs", *ChemMedChem* **2011**, *6*, 963–974.

[23] L. Pérez-Benito, A. Henry, M. T. Matsoukas, L. Lopez, D. Pulido, M. Royo, A. Cordomí, G. Tresadern, L. Pardo, "The size matters? A computational tool to design bivalent ligands", *Bioinformatics* **2018**, *34*, 3857–3863.

[24] N. R. Latorraca, A. J. Venkatakrishnan, R. O. Dror, "GPCR Dynamics: Structures in Motion", *Chemical reviews* **2017**, *117*, 139–155.

[25] J. A. Maier, C. Martinez, K. Kasavajhala, L. Wickstrom, K. E. Hauser, C. Simmerling, "ff14SB: Improving the Accuracy of Protein Side Chain and Backbone Parameters from ff99SB", *Journal of chemical theory and computation* **2015**, *11*, 3696–3713.

[26] C. J. Dickson, B. D. Madej, Å. A. Skjevik, R. M. Betz, K. Teigen, I. R. Gould, R. C. Walker, "Lipid14: The Amber Lipid Force Field", *Journal of chemical theory and computation* **2014**, *10*, 865–879.

[27] W. L. Jorgensen, J. Chandrasekhar, J. D. Madura, R. W. Impey, M. L. Klein, "Comparison of simple potential functions for simulating liquid water", *The Journal of Chemical Physics* **1983**, *79*, 926–935.

[28] X. He, V. H. Man, W. Yang, T. S. Lee, J. Wang, "A fast and high-quality charge model for the next generation general AMBER force field", *The Journal of chemical physics* **2020**, *153*.

[29] C. I. Bayly, P. Cieplak, W. D. Cornell, P. A. Kollman, "A well-behaved electrostatic potential based method using charge restraints for deriving atomic charges: the RESP model", *The Journal of physical chemistry* **1993**, *97*, 10269–10280.

[30] T. J. Dolinsky, J. E. Nielsen, J. A. McCammon, N. A. Baker, "PDB2PQR: an automated pipeline for the setup of Poisson-Boltzmann electrostatics calculations", *Nucleic acids research* **2004**, *32*.

[31] C. R. Søndergaard, M. H. Olsson, M. Rostkowski, J. H. Jensen, "Improved Treatment of Ligands and Coupling Effects in Empirical Calculation and Rationalization of pKa Values", *Journal of chemical theory and computation* **2011**, *7*, 2284–2295.

[32] E. Mayol, A. Garcia-Recio, J. K. Tiemann, P. W. Hildebrand, R. Guixa-Gonzalez, M. Olivella, A. Cordomi, "HomolWat: a web server tool to incorporate 'homologous' water molecules into GPCR structures", *Nucleic acids research* **2020**, *48*, W54–W59.

[33] S. Schott-Verdugo, H. Gohlke, "PACKMOL-Memgen: A Simple-To-Use, Generalized Workflow for Membrane-Protein-Lipid-Bilayer System Building", *Journal of chemical information and modeling* **2019**, *59*, 2522–2528.

[34] D. P. Tieleman, "Methods and Parameters for Membrane Simulations", *Molecular Simulations and Biomembranes* **2010**, 1–25.

[35] M. J. Abraham, T. Murtola, R. Schulz, S. Páll, J. C. Smith, B. Hess, E. Lindah, "GROMACS: High performance molecular simulations through multi-level parallelism from laptops to supercomputers", *SoftwareX* **2015**, *1-2*, 19–25.

[36] M. Torrens-Fontanals, T. M. Stepniewski, D. Aranda-García, A. Morales-Pastor, B. Medel-Lacruz, J. Selent, "How Do Molecular Dynamics Data Complement Static Structural Data of GPCRs", *International journal of molecular sciences* **2020**, *21*, 1–26.

[37] N. Michaud-Agrawal, E. J. Denning, T. B. Woolf, O. Beckstein, "MDAnalysis: a toolkit for the analysis of molecular dynamics simulations", *Journal of computational chemistry* **2011**, *32*, 2319–2327.

[38] R. J. Gowers, M. Linke, J. Barnoud, T. J. E. Reddy, M. N. Melo, S. L. Seyler, J. Domanski, D. L. Dotson, S. Buchoux, I. M. Kenney, O. Beckstein, "MDAnalysis: A Python Package for the Rapid Analysis of Molecular Dynamics Simulations", *Proceedings of the 15th Python in Science Conference* **2019**, 98–105.

[39] C. A. Flanagan, "GPCR-radioligand binding assays", *Methods in Cell Biology* **2016**, *132*, 191–215.

[40] J. J. Maguire, R. E. Kuc, A. P. Davenport, "Radioligand binding assays and their analysis", *Methods in molecular biology* **2012**, *897*, 31–77.

[41] A. Miyawaki, "Green fluorescent protein glows gold", *Cell* **2008**, *135*, 987–990.

[42] I. Ghosh, A. D. Hamilton, L. Regan, "Antiparallel leucine zipper-directed protein reassembly: Application to the green fluorescent protein [12]", *Journal of the American Chemical Society* **2000**, *122*, 5658–5659.

[43] T. K. Kerppola, "Design and implementation of bimolecular fluorescence complementation (BiFC) assays for the visualization of protein interactions in living cells", *Nature protocols* **2006**, *1*, 1278–1286.

[44] S. R. Schwarze, A. Ho, A. Vocero-Akbani, S. F. Dowdy, "In vivo protein transduction: delivery of a biologically active protein into the mouse", *Science* **1999**, *285*, 1569–1572.

[45] A. S. Dixon, M. K. Schwinn, M. P. Hall, K. Zimmerman, P. Otto, T. H. Lubben, B. L. Butler, B. F. Binkowski, T. MacHleidt, T. A. Kirkland, M. G. Wood, C. T. Eggers, L. P. Encell, K. V. Wood, "NanoLuc Complementation Reporter Optimized for Accurate Measurement of Protein Interactions in Cells", *ACS chemical biology* **2016**, *11*, 400–408.

Chapter 4

Designing homobivalent ligands for the cannabinoid CB_2 receptor

While most GPCRs recognize polar ligands, GPCRs for lipid mediators are activated by hormone-like signaling molecules derived from lipid species, which possess long hydrophobic moieties. This subfamily is mostly composed of the sphingosine-1-phosphate (S1P), lysophosphatidic acid (LPA) and cannabinoid (CB_1R and CB_2R) receptors [1]. In the crystal structures of these receptors [2] the extracellular N-terminus and extracellular loop 2 folds over the ligand binding pocket blocking the access to the orthosteric binding cavity from the extracellular environment. These structures together with binding pathway simulations suggest that the entrance of ligands to the orthosteric site within the 7TM domain occurs from the membrane bilayer [3, 4], through a narrow channel between TMs 1 and 7 that connects the orthosteric binding site to the lipid bilayer [3]. Indeed, the pathway of ligand entry to the cannabinoid CB_2 receptor (CB_2R), determined by MD simulations, defines two transient binding sites [5]: a membrane-facing pocket between TMs 1 and 7 [6] and a bundle-facing allosteric pocket located near the orthosteric site [7]. Notably, the access to the ligand pocket of the MT1 melatonin receptor that binds polar ligands (serotonin-derived compounds) is also

via the lipid bilayer [8]. Thus, the design of bivalent ligands for lipid GPCRs is more challenging than for other GPCRs that fully expose the binding site to the extracellular environment, due to the narrow channel linking the binding site and the lipid bilayer.

In the following two case studies, we have designed bivalent ligands for the cannabinoid CB_2R. We have selected CB_2R, instead of CB_1R, due to its lack of adverse psychotropic effects along with its wide therapeutic application in pathologies such as cancer, neuroinflammation and pain [9]. Bivalent ligands have already been published for CB_1R [10–12] and CB_2R [13]. All these ligands were reported before the release of crystal structures, thus, their binding characteristics remain unclear [14, 15]. Here, we have used the released structure of CB_2R in its active G_i-bound conformation [16] to identify the binding mode of the designed ligands.

4.1. Case study 1. Discovery of homobivalent bitopic ligands of the cannabinoid CB_2 receptor

Published as co-first author in

Paula Morales[1], Gemma Navarro[1], Marc Gómez-Autet[1], Laura Redondo, Javier Fernández-Ruiz, Laura Pérez-Benito, Arnau Cordomí, Leonardo Pardo[*], Rafael Franco[*], Nadine Jagerovic[*]. **Discovery of Homobivalent Bitopic Ligands of the Cannabinoid CB_2 Receptor.** Chemistry – A European Journal, 2020, 26(68), 15839–15842.

[1]These authors contributed equally.

4.1.1. Introduction

Novel approaches to overcome the selectivity problem for the orthosteric binding site of GPCRs include the discovery of bitopic ligands that bind the orthosteric site as well as a less conserved site within the same receptor unit [17–19] (see *Chapter 1 Introduction*). This type of complementary cavity is often located at the entrance of the orthosteric binding site, as identified in ligand binding pathway simulations, which have been named extracellular vestibule [20] or entrance [21], or secondary [22] or metastable [23] binding site, or exosite [24]. In this work, we will name this cavity as receptor vestibule or exosite. Bitopic ligands which bind these two sites have been reported to improve selectivity [24, 25], off-rates and signaling bias [17, 26, 27], maintaining bioavailability and brain penetration properties in mice [28].

In this case of study, we have designed, synthesized and functionally characterized the first bitopic ligands for the cannabinoid CB_2R to selectively target CB_2 vs CB_1 receptors. These ligands simultaneously bind the orthosteric binding site and the membrane-facing vestibule. Their binding mode has been studied by molecular dynamic simulations and site-directed mutagenesis.

4.1.2. Results and discussion

Molecular design

The design of bitopic ligands requires the selection of a moiety able to bind the orthosteric site (pharmacophore). In this regard, we have selected chromenopyrazole derivatives A and B (Figure 4.1), which have been previously identified as CB_2R orthosteric agonists [29]. Then, it is needed to develop a second pharmacophore unit for the vestibule or exosite. This is challenging because this additional cavity has not been properly characterized yet for most GPCRs. We have taken advantage of the simulated binding process of a lipid inhibitor to the S1P1 receptor [3]. The process consists in the diffusion of the ligand through the bilayer leaflet to contact the vestibule at the top of TM 7 (the rate-limiting step), subsequently moving from this lipid-facing vestibule to the orthosteric binding cavity through the channel between TMs 1 and 7. We propose that lipid GPCRs are capable to recognize orthosteric ligands at the vestibule of the receptor. Thus, we have also selected the chromenopyrazole moiety as the second pharmacophore so that the designed bitopic ligands are symmetrical (it contains two copies of the same pharmacophore). In addition, an appropriate length spacer to cover the distance between both pharmacophores is required. Importantly, this approach has been recently supported in the model of the bitopic ligand CTL01-05-B-A05, a symmetrical agomelatine molecule linked by an ethoxyethane spacer, which binds both the orthosteric binding site and the exosite of the MT1 melatonin receptor [8].

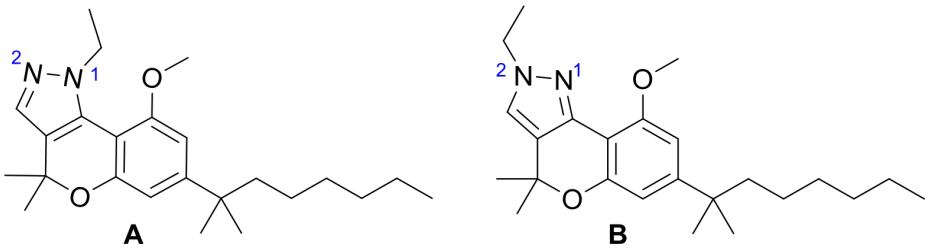

Figure 4.1: Structures of chromenopyrazoles A and B [29]. These compounds are isomers differing in the position of the N-Ethyl at the pyrazole (N1- or N2-Ethyl).

The orientation of the spacer was properly characterized by performing *ab initio* geometry optimization of the pharmacophores (Figure 4.2A-C). The most favorable conformations of the N1-Ethyl and N2-Ethyl analogs show different dihedral angles which favor two distinct intramolecular hydrogen bonds (Figure 4.2B-E, in yellow). These different intramolecular hydrogen bonds of the methoxy moiety, to which the methylene spacer is attached, explains the difference in the optimal spacer length in the N1- and N2-Ethyl derivatives (Tables 4.1 and 4.2).

Chromenopyrazole A, in its most stable conformation (Figure 4.2), was docked into the orthosteric and vestibule sites of CB_2R, and its stability was assessed by molecular dynamic (MD) simulations (Figure 4.3). Results showed that pharmacophore units remain highly stable at the orthosteric site and moderately stable at the exosite. Visual inspection of the models shows that the -CH_3 group of the methoxy moieties of both pharmacophores are suitable attachment points to link the spacer moiety. Linker lengths from six to sixteen methylene units were chosen for the bivalent molecules.

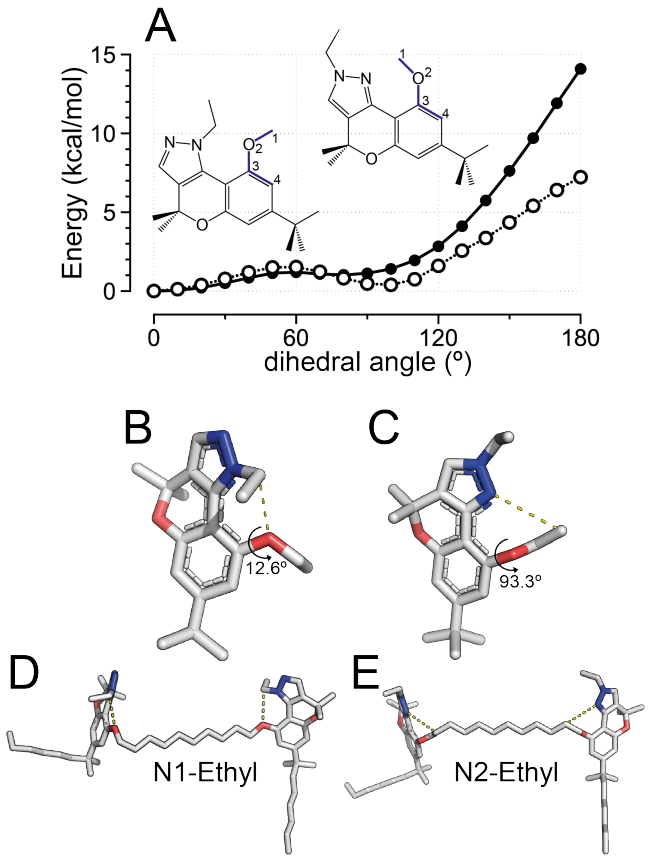

Figure 4.2: (A) *Ab initio* torsional energy profile (HF/6-31G*//HF/6-31G*) of the C1-O2-C3-C4 dihedral angle (in blue) for chromenopyrazole derivatives A (N1-Ethyl, black circle) and B (N2-Ethyl, white circle) in which the hexyl chains were substituted by methyl. (B, C) *Ab initio* full geometry optimization (MP2/6-31G*) of analogous compounds using the two energy minima (dihedral angles of ≈0° and ≈90°), obtained in panel A, as starting points. -OCH_3 was substituted by -OCH_2CH_3. The most favorable conformations of the N1-Ethyl and N2-Ethyl analogs correspond to dihedral angles of 12.6° (B) and 93.3° (C), respectively. This favors two distinct intramolecular hydrogen bonds (in yellow) between the oxygen atom of the -OCH_2CH_3 group and the -CH group of the N1-attached ethyl moiety (B), and between the -CH- group of -OCH_2CH_3 and the N1 atom of the chromenopyrazole moiety (C). (D, E) Conformations obtained in panels B and C, were used for *ab initio* full geometry optimization (HF/6-31G*) of derivatives **22** (N1-Ethyl, n=8, panel D), **25** (N2-Ethyl, n=10, panel E) and **27** (N2-Ethyl, n=12, not shown) (Figure 4.4 and Table 4.1), and for deriving RESP atomic charges (HF/6-31G*). The calculations were performed with Gaussian 09.

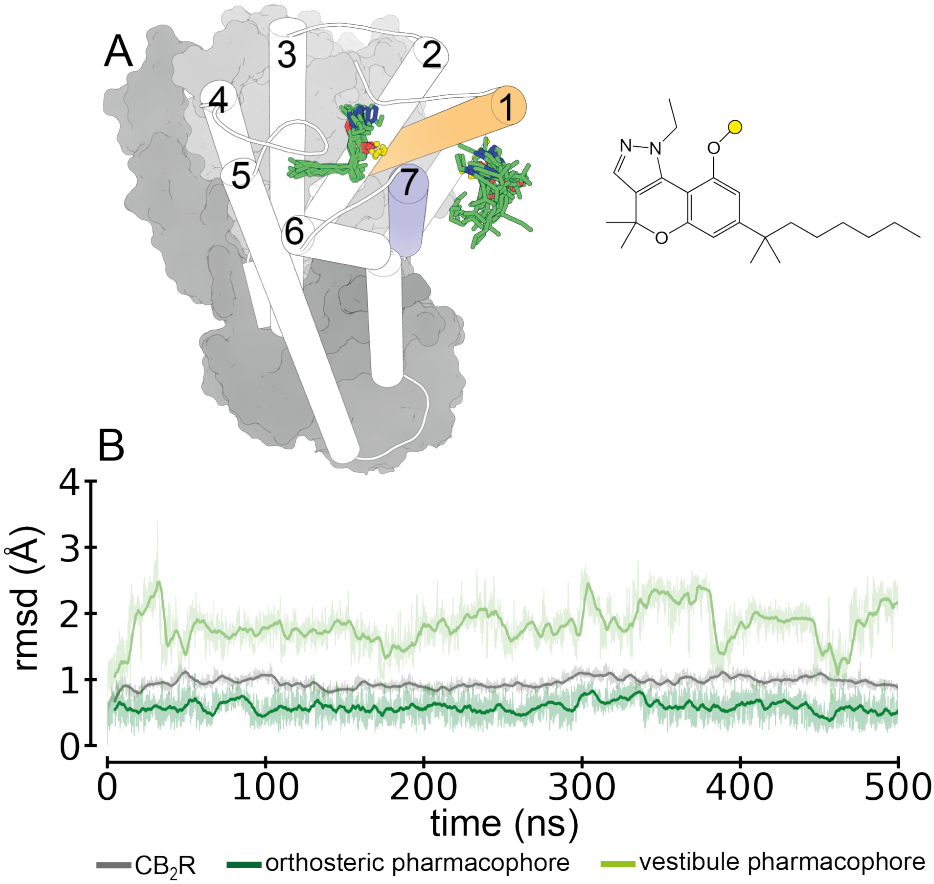

Figure 4.3: (A) MD simulation of chromenopyrazole derivative A (docked into the orthosteric site between TMs 2-3, 5-6 and the lipid-facing vestibule in TMs 1 and 7) bound to CB_2R (TM helices are depicted as cylinders and loops as ribbons) in complex with G_i (α- and $\beta\gamma$-subunits in dark and light gray surfaces, respectively) (PDB ID 6PT0 [16]). The structures of derivative A are extracted from the simulations (10 structures collected every 50 ns), whereas the structure of CB_2R-G_i complex corresponds to the initial structure. (B) The MD simulation was monitored by the root mean-square deviation (rmsd) of the backbone atoms of the TM helices of CB_2R (gray) and heavy atoms of the pharmacophore moieties located at the orthosteric (dark green) and vestibule (light green) binding sites. These results showed that pharmacophore units remain highly stable at the orthosteric site and moderately stable at the vestibule. The proposed attachment points (yellow sphere) are self-oriented in space and can be used for linking the spacer group. See *Chapter 3 Methods* for the details of the MD simulation.

Chemical synthesis

Bivalent chromenopyrazoles and their monovalent analogues were synthesized by Paula Morales and Nadine Jagerovic at the Medicinal Chemistry Institute, Spanish Research Council (CSIC), Madrid (Spain), using the Scheme shown in Figure 4.4.

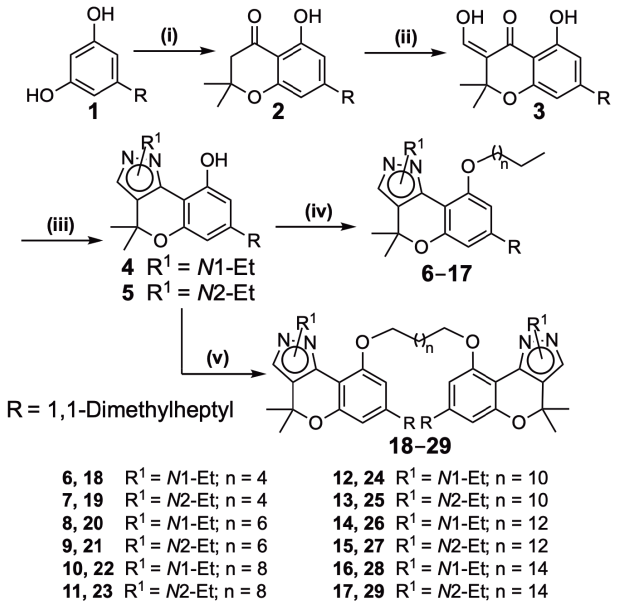

Figure 4.4: Synthesis of 9-alkoxychromenopyrazoles **6-17** and bivalent chromenopyrazoles **18-29**. Reagents and conditions: (i) 3,3-dimethylacrylic acid, methanesulfonic acid, P_2O_5, 8 h, 70 °C, 81%; (ii) a) NaH, THF, MW, 25 min, 45 °C; b) ethyl formate, MW, 25 min, 45 °C, 76%; (iii) corresponding hydrazine, EtOH, 1-4 h, 40 °C, 28-74%; (iv) a) NaH, anhydrous THF, 10 min, b) 1-bromoalkane, reflux, 2-12 h, 32-75%; (v) a) Cs_2CO_3, anhydrous THF, 10 min, b) 1,(n+2)-dibromoalkane, reflux, 8-72 h, 6-59%.

Ligand binding and functional assays

In vitro binding affinities of the alleged bitopic ligands **18-29** (Table 4.1) were obtained from [^{3}H]CP-55,940 competition-binding (see *Chapter 3 Methods*) assays using membrane fractions of the human CB_1R and CB_2R respectively expressed in HEK-293T cells by

Paula Morales and Nadine Jagerovic at the Medicinal Chemistry Institute, Spanish Research Council (CSIC), Madrid (Spain). None of the monovalent chromenopyrazoles exhibits affinity towards any of the cannabinoid receptors (not shown). Addition of the second pharmacophore makes bivalent ligands capable of binding CB_2R in a selective manner. Optimal spacer length for N1- and N2-ethyl derivatives is from 10 (n=8) to 14 (n=12) methylene units.

Compd	**R[1]**	***N*[a]**	**CB_1R K_i [µM][b]**	**CB_2R K_i [µM][b]**
18	*N*1-Et	4	> 40	28.1 ± 1.6
19	*N*2-Et	4	> 40	12.4 ± 2.0
20	*N*1-Et	6	> 40	2.2 ± 0.7
21	*N*2-Et	6	nd	nd
22	*N*1-Et	8	> 40	0.9 ± 0.2
23	*N*2-Et	8	> 40	5.8 ± 1.5
24	*N*1-Et	10	> 40	0.4 ± 0.14
25	*N*2-Et	10	> 40	0.3 ± 0.1
26	*N*1-Et	12	> 40	0.8 ± 0.1
27	*N*2-Et	12	> 40	0.3 ± 0.1
28	*N*1-Et	14	> 40	> 40
29	*N*2-Et	14	> 40	2.12 ± 0.21
A[30]	*N*1-Et	-	5.0 ± 0.7	0.16 ± 0.03
B[30]	*N*2-Et	-	2.9 ± 0.5	0.09 ± 0.02
WIN[c]	-	-	0.04 ± 0.01	0.003 ± 0.002

Table 4.1: Binding affinities of bivalent chromenopyrazoles (**18-29**) for hCB_1R and hCB_2R. [a] *n* refers to Figure 4.4. Total number of methylenes in the spacer is n+2. [b] Values obtained from competition curves using [^{3}H]CP55,940 as radioligand for hCB_1R and hCB_2R and are expressed as the mean ± SEM of at least three experiments. nd: not determined. [c] WIN55,212,2.

Compounds with CB_2R affinity constants in the low micromolar range (**22**, **24-27**) were selected for functional evaluation by measuring their effect on forskolin-induced cAMP levels in HEK-293 cells expressing hCB_2R (Figure 4.5A) by Gemma Navarro and Rafael Franco at the Department of Biochemistry and Physiology, Faculty of Pharmacy and Food Sciences, Universitat de Barcelona, Barcelona

(Spain). Dose-response experiments demonstrated that these compounds can inhibit cAMP accumulation as efficiently as CP55,940 but with a slightly drop of potency (**27**: pEC_{50}=7.6 vs. CP55,940: pEC_{50}=8.2) (Table 4.2).

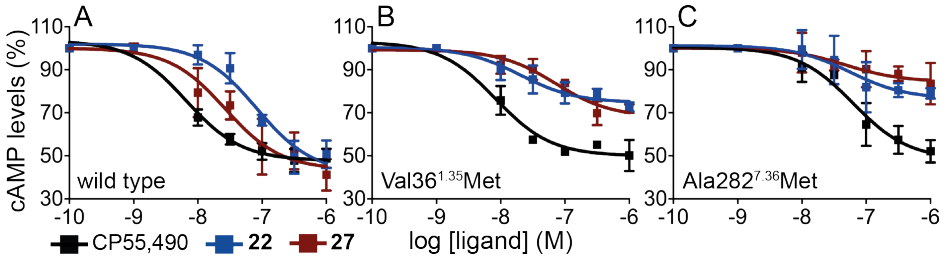

Figure 4.5: Decrease of forskolin-induced cAMP (normalized to 100%), in HEK-293T cells, upon stimulation of wild type CB_2R (A) and Val36 $^{1.35}$Met (B) and Ala282$^{7.36}$Met (C) mutant receptors with the CP55,940 agonist and ligands **22** and **27**.

	Wild type		**Val36$^{1.35}$Met**		**Ala282$^{7.36}$Met**	
	pEC_{50}	**E_{max}**[a]	**pEC_{50}**	**E_{max}**[a]	**pEC_{50}**	**E_{max}**[a]
22	7.1 ± 0.2	42 ± 5.4	7.7 ± 0.1	75 ± 1.5	7.2 ± 0.2	77 ± 2.5
24	7.2 ± 0.2	45 ± 6.3	nd		nd	
25	7.2 ± 0.2	40 ± 5.9	nd		nd	
26	6.5 ± 0.2	52 ± 4.1	nd		nd	
27	7.6 ± 0.1	44 ± 3.7	7.1 ± 0.2	68 ± 3.5	7.3 ± 0.2	84 ± 1.4
CP[b]	8.2 ± 0.1	48 ± 1.7	8.1 ± 0.1	50 ± 2.3	7.2 ± 0.1	48 ± 3.43

Table 4.2: Functional properties of compounds **22**, **24**-**27** and the reference compound CP55,940 at wild type and mutant CB_2R. [a] E_{max} (%), the maximum inhibition of forskolin-stimulated cAMP levels (normalized to 100%), values were calculated using nonlinear regression analysis. Data are expressed as the mean ± SEM of at least three independent experiments performed in triplicates. [b] CP is CP55,940. nd: not determined.

Molecular modelling

In order to assess the binding mode of homobivalent chromenopyrazoles **22**, **25** and **27** (10, 12 and 14 methylene units), we docked their most favorable conformation (Figure 4.2) into CB_2R in its active state in such a manner that both pharmacophoric units bind

into the orthosteric and vestibule sites (Figure 4.6A). Unbiased MD simulations show that these chain lengths can simultaneously bind both sites (Figure 4.7). The methylene spacer expands toward the lipid-facing vestibule interacting with the hydrophobic side chains of Phe91$^{2.61}$, Ala282$^{7.36}$, Met286$^{7.40}$, and Val36$^{1.35}$. In the vestibule, the chromenopyrazole moiety forms aromatic-aromatic interactions with Phe283$^{7.37}$. In the simulations Phe283$^{7.37}$ adopts the trans conformation that opens the channel between TMs 1 and 7 and permits the ligand to reach the membrane, in contrast to the *gauche*$^{+}$ conformation observed in the crystal structure of CB_2R [16, 30] that closes the channel. The heptyl chain is accommodated in a hydrophobic cavity of TMs 1 and 7, facing the membrane, which is formed by Leu39$^{1.38}$, Cys40$^{1.39}$, Met286$^{7.40}$, Leu43$^{1.39}$, Ile290$^{7.44}$, Met293$^{7.47}$ and Leu46$^{1.45}$. In the case of the N1-Ethyl derivative the lone pair in the N2 atom forms a hydrogen bond with Gln32$^{1.31}$. A detailed description of these interactions is shown in Figure 4.8.

Figure 4.6B shows the mesh surface formed by Val36$^{1.35}$ and Ala282$^{7.36}$. Clearly, these TMs side chains, which are located midway between the orthosteric site and the receptor vestibule, delimit the channel between TMs 1 and 7. Thus, in order to validate the proposed binding mode of bitopic ligands, Gemma Navarro and Rafael Franco at the Department of Biochemistry and Physiology, Faculty of Pharmacy and Food Sciences, Universitat de Barcelona, Barcelona (Spain) mutated the side chains of Val36$^{1.35}$ (Figure 4.5B) and Ala282$^{7.36}$ (Figure 4.5C) to the much larger Met side chain. As expected, these mutations do not influence the function of the orthosteric agonist CP55,490, but clearly impairs signaling of bitopic ligands **22** and **27** (Table 4.2), by occupying the volume of the channel. Notably, these results contrast with other MD simulations, suggesting the entrance of the ligands from the extracellular environment [31, 32].

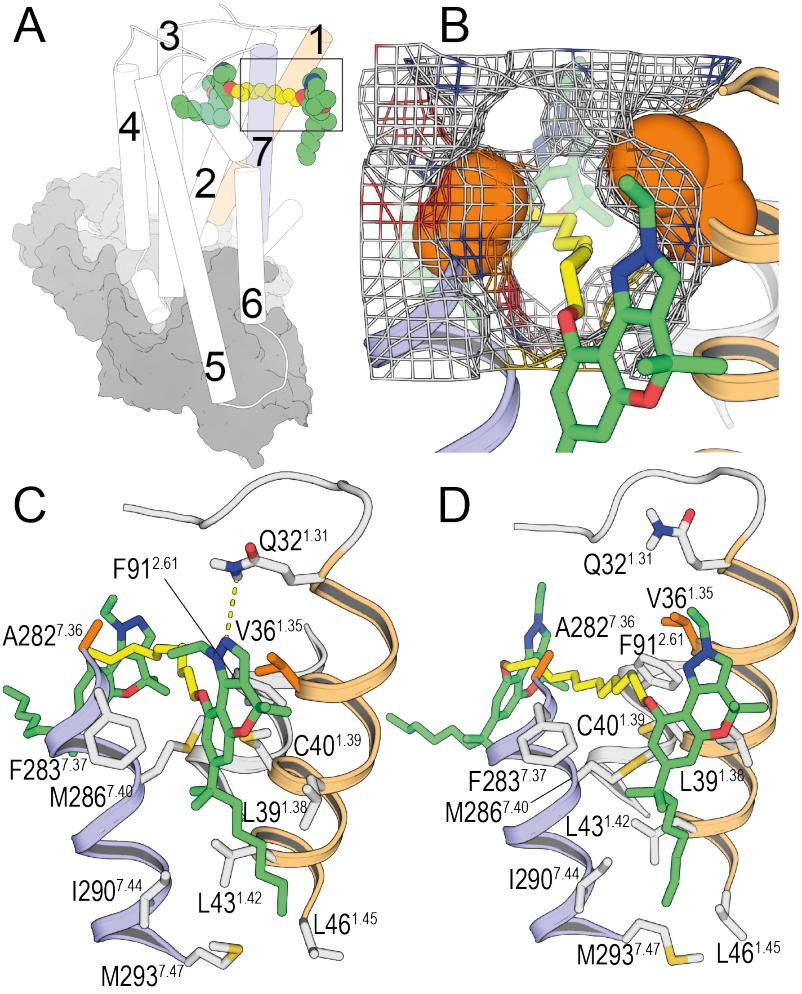

Figure 4.6: (A) General view of the binding mode of bitopic ligand **22** into the orthosteric site and the vestibule of the CB_2R-G_i complex (depicted as cylinders for CB_2R and grey surfaces for G_i) (PDB ID 6PT0 [16]). (B) Mesh surface of Val36$^{1.35}$ and Ala282$^{7.36}$ (spheres in orange) that formed the channel between TMs 1 and 7. (C, D) Detailed views of the binding mode of **22** (C) and **25** (D) into the receptor vestibule obtained during the MD simulations (the longer spacer of **27** permits higher flexibility at the vestibule and some of these interactions are not observed, Figure 4.8). TMs 1 and 7 are shown in orange and blue, respectively; Val36$^{1.35}$ and Ala282$^{7.36}$, which were mutated to Met, are shown in orange; and the pharmacophore units and spacer of bitopic ligands are shown in green and yellow, respectively.

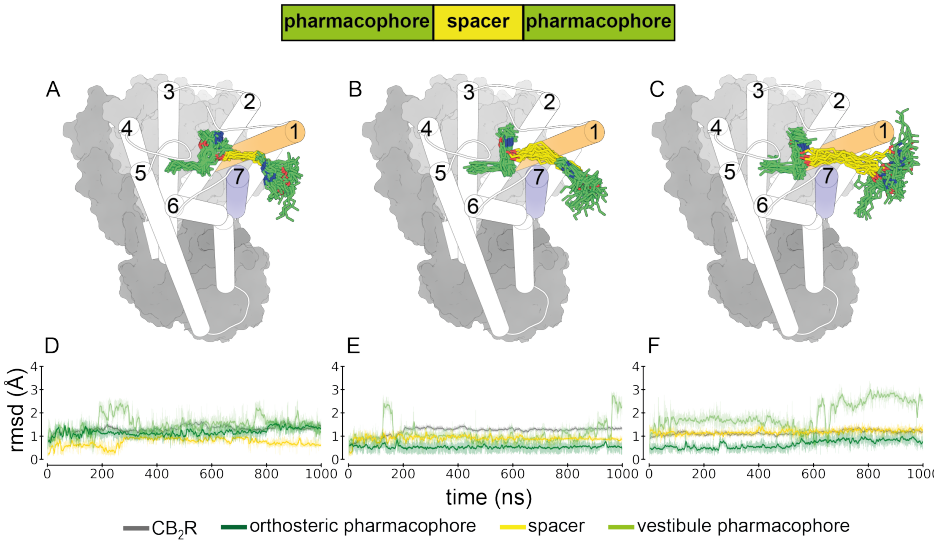

Figure 4.7: Evolution of homobivalent bitopic ligands **22** (A, D), **25** (B, E) and **27** (C, F) as devised from unbiased 1μs MD simulations (see *Chapter 3 Methods* for computational details and Figure 4.2 for their *ab initio* full geometry optimization). One replica is displayed for better visualization although an additional replica showed consistent behavior. The structures of **22**, **25** and **27** are extracted from the simulations (10 structures collected every 100 ns), whereas the structure of CB_2R (TM helices are depicted as cylinders and loops as ribbons) in complex with G_i (α- and βγ-subunits in dark and light gray surfaces, respectively) corresponds to the initial structure (PDB ID 6PT0 [16]). The stabilities of the ligand-receptor complexes are analyzed via root mean-square deviations (rmsd) of the backbone atoms of the TM helices of CB_2R (gray), heavy atoms of the pharmacophore moieties located at the orthosteric (dark green) and vestibule (light green) binding sites, and the spacer (yellow), in panels D, E and F. As expected, rmsd values of the pharmacophore group at the vestibule are larger than those of the orthosteric site due to a more open, less restrictive, binding cavity. Clearly, rmsd values of the pharmacophore group at the vestibule are larger for compound **27** with 14 methylene units (n=12) as spacer than for compounds **22** with 10 methylene units (n=8) or **25** with 12 methylene units (n=10). The longer spacer of **27** permits higher flexibility at the vestibule.

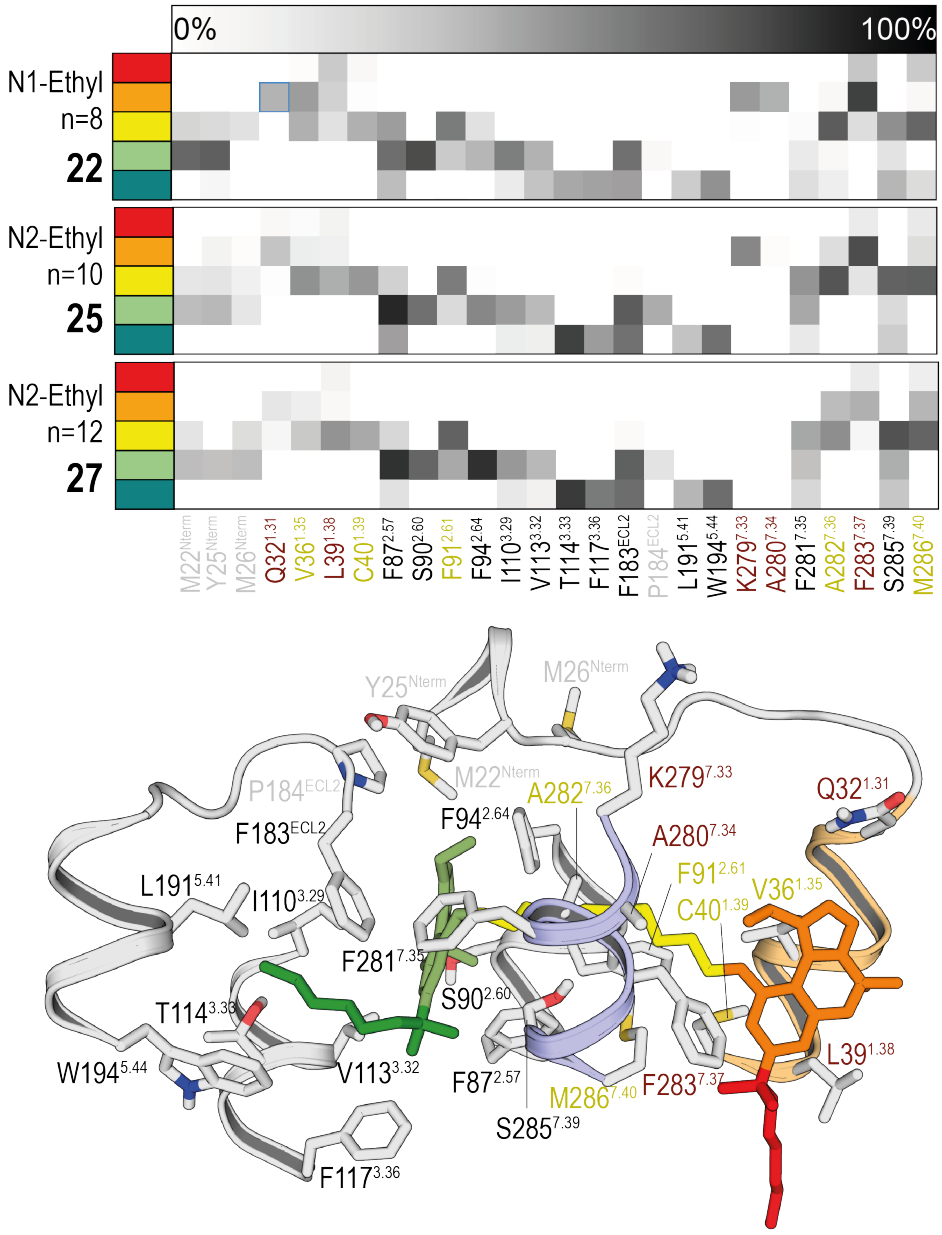

Figure 4.8: Heatmaps depicting the Van der Waals interactions of bitopic ligands **22** (N1-Ethyl, n=8, 10 methylene units), **25** (N2-Ethyl, n=10, 12 methylene units), and **27** (N2-Ethyl, n=12, 14 methylene units) with amino acids of CB_2R (PDB ID 6PT0 [16]). In order to determine the most important residues of CB_2R

that interact with the ligand, the ligand-receptor interactions were quantified during the 6x1μs (two replicas per ligand) of unrestrained MD simulation (see *Chapter 3 Methods* for computational details and Figure 4.7). The interactions were quantified with GetContacts (https://getcontacts.github.io/interactions.html). Average frequencies have been calculated as the mean proportion between replicas of frames in which the interaction occurs, according to GetContacts interaction criteria. Average frequencies of van der Waals interactions are shown using a grey gradient while consistent hydrogen bond interactions are pinpointed with a blue square. The color code for the moieties of the ligand is: the heptyl and chromenopyrazole moieties of the orthosteric pharmacophore in dark and light green, respectively, the spacer in yellow, and the heptyl and chromenopyrazole moieties of the vestibule pharmacophore in red and orange, respectively. The color code for CB_2R is: the amino acids of the orthosteric binding site are labeled in black, the amino acids that interact with the spacer are labeled in yellow, the amino acids of the vestibule binding site are labeled in red, and the amino acids at the extracellular part defining the cavity in gray. A representative model of bitopic ligand **22** and all the side chains of CB_2R (in white sticks) is depicted. TMs 1 and 7 are shown in light orange and blue, respectively.

4.1.3. Conclusions

In summary, we present herein the discovery of CB_2R homobivalent bitopic ligands. These compounds were designed as symmetrical bivalent compounds using the previously reported chromenopyrazole scaffold as potential pharmacophore for both units linked by a methylene spacer. Binding and functional cAMP studies revealed their ability to selectively activate CB_2R versus CB_1R. The longer $Ile^{1.35}$ in CB_1R than $Val^{1.35}$ in CB_2R seems responsible for the observed selectivity (Figure 4.9). MD simulations and site-directed mutagenesis studies show that these bitopic ligands bind into the orthosteric site and in a vestibule/exosite located at the ligands entry/egress channel that connects the orthosteric site with the lipid bilayer membrane. Whether these bitopic ligands at CB_2R show beneficial therapeutic application needs further investigation, such as structure-activity relationship studies to improve potency.

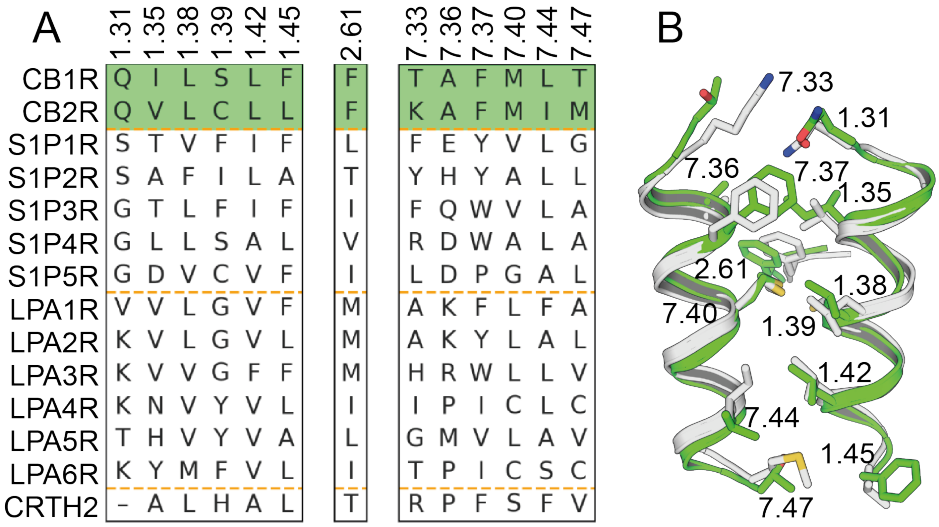

Figure 4.9: (A) Multiple sequence alignment, among CB_1R and CB_2R, the sphingosine-1-phosphate (S1P1R-S1P5R), lysophosphatidic acid (LPA1R-LPA6R) and prostaglandin D_2 (CRTH2) receptors, of the amino acids forming the channel between TMs 1 and 7. (B) Location of these amino acids in the crystal structures of CB_1R-G_i (PDB id 6N4B, in green) and CB_2R-G_i (PDB id 6PT0, in white) complexes. Addition of the second pharmacophore, which interacts with these amino acids, makes bivalent ligands fully selective toward CB_2R (Table 4.1). The major change between CB_1R and CB_2R is at position 7.33 (Thr in CB_1R and Lys in CB_2R), however, this amino acid does not frequently interact with all ligands (Figure 4.8). A minor change is at the key position 1.35 (Figures 4.5-4.6, Table 4.2), the β-branched and very rigid Val side chain in CB_2R, and the likewise β-branched, but longer, Ile in CB_1R. We propose that this additional methyl group of Ile in CB_1R crashes with the bivalent ligand, which explains the observed selectivity.

4.2. Case study 2. Homodimerization of CB_2 cannabinoid receptor triggered by a bivalent ligand enhances cellular signaling

Submitted as co-first author in

Gemma Navarro[1], Marc Gómez-Autet[1], Paula Morales[1], Joan Biel Rebassa, Claudia Llinas del Torrent, Nadine Jagerovic[*], Leonardo Pardo[*], Rafael Franco[*]. **Homodimerization of CB2 cannabinoid receptor triggered by a bivalent ligand enhances cellular signaling.** Submitted.

[1]These authors contributed equally.

4.2.1. Introduction

Understanding the modes of activation of GPCRs from a structural point of view (see *Chapter 1 Introduction*) is essential for deciphering the significance and relevance of the research presented here. In class A GPCRs, endogenous ligands bind to a conserved pocket within the 7TMs of the receptor that optimally accommodates their electrostatic and steric properties [33]. Agonist binding to this extracellular orthosteric site triggers local structural changes, which vary among GPCR families, in the immediate proximity of the highly conserved PIF motif. The agonist-induced arrangement of the PIF side chains is transmitted into larger-scale helix movements at the intracellular site via the highly conserved NPxxY and DRY motifs and Y5.58 [34, 35], so that an intracellular cavity is opened through the outward

movement of TMs 5 and 6 [36]. Opening of this cavity permits the C-terminal α5 helix of G-proteins [37], the finger loop of β-arrestins [38], or the N-terminal αN helix of GPCR kinases [39] to bind the receptor for downstream signaling pathways. The greater efficacy of some extracellular ligands to stimulate a particular transducer is known as ligand bias [40].

The size of a G protein or β-arrestin is larger than the 7TM domain of a GPCR and, despite a monomeric GPCR can activate a G protein [41], it is also feasible a 2:1 (receptor:G protein/arrestin) stoichiometry [42]. Single-molecule microscopy techniques [43] have shown that GPCRs are present in a dynamic equilibrium between monomers, dimers, and tetramers [44–47] (see *Chapter 1 Introduction*). The formation of homo- or hetero-oligomers [48–53] may alter the signaling response compared to receptors expressed individually on the cell surface [48, 49, 53]. In fact, the formation of oligomers can influence G protein or β-arrestin binding [47, 54]. However, the mechanism by which the second protomer of the homodimer modulates the G protein or β-arrestin remain(s) unknown.

Here, we have checked whether the set of compounds described in the previous case study (see section 4.1) can modulate the dynamics of CB_2R homodimerization, as it has been suggested for other bivalent compounds for other GPCRs (e.g. for dopamine D_2-D_2 receptor homodimer [55] and for adenosine A_{2A}-dopamine D_2 receptor heteromer [56]). Importantly, we show that the formation of CB_2R homodimerization promoted by the bivalent ligand provides unique pharmacological properties, such as increased potency in G_i binding and enhanced β-arrestin recruitment. Thus, the research described herein highlights the intricacies of GPCR modulation and presents a novel approach, using homobivalent ligands, to influence the dynamics of GPCR homodimerization and signaling.

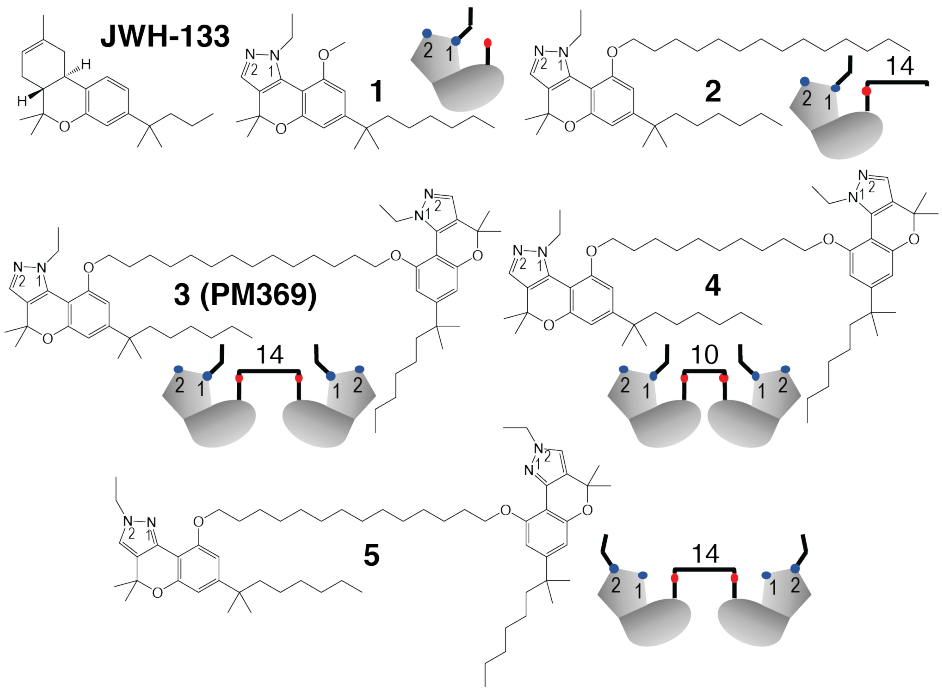

Figure 4.10: Chemical structures and cartoon representations of compounds **3** (PM369), **1**, **2**, **4**, and **5** previously reported by us [6] (section 4.1), and the reference CB_2R agonist JWH-133, used in this manuscript.

4.2.2. Results and discussion

A homobivalent ligand of CB_2R modulates the dynamics of receptor homodimerization

From the computational models (see Figure 4.6) of the compounds (Figure 4.10) described in the previous case study (see section 4.1), we observed that one of the chromenopyrazole pharmacophores was located at the membrane-facing part, thus exposed to a putative second protomer. Taking into account this observation, the group of Gemma Navarro and Rafael Franco at the Department of Biochemistry and Physiology, Faculty of Pharmacy and Food Sciences, Universitat de Barcelona, Barcelona (Spain) tested the ability of these compounds to modulate the dynamics of CB_2R homodimerization. With this aim, they used bioluminescence resonance energy transfer ($BRET^2$) assays in cells expressing CB_2R fused with Renilla luciferase (CB_2R-Rluc) as BRET donor and fused to the GFP^2 green fluorescent protein (CB_2R-GFP^2) as BRET acceptor (see *Chapter 3 Methods*). Homodimers of CB_2R were detected in HEK-293T cells, whereas $GABA_{B1}R$-Rluc, used as a negative control, could not interact with CB_2R-GFP^2 (Figure 4.11A). $BRET^2$ values increased in a statistically significant manner with the treatment of homobivalent ligand PM369 (N1-ethyl with 14 methylene units; structure shown in Figure 4.10), relative to untreated cells, but not in the presence of **1** (a pharmacophore unit; structure shown in Figure 4.10) or **2** (a monovalent compound that lacks the second pharmacophore; structure shown in Figure 4.10), used as negative controls (Figures 4.11C,D). Importantly, the shorter homobivalent N1-ethyl ligand of 10 methylene units (**4**; structure shown in Figure 4.10) did not increase BRET values, suggesting the need for a specific linker size to interact with the second protomer of CB_2R and favor homodimerization. It is also noteworthy that the homobivalent N2-ethyl ligand with 14 methylene units (**5**; structure shown in Figure 4.10) did not increase BRET values (Figure 4.11B). This suggests that the pyrazole ring of the second pharmacophore plays a key role in the recognition of the second protomer of the CB_2R homodimer.

To further test that the increase in CB_2R homodimerization is triggered by the homobivalent ligand PM369, they performed similar experiments in mutant CB_2Rs. They mutated $Val113^{3.32}$, which is centrally located in the orthosteric cavity, and $Val36^{1.35}$, delimiting the channel between TMs 1 and 7, to the much larger Met side chain (Figure 4.11D). Clearly, in the $Val113^{3.32}Met$ mutant, PM369 does not increase BRET signal, indicating that the first pharmacophore must bind the orthosteric site; and the $Val36^{1.35}Met$ mutants does not increase BRET signal either, indicating that the second pharmacophore must bind the membrane-facing pocket between TMs 1 and 7 for CB_2R homodimerization.

Computational model of homobivalent ligand PM369 bound to the CB_2R-CB_2R homodimer in complex with G_i

An inactive CB_2R protomer was added (see *Chapter 3 Methods*) to our previously reported model of the active CB_2R-G_i complex bound to the homobivalent N1-ethyl ligand PM369 with 14 methylene units (see Figure 4.6). We have recently shown that the binding pathway to the orthosteric site of CB_2R consists of the ligand diffusing in the bilayer leaflet to contact a membrane-facing pocket between TMs 1 and 7 that is transiently occupied before entering to the orthosteric binding site through a tunnel formed between TMs 1 and 7 [5]. This membrane-facing binding site of the receptor has probably been evolutionary designed to transiently recognize endogenous cannabinoid that possess long hydrophobic moieties. It is, thus, reasonable to assume, as a working hypothesis, that the second pharmacophore of the bivalent ligand is also recognized by this favorable membrane-facing site between TMs 1 and 7 of the second protomer. Accordingly, in the constructed model (Figure 4.12A), the first chromenopyrazole pharmacophore of homobivalent ligand PM369 binds the orthosteric site of active CB_2R bound to G_i, the 14 methylene units of the spacer expands through the tunnel between TMs 1 and 7 of the active CB_2R-G_i protomer, and the second chromenopyrazole pharmacophore binds the membrane-facing pocket between TMs 1 and 7 of the inactive

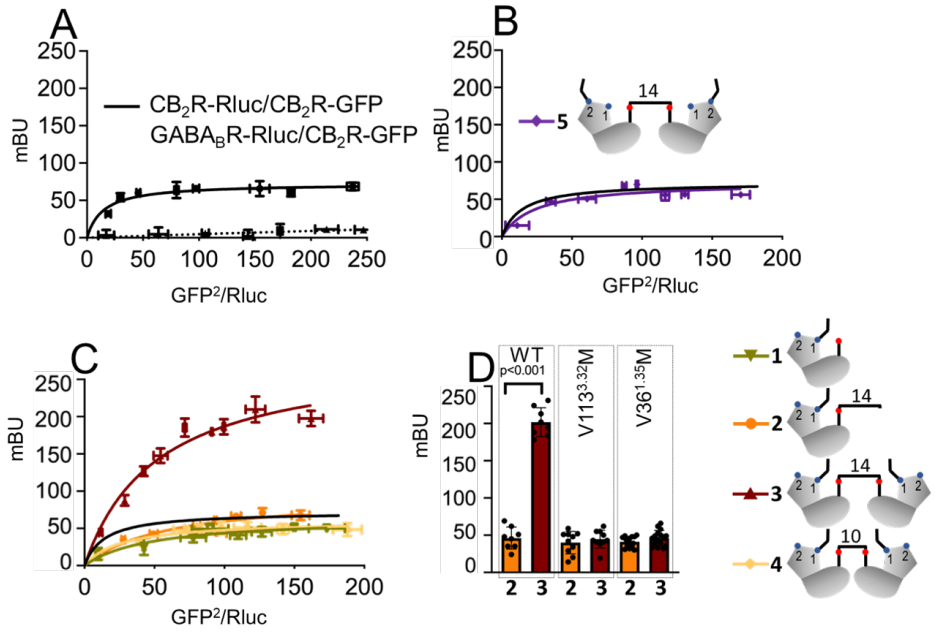

Figure 4.11: Homodimerization of CB_2R in the presence of symmetrical homobivalent ligands. BRET assays were performed in HEK-293T cells transfected with a constant amount of cDNA for CB_2R-Rluc (0.3 µg) (A-C) or $GABA_B$-Rluc (0.5 µg) (as negative control) (A) and increasing amounts of cDNA for CB_2R-GFP^2 (0.05 to 0.6 µg) (A-C). (B, C) Cells were treated with the indicated compounds **3** (PM369), **2**, **4**, **5**, and **1** (100 nM) (see Figure 4.10). (D) Maximal BRET values obtained in HEK-293T cells transfected with a constant amount of cDNA for CB_2R (WT/$Val113^{3.32}$Met/ $Val36^{1.35}$Met)-Rluc (0.3 µg) and increasing amounts of cDNA for CB_2R (WT/$Val113^{3.32}$Met/ $Val36^{1.35}$Met)-GFP^2 (0.05 to 0.6 µg) in the presence of compounds **2** and PM369.

second CB_2R protomer. To evaluate the stability of PM369 in the CB_2R-CB_2R homodimer, we performed unbiased MD simulations (see *Chapter 3 Methods*). Clearly, root-mean square deviations (rmsds) of the heavy atoms of the CB_2R-G_i-bound first pharmacophore (≈1 Å) and the CB_2R-bound second pharmacophore (<2 Å) remained low across three replicas of 1 µs unbiased MD simulation (Figure 4.13), suggesting that both pharmacophores optimally interact with the orthosteric and membrane-facing sites. Likewise, the rmsd values of the extended chain of 14 methylene units are also low (≈1 Å), indicating that the spacer length is optimal to bridge both sites, as determined in BRET assays above (Figure 4.11C). Furthermore, the low rmsd values (<2.5 Å) of the second inactive CB_2R protomer, comparable to the active CB_2R protomer (<2.5 Å), suggest that the initial position modeled through the TM 1/7 interface remains unchanged during the unbiased MD simulation (Figure 4.13). Inward shifts of TMs 1 and 2 have been described during the process of activation of the closely related CB_1R [57]. Thus, we evaluated the influence of homobivalent ligand PM369 in the extracellular conformation of TMs 1, 2 and 7 of both the active CB_2R-G_i and inactive CB_2R protomers (Figure 4.14). The MD simulations show that PM369 does not alter the conformation of TM 2 of either active or inactive CB_2R with respect to apo CB_2R. Notably, inward shifts of TMs 1 (distinctive of the activation process) and 7 are observed in the active protomer, and an outward shift of TM 1 is observed in the inactive protomer. It has been previously shown that the outward conformation of TM 1, driven in this case by an antagonist of $A_{2A}R$, facilitated the formation of the TM 1/7 interface between protomers in the $A_{2A}R$-CB_2R heteromer [58].

Figure 4.12B shows heatmaps of the predicted interactions of the second chromenopyrazole pharmacophore of 3 (PM369) with amino acids of the membrane-facing pocket between TMs 1 and 7 of the inactive CB_2R protomer. A chemical signature of cannabinoid agonists is branched dimethyl moieties that induce receptor activation through hydrophobic interactions with Phe117$^{3.36}$ in the $g+$ conformation and Val261$^{6.51}$ [31, 59]. The pharmacophore group of homobivalent ligand **3** (PM369) contains these branched dimethyl moieties at the chromenopyrazole ring and the heptyl chain close to the aromatic

ring (Figure 4.10). Notably, the membrane-facing site between TMs 1 and 7 contains site 1, delineated by Val36$^{1.35}$ and Ala282$^{7.36}$, to accommodate the dimethyl group of the chromenopyrazole ring and site 2, delineated by Leu39$^{1.38}$ and Met286$^{7.40}$, to accommodate the dimethyl group of the heptyl chain (Figure 4.12B). The highly polarizable sulfur atom of Met can form stronger hydrophobic interactions with methyl groups that aromatic or hydrophobic side chains [60]. Furthermore, this membrane-facing site contains the aromatic Phe283$^{7.37}$ side chain that forms aromatic-aromatic interactions with the aromatic chromenopyrazole ring of the ligand, and the polar Gln32$^{1.31}$ and Lys279$^{7.33}$ that act as hydrogen bond donor in the interaction with the N2 atom of the N1-ethyl isomer of the pyrazole ring. Importantly, the N2-ethyl isomer cannot achieve this key interaction, due to a different orientation of the N1 atom, which explains that homobivalent ligand **5** could not increase BRET values (Figure 4.11B).

Homobivalent ligand PM369 potentiates cellular signaling

The group of Gemma Navarro and Rafael Franco at the Department of Biochemistry and Physiology, Faculty of Pharmacy and Food Sciences, Universitat de Barcelona, Barcelona (Spain) has first compared the agonist-induced response of the chromenopyrazole pharmacophore **1** with JWH-133, a potent and selective CB_2R agonist, both binding exclusively at the orthosteric site. Cells stimulated with forskolin and treated with JWH-133 or compound **1** showed reduced cAMP production, as expected for G_i-coupled receptors (Figure 4.15A). However, the chromenopyrazole **1** is considered a partial agonist referred to JWH-133 due to a decrease of cAMP of less magnitude. Notably, homobivalent ligand PM369 is as efficient as JWH-133 in reducing cAMP production, unlike its corresponding monovalent ligand **2** that lacks the second pharmacophore and is considered as a negative control. Moreover, PM369 left-shifts the dose-response curve by one log unit relative to JWH-133, indicating an increase in potency.

We aim to understand the mechanisms by which the second phar-

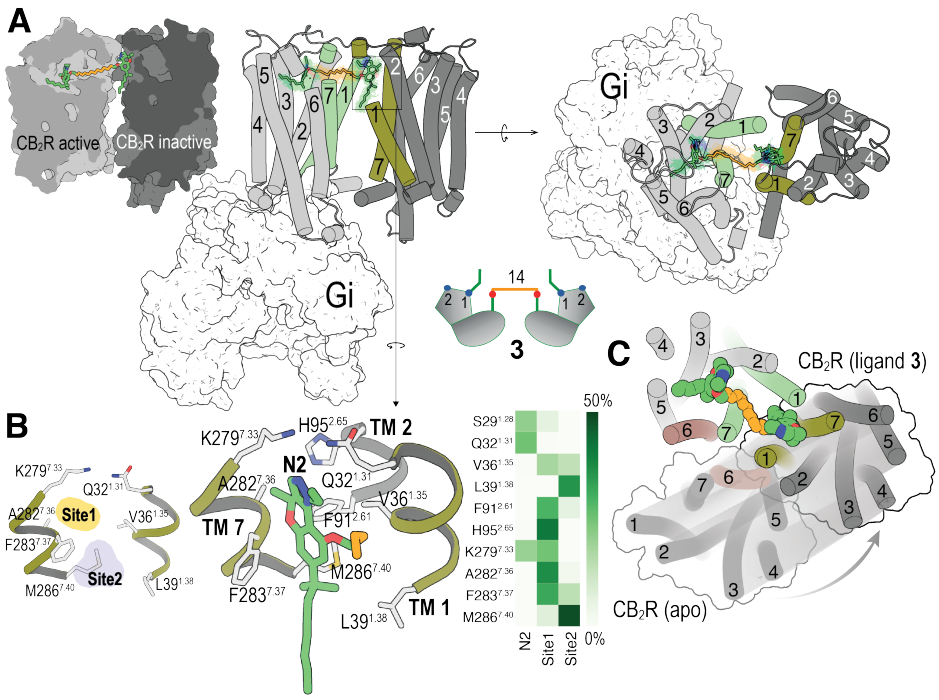

Figure 4.12: Computational model of the CB_2R-CB_2R homodimer in complex with G_i. (A) Cross-section through the CB_2R-CB_2R homodimer, highlighting homobivalent ligand PM369 (color sticks) binding the orthosteric site of active CB_2R and the membrane-facing pocket of inactive CB_2R. A representative structure (color sticks) and 100 structures collected every 10 ns (translucent lines) of homobivalent ligand PM369, as devised from unbiased 1 µs MD simulations in views parallel and perpendicular to the membrane plane. The structure of CB_2R-CB_2R (TM helices are depicted as cylinders) in complex with G_i (white surface) corresponds to the initial structure. One replica is displayed for better visualization although additional replicas showed consistent behavior (Figure 4.13). (B) Detailed views and heatmaps (calculated with GetContacts, https://getcontacts.github.io/interactions.html) depicting the predicted interactions between the aromatic chromenopyrazole ring of PM369 and Phe283$^{7.37}$ of inactive CB_2R protomer, between the N2 atom of the N1-ethyl isomer of the pyrazole ring and Gln32$^{1.31}$ and Lys279$^{7.33}$, and between branched dimethyl moieties at the chromenopyrazole ring and the heptyl chain with Val36$^{1.35}$ and Ala282$^{7.36}$ (site 1), and Leu39$^{1.38}$ and Met286$^{7.40}$ (site 2), respectively. (C) Computational molecular models of the CB_2R-CB_2R homodimer built using the TM 6 interface (in red) for apo (previously determined by BiFC assays in combination with disruptive peptides [58]) and the TM 1/7 interface (in green)

for homobivalent ligand PM369. To facilitate visualization of the dynamic dimerization interface of the CB_2R-CB_2R homodimer, the TM 6 and TM 1/7 interfaces are displayed in the same panel, as well as the geometrical morphing between both conformations.

macophore of PM369 that binds to the membrane-facing pocket between TMs 1 and 7 of the inactive second protomer enhances agonist-induced receptor activation. Previous work using bimolecular fluorescence complementation (BiFC) experiments, in which HEK-293T cells were co-transfected with CB_2Rs separately fused to complementary halves of the yellow fluorescent protein (N-terminal, CB_2R-nYFP; or C-terminal, CB_2R-cYFP), in combination with disruptive peptides targeting a specific dimer interface (see *Chapter 3 Methods*), showed that fluorescence of CB_2R-nYFP/CB_2R-cYFP was mainly reduced by the TM6 peptide of CB_2R with minor, but statistically significant, contributions of TM1, TM5, and TM7 [58]. This suggested that, in the absence of the ligand (apo CB_2R), the CB_2R homodimer is dynamically tuneable, and several dimer interfaces co-exist and interconvert as also described for neurotensin receptor 1 [45]. In a CB_2R-CB_2R homodimer formed through the TM 6 interface, one of the protomers might partially prevent the outward movement of TM 6 of the partner protomer, challenging the opening of the intracellular cavity for receptor activation and G_i binding. Therefore, homobivalent ligand PM369 has two effects in the process of receptor activation. First, binding of the second pharmacophore group to the membrane-facing pocket between TMs 1 and 7 of the inactive second protomer interconverts the CB_2R-CB_2R homodimer from TM 6 to the TM 1/7 interface, facilitating the opening of the intracellular cavity for G protein binding at the partner receptor. Second, binding of the first pharmacophore group to the orthosteric site activates the molecular switches for receptor activation with improved efficacy, like the full agonist JWH-133. The increase in potency is attributed to the multiple contacts of the second pharmacophore with the membrane-facing site between TMs 1 and 7 (Figure 4.12B). Figure 4.12C shows the proposed structure of the CB_2R-CB_2R homodimer bound to the

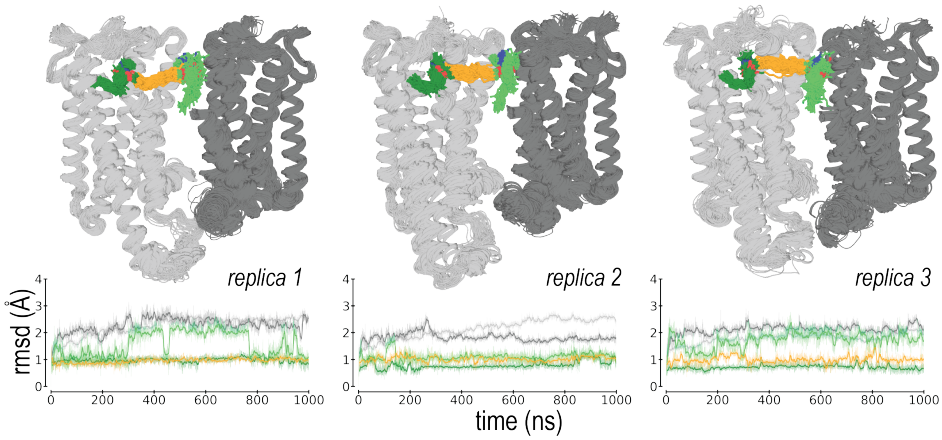

Figure 4.13: Molecular dynamic simulations of the CB_2R-CB_2R homodimer in complex with G_i. Evolution of the first chromenopyrazole pharmacophore (dark green), binding to the orthosteric site of active CB_2R (light gray) bound to G_i (not shown for clarity), the 14 methylene units of the spacer (orange), and the second chromenopyrazole pharmacophore (light green), binding to the membrane-facing pocket of inactive CB_2R (dark gray), of homobivalent ligand PM369 as devised from three replicas of unbiased 1 µs MD simulations. The stabilities of these moieties of PM369 were analyzed via root mean-square deviations (rmsd) of the heavy atoms, and the stabilities of active and inactive CB_2R were analyzed via rmsd of the backbone atoms.

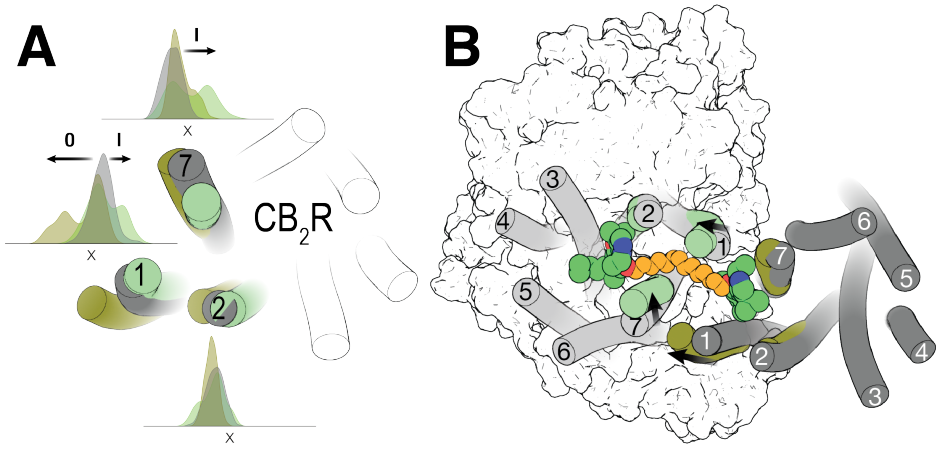

Figure 4.14: Homobivalent ligand PM369 driven rearrangements of TMs 1, 2 and 7. (A) Superimposition of the conformation of TMs 1, 2 and 7 as observed in MD simulations of apo CB_2R (grey), previously performed in [58], and inactive CB_2R (olive) and active CB_2R-G_i (light green) as observed in MD simulations of homobivalent ligand PM369 bound to the CB_2R-CB_2R homodimer in complex with G_i. Distribution of the x-values of the center of mass of the amino acids 1.32-1.35 in TM 1, 2.52-2.55 in TM 2, and 7.31-7.34 in TM 7 of CB_2R during three replicas of unbiased 1 µs MD simulation are shown. Arrows show the most remarkable Inward and Outward movements. The xy plane is as defined by the Orientations of Proteins in Membranes (OPM) [61]. (B) Significant movements (black arrows) of TMs 1 and 7 observed in the MD simulations of homobivalent ligand PM369 bound to the CB_2R-CB_2R homodimer in complex with G_i, relative to their orientation in the initial structure (grey).

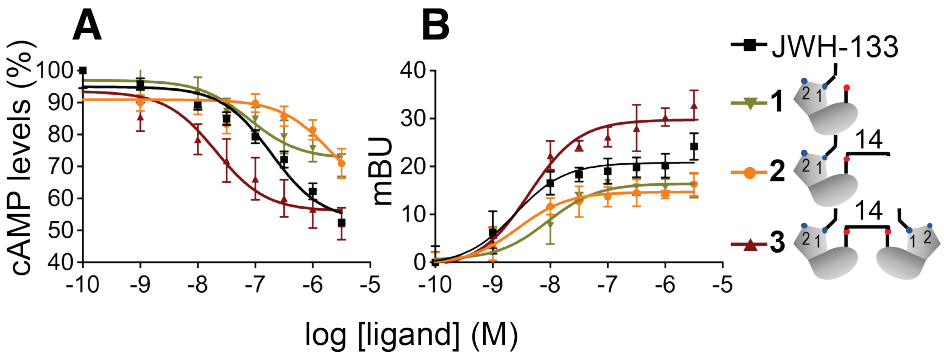

Figure 4.15: Functional characterization of the CB_2R-CB_2R homodimer in transfected HEK-293T cells. (A) cAMP levels were determined in HEK-293T cells transfected with CB_2R (0.5 µg cDNA). (B) β-arrestin 2 recruitment experiments were performed in HEK-293T cells transfected with β-arrestin 2-Rluc (0.5 µg) and CB_2R-YFP (0.5 µg) cDNAs. (A, B) Cells were stimulated with increasing concentrations (0.1 NM to 3 µM) of the full agonist JWH-133 (100 nM) or with compounds **1**, **2**, and PM369. cAMP accumulation was collected upon stimulation with forskolin (Fk, 500 nM).

homobivalent ligand PM369, together with apo CB_2R-CB_2R homodimer, constructed via the TM 6 interface, to facilitate visualization of the dynamic dimerization interfaces of the homodimer. The intracellular cavity, opened upon receptor activation by the outward movement of TM 6, to accommodate the C-terminal α5 helix of the Gα subunit [16], also binds the finger loop of arrestin [62]. Accordingly, homobivalent ligand PM369 should also have a significant effect in β-arrestin-2 recruitment. Like in cAMP measurements, JWH-133 recruited β-arrestin-2 more efficiently than the chromenopyrazole pharmacophore **1** (Figure 4.15B). Surprisingly, PM369 not only improved β-arrestin-2 recruitment relative to chromenopyrazole **1**, but also surpassed the efficacy of the full agonist JWH-133, unlike the corresponding monovalent ligand **2** (negative control). Therefore, the TM 1/7 interface of the CB_2R-CB_2R homodimer, triggered by PM369, facilitates β-arrestin-2 recruitment.

Computational model of the CB_2R-CB_2R homodimer in complex with β-arrestin

To understand the mechanism by which homodimerization via the TM 1/7 interface facilitates β-arrestin-2 recruitment, we constructed a computational model of the CB_2R-CB_2R homodimer bound to β-arrestin-2 (see *Chapter 3 Methods*). Arrestins are organized in a fold consisting of N- and C- domains [63], at whose interface is the finger loop that inserts into the receptor intracellular binding cavity opened with the outward movement of TMs 5 and 6 (Figure 4.16A). Biophysical and structural studies have revealed conformational variability of arrestin while coupled to the receptor [11]. These multiple conformations are shown in Figure 4.16B in which the available GPCR-bound β-arrestin structures are superimposed to the active protomer of the CB_2R-CB_2R homodimer. Two clusters of arrestin orientations can be visually distinguished: the NTS_1R-bound and the V_2R/5-$HT_{2B}R$/β_1R/$CB_1R^{(8WU1)}$/M_2R/$CB_1R^{(8WRZ)}$-bound orientations. Furthermore, a lateral view of the structures forming the later cluster also shows two distinct tilt angles of β-arrestin relative to the bound receptor (Figures 4.16C,D). However, two different groups have recently published the structure of β-arrestin bound to the highly homologous CB_1R. Liao et al. showed that the tilt angle of β-arrestin bound to CB_1R (72^{o}) is like the complexes formed with β_1R (75^{o}) or M_2R receptor (75^{o}) [62] (Figure 4.16C). In contrast, the structure reported by Wang et al. [64] adopts a tilt angle of 46^{o} comparable to the value observed in the complex with V_2R (Figure 4.16D). In these structures the C-domain of β-arrestin is oriented towards the cell membrane, where the C-edge loop acts as a membrane anchor [65]; whereas Lys158 localized at the tip of the N-domain of β-arrestin is facing the inactive protomer of the CB_2R-CB_2R homodimer (Figures 4.16E,F). However, in the 8WRZ structure of Wang et al. Lys158 points towards ICL3 of the inactive protomer (Figure 4.16F), whereas in the 8WU1 structure of Liao et al. Lys158 points towards H8 and it is Arg162 that points towards ICL3 (Figure 4.16E). Unfortunately, the interactions of Lys158 with the inactive CB_2R protomer cannot be assigned non-arbitrarily, as they depend on the modeled conforma-

tion of β-arrestin. However, this analysis supports our proposal that β-arrestin stablishes new contacts with the inactive CB_2R protomer of the CB_2R-CB_2R homodimer in the TM 1/7 interface.

4.2.3. Conclusions

Bitopic and bivalent ligands are single chemical entities composed of two pharmacophore units, covalently linked by an appropriate spacer, that bind the orthosteric site as well as a less conserved site within the same receptor unit or bridge two receptor units [23, 66]. Many of the synthesized bivalent ligands for cannabinoid receptors in particular, and GPCRs in general, contain spacers too short for simultaneous binding of both orthosteric sites of the (homo/hetero)dimer [14, 15]. It has been suggested that these short bivalent ligands might bind the orthosteric pocket of one protomer and a complementary site, different from the orthosteric, of the second protomer [15]. Alternatively, these short ligands can bind to both orthosteric sites of the (homo/hetero)dimer, not simultaneously, but via a 'flip-flop' mechanism or cooperatively [17].

Here, we have tested whether previously reported compounds, formed by equal chromenopyrazole moieties as pharmacophores connected by spacers whose lengths vary from six to sixteen methylene units [6], can modulate the dynamics of CB_2R homodimerization by simultaneously binding both protomers of the CB_2R-CB_2R homodimer. Notably, only homobivalent ligand PM369 with 14 methylene units, but none of the other tested compounds, increased BRET values relative to untreated cells. Computational and experimental results showed that the first chromenopyrazole pharmacophore of PM369 binds the orthosteric site of active CB_2R bound to G_i, the 14 methylene units of the spacer expands through the tunnel between TMs 1 and 7 of the active CB_2R-G_i protomer, and the second chromenopyrazole pharmacophore binds the membrane-facing pocket between TMs 1 and 7 (complementary site) of the inactive second CB_2R protomer. This binding mode of PM369 triggers the formation of the CB_2R-CB_2R homodimer via the TM 1/7 interface. This provides unique pharmacological properties, such as increased potency

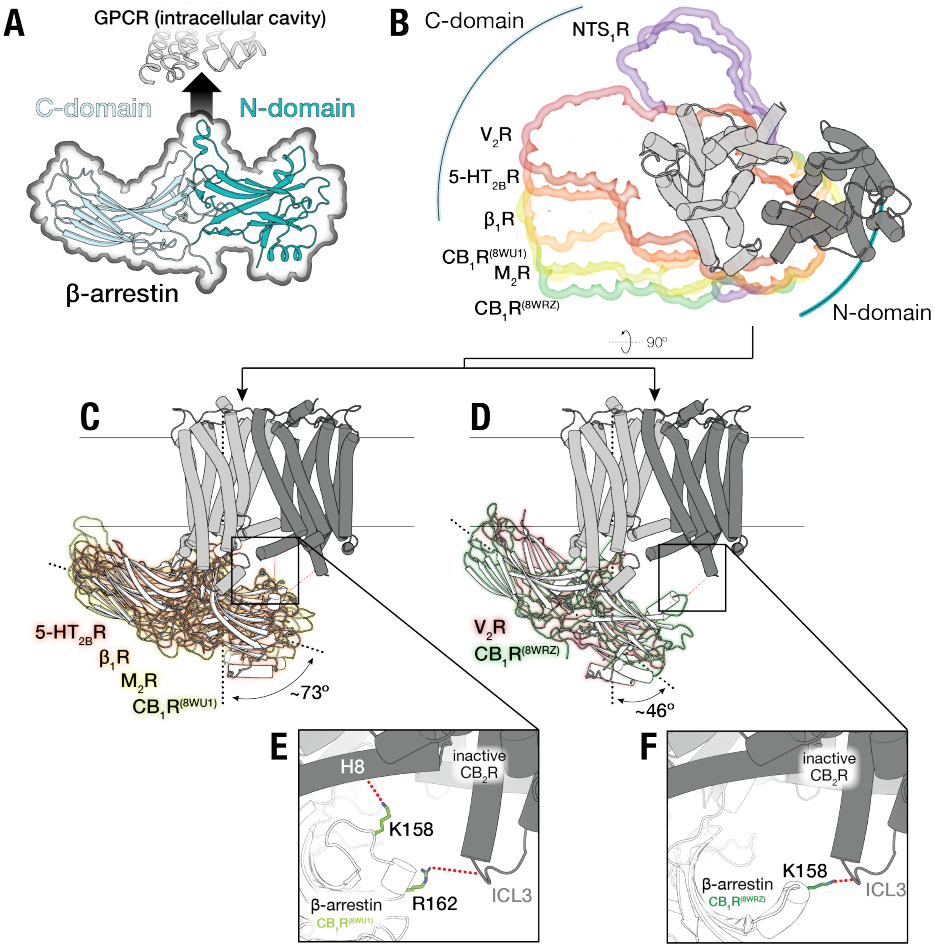

Figure 4.16: Computational model of the CB_2R-CB_2R homodimer in complex with β-arrestin 2. (A) Structure of β-arrestin in a fold consisting of C- and N-domains, in light cyan and teal, respectively, at whose interface is the finger loop that inserts into the receptor intracellular binding cavity. (B) Available GPCR-bound β-arrestin structures [NTS_1R- (PDB IDs 6UP7, 6PWC)/V_2R- (PDB ID 7R0C)/5-$HT_{2B}R$- (PDB ID 7SRS)/β_1R- (PDB ID 6TKO)/M_2R- (PDB ID 6U1N)/CB_1R- (PDB ID 8WU1, 8WRZ) bound) superimposed to the active protomer (light gray) of the CB_2R-CB_2R homodimer. (C, D) Lateral view of GPCR-bound β-arrestin structures showing two distinct tilt angles of β-arrestin relative to the bound receptor. (E, F) Detailed views of the interaction between Lys158 located at the tip of the N-domain of β-arrestin and the inactive CB_2R protomer.

in G_i binding and increased recruitment of β-arrestin. It was previously shown by others that oligomerization of the platelet-activating factor receptor either via TM 1 or TM 4/5 interfaces decreased recruitment of β-arrestin [54]. Therefore, these results suggest that only certain conformation(s) of the homodimer, stabilized in this work by homobivalent ligand PM369, is(are) able to recruit β-arrestin more efficiently.

By promoting homodimerization and altering downstream signaling events, PM369 is explored as a tool to better understand GPCR pharmacology. However, these findings also suggest that PM369 could offer new therapeutic strategies by controlling the signaling pathways mediated by CB_2R. CB_2R plays a crucial role in modulating immune responses and inflammation [67]. Its upregulation under pathological conditions and its association with anti-inflammatory effects highlight the therapeutic potential of targeting CB_2R in various disease states such as autoimmune diseases, neuroinflammation, tissue injury [68, 69]. Altogether, these novel results open new possibilities to control GPCR signaling.

Bibliography

[1] G. Pándy-Szekeres, C. Munk, T. M. Tsonkov, S. Mordalski, K. Harpsøe, A. S. Hauser, A. J. Bojarski, D. E. Gloriam, "GPCRdb in 2018: adding GPCR structure models and ligands", *Nucleic acids research* **2018**, *46*, D440–D446.

[2] M. Audet, R. C. Stevens, "Emerging structural biology of lipid G protein-coupled receptors", *Protein science* **2019**, *28*, 292–304.

[3] N. Stanley, L. Pardo, G. D. Fabritiis, "The pathway of ligand entry from the membrane bilayer to a lipid G protein-coupled receptor", *Scientific Reports* **2016**, *6*, 22639.

[4] L. Wang, D. Yao, R. N. Deepak, H. Liu, Q. Xiao, H. Fan, W. Gong, Z. Wei, C. Zhang, "Structures of the Human PGD2 Receptor CRTH2 Reveal Novel Mechanisms for Ligand Recognition", *Molecular Cell* **2018**, *72*, 48–59.e4.

[5] N. Casajuana-Martin, G. Navarro, A. Gonzalez, C. L. D. Torrent, M. Gómez-Autet, A. Q. García, R. Franco, L. Pardo, "A Single Point Mutation Blocks the Entrance of Ligands to the Cannabinoid CB2Receptor via the Lipid Bilayer", *Journal of Chemical Information and Modeling* **2022**, *62*, 5771–5779.

[6] P. Morales, G. Navarro, M. Gómez-Autet, L. Redondo, J. Fernández-Ruiz, L. Pérez-Benito, A. Cordomí, L. Pardo, R. Franco, N. Jagerovic, "Discovery of Homobivalent Bitopic Ligands of the Cannabinoid CB2 Receptor", *Chemistry - A European Journal* **2020**, *26*, 15839–15842.

[7] G. Navarro, A. Gonzalez, A. Sánchez-Morales, N. Casajuana-Martin, M. Gómez-Ventura, A. Cordomí, F. Busqué, R. Alibés, L. Pardo, R. Franco, "Design of Negative and Positive Allosteric Modulators of the Cannabinoid CB2Receptor Derived from the Natural Product Cannabidiol", *Journal of Medicinal Chemistry* **2021**, *64*, 9354–9364.

[8] B. Stauch, L. C. Johansson, J. D. McCorvy, N. Patel, G. W. Han, X. P. Huang, C. Gati, A. Batyuk, S. T. Slocum, A. Ishchenko, W. Brehm, T. A. White, N. Michaelian, C. Madsen, L. Zhu, T. D. Grant, J. M. Grandner, A. Shiriaeva, R. H. Olsen, A. R. Tribo, S. Yous, R. C. Stevens, U. Weierstall, V. Katritch, B. L. Roth, W. Liu, V. Cherezov, "Structural basis of ligand recognition at the human MT1 melatonin receptor", *Nature* **2019**, *569*, 284–288.

[9] A. Dhopeshwarkar, K. Mackie, "CB2 Cannabinoid receptors as a therapeutic target-what does the future hold?", *Molecular pharmacology* **2014**, *86*, 430–437.

[10] Y. Zhang, A. Gilliam, R. Maitra, M. I. Damaj, J. M. Tajuba, H. H. Seltzman, B. F. Thomas, "Synthesis and biological evaluation of bivalent ligands for the cannabinoid 1 receptor", *Journal of medicinal chemistry* **2010**, *53*, 7048–7060.

[11] C. Fernández-Fernández, J. Decara, F. J. Bermúdez-Silva, E. Sánchez, P. Morales, M. Gõmez-Cañas, M. Gõmez-Ruíz, L. F. Callado, P. Goya, F. R. D. Fonseca, M. I. Martín, J. Fernández-Ruíz, J. J. Meana, N. Jagerovic, "Description of a bivalent cannabinoid ligand with hypophagic properties", *Archiv der Pharmazie* **2013**, *346*, 171–179.

[12] G. Huang, D. Pemp, P. Stadtmüller, M. Nimczick, J. Heilmann, M. Decker, "Design, synthesis and in vitro evaluation of novel uni- and bivalent ligands for the cannabinoid receptor type 1 with variation of spacer length and structure", *Bioorganic & medicinal chemistry letters* **2014**, *24*, 4209–4214.

[13] M. Nimczick, D. Pemp, F. H. Darras, X. Chen, J. Heilmann, M. Decker, "Synthesis and biological evaluation of bivalent cannabinoid receptor ligands based on hCB2R selective benzimidazoles reveal unexpected intrinsic properties", *Bioorganic & medicinal chemistry* **2014**, *22*, 3938–3946.

[14] M. Glass, K. Govindpani, D. P. Furkert, D. P. Hurst, P. H. Reggio, J. U. Flanagan, "One for the Price of Two...Are Bivalent Ligands Targeting Cannabinoid Receptor Dimers Capable of Simultaneously Binding to both Receptors?", *Trends in Pharmacological Sciences* **2016**, *37*, 353–363.

[15] L. Pérez-Benito, A. Henry, M. T. Matsoukas, L. Lopez, D. Pulido, M. Royo, A. Cordomí, G. Tresadern, L. Pardo, "The size matters? A computational tool to design bivalent ligands", *Bioinformatics* **2018**, *34*, 3857–3863.

[16] C. Xing, Y. Zhuang, T. H. Xu, Z. Feng, X. E. Zhou, M. Chen, L. Wang, X. Meng, Y. Xue, J. Wang, H. Liu, T. F. McGuire, G. Zhao, K. Melcher, C. Zhang, H. E. Xu, X. Q. Xie, "Cryo-EM Structure of the Human Cannabinoid Receptor CB2-Gi Signaling Complex", *Cell* **2020**, *180*, 645–654.e13.

[17] J. R. Lane, P. M. Sexton, A. Christopoulos, "Bridging the gap: Bitopic ligands of G-protein-coupled receptors", *Trends in Pharmacological Sciences* **2013**, *34*, 59–66.

[18] K. Mohr, J. Schmitz, R. Schrage, C. Tränkle, U. Holzgrabe, "Molecular alliance-from orthosteric and allosteric ligands to dualsteric/bitopic agonists at G protein coupled receptors", *Angewandte Chemie* **2013**, *52*, 508–516.

[19] S. J. Bradley, A. B. Tobin, "Design of Next-Generation G Protein-Coupled Receptor Drugs: Linking Novel Pharmacology and In Vivo Animal Models", *Annual review of pharmacology and toxicology* **2016**, *56*, 535–559.

[20] R. O. Dror, A. C. Pan, D. H. Arlow, D. W. Borhani, P. Maragakis, Y. Shan, H. Xu, D. E. Shaw, "Pathway and mechanism of drug binding to G-protein-coupled receptors", *Proceedings of the National Academy of Sciences of the United States of America* **2011**, *108*, 13118–13123.

[21] C. Wang, Y. Jiang, J. Ma, H. Wu, D. Wacker, V. Katritch, G. W. Han, W. Liu, X. P. Huang, E. Vardy, J. D. McCorvy, X. Gao, X. E. Zhou, K. Melcher, C. Zhang, F. Bai, H. Yang, L. Yang, H. Jiang, B. L. Roth, V. Cherezov, R. C. Stevens, H. E. Xu, "Structural basis for molecular recognition at serotonin receptors", *Science (New York N.Y.)* **2013**, *340*, 610–614.

[22] A. González, T. Perez-Acle, L. Pardo, X. Deupi, "Molecular basis of ligand dissociation in β-adrenergic receptors", *PloS one* **2011**, *6*.

[23] P. Fronik, B. I. Gaiser, D. S. Pedersen, "Bitopic Ligands and Metastable Binding Sites: Opportunities for G Protein-Coupled Receptor (GPCR) Medicinal Chemistry", *Journal of Medicinal Chemistry* **2017**, *60*, 4126–4134.

[24] M. Masureel, Y. Zou, L. P. Picard, E. van der Westhuizen, J. P. Mahoney, J. P. Rodrigues, T. J. Mildorf, R. O. Dror, D. E. Shaw, M. Bouvier, E. Pardon, J. Steyaert, R. K. Sunahara, W. I. Weis, C. Zhang, B. K. Kobilka, "Structural insights into binding specificity, efficacy and bias of a β 2 AR partial agonist", *Nature Chemical Biology* **2018**, *14*, 1059–1066.

[25] R. A. Medina, H. Vázquez-Villa, J. C. Gómez-Tamayo, B. Benhamú, M. Martín-Fontecha, T. D. L. Fuente, G. Caltabiano, P. B. Hedlund, L. Pardo, M. L. López-Rodríguez, "The extracellular entrance provides selectivity to serotonin 5-HT 7 receptor antagonists with antidepressant-like behavior in vivo", *Journal of Medicinal Chemistry* **2014**, *57*, 6879–6884.

[26] C. Valant, J. R. Lane, P. M. Sexton, A. Christopoulos, "The best of both worlds? Bitopic orthosteric/allosteric ligands of g protein-coupled receptors", *Annual review of pharmacology and toxicology* **2012**, *52*, 153–178.

[27] B. I. Gaiser, M. Danielsen, E. Marcher-Rørsted, K. R. Jørgensen, T. M. Wróbel, M. Frykman, H. Johansson, H. Bräuner-Osborne, D. E. Gloriam, J. M. Mathiesen, D. S. Pedersen, "Probing the Existence of a Metastable Binding Site at the β2-Adrenergic Receptor with Homobivalent Bitopic Ligands", *Journal of medicinal chemistry* **2019**, *62*, 7806–7839.

[28] L. Tan, Q. Zhou, W. Yan, J. Sun, A. P. Kozikowski, S. Zhao, X. P. Huang, J. Cheng, "Design and Synthesis of Bitopic 2-Phenylcyclopropylmethylamine (PCPMA) Derivatives as Selective Dopamine D3 Receptor Ligands", *Journal of medicinal chemistry* **2020**, *63*, 4579–4602.

[29] P. Morales, M. Gómez-Cañas, G. Navarro, D. P. Hurst, F. J. Carrillo-Salinas, L. Lagartera, R. Pazos, P. Goya, P. H. Reggio, C. Guaza, R. Franco, J. Fernández-Ruiz, N. Jagerovic, "Chromenopyrazole, a Versatile Cannabinoid Scaffold with in Vivo Activity in a Model of Multiple Sclerosis.", *Journal of medicinal chemistry* **2016**, *59*, 6753–6771.

[30] X. Li, T. Hua, K. Vemuri, J. H. Ho, Y. Wu, L. Wu, P. Popov, O. Benchama, N. Zvonok, K. Locke, L. Qu, G. W. Han, M. R. Iyer, R. Cinar, N. J. Coffey, J. Wang, M. Wu, V. Katritch, S. Zhao, G. Kunos, L. M. Bohn, A. Makriyannis, R. C. Stevens, Z. J. Liu, "Crystal Structure of the Human Cannabinoid Receptor CB2", *Cell* **2019**, *176*, 459–467.e13.

[31] T. Hua, X. Li, L. Wu, C. Iliopoulos-Tsoutsouvas, Y. Wang, M. Wu, L. Shen, C. A. Brust, S. P. Nikas, F. Song, X. Song, S. Yuan, Q. Sun, Y. Wu, S. Jiang, T. W. Grim, O. Benchama, E. L. Stahl, N. Zvonok, S. Zhao, L. M. Bohn, A. Makriyannis, Z. J. Liu, "Activation and Signaling Mechanism Revealed by Cannabinoid Receptor-Gi Complex Structures", *Cell* **2020**, *180*, 655–665.e18.

[32] N. Saleh, O. Hucke, G. Kramer, E. Schmidt, F. Montel, R. Lipinski, B. Ferger, T. Clark, P. W. Hildebrand, C. S. Tautermann, "Multiple Binding Sites Contribute to the Mechanism of Mixed Agonistic and Positive Allosteric Modulators of the Cannabinoid CB1 Receptor", *Angewandte Chemie* **2018**, *57*, 2580–2585.

[33] A. J. Venkatakrishnan, X. Deupi, G. Lebon, C. G. Tate, G. F. Schertler, M. M. Babu, "Molecular signatures of G-protein-coupled receptors", *Nature* **2013**, *494*, 185–194.

[34] W. I. Weis, B. K. Kobilka, "The Molecular Basis of G Protein–Coupled Receptor Activation", *Annual Review of Biochemistry* **2018**, *87*, 897–919.

[35] Q. Zhou, D. Yang, M. Wu, Y. Guo, W. Guo, L. Zhong, X. Cai, A. Dai, W. Jang, E. Shakhnovich, Z. J. Liu, R. C. Stevens, N. A. Lambert, M. M. Babu, M. W. Wang, S. Zhao, "Common activation mechanism of class a GPCRs", *eLife* **2019**, *8*, 1–31.

[36] J. H. Park, P. Scheerer, K. P. Hofmann, H. W. Choe, O. P. Ernst, "Crystal structure of the ligand-free G-protein-coupled receptor opsin", *Nature* **2008**, *454*, 183–187.

[37] S. G. F. Rasmussen, B. T. DeVree, Y. Zou, A. C. Kruse, K. Y. Chung, T. S. Kobilka, F. S. Thian, P. S. Chae, E. Pardon, D. Calinski, J. M. Mathiesen, S. T. a Shah, J. a Lyons, M. Caffrey, S. H. Gellman, J. Steyaert, G. Skiniotis, W. I. Weis, R. K. Sunahara, B. K. Kobilka, "Crystal structure of the β2 adrenergic receptor-Gs protein complex.", *Nature* **2011**, *477*, 549–55.

[38] W. Huang, M. Masureel, Q. Qu, J. Janetzko, A. Inoue, H. E. Kato, M. J. Robertson, K. C. Nguyen, J. S. Glenn, G. Skiniotis, B. K. Kobilka, "Structure of the neurotensin receptor 1 in complex with β-arrestin 1", *Nature* **2020**, *579*, 303–308.

[39] Q. Chen, M. Plasencia, Z. Li, S. Mukherjee, D. Patra, C. L. Chen, T. Klose, X. Q. Yao, A. A. Kossiakoff, L. Chang, P. C. Andrews, J. J. Tesmer, "Structures of rhodopsin in complex with G-protein-coupled receptor kinase 1", *Nature* **2021**, *595*, 600–605.

[40] P. Kolb, T. Kenakin, S. P. Alexander, M. Bermudez, L. M. Bohn, C. S. Breinholt, M. Bouvier, S. J. Hill, E. Kostenis, K. A. Martemyanov, R. R. Neubig, H. O. Onaran, S. Rajagopal, B. L. Roth, J. Selent, A. K. Shukla, M. E. Sommer, D. E. Gloriam, "Community guidelines for GPCR ligand bias: IUPHAR review 32", *British Journal of Pharmacology* **2022**, *179*, 3651–3674.

[41] M. R. Whorton, M. P. Bokoch, S. G. Rasmussen, B. Huang, R. N. Zare, B. Kobilka, R. K. Sunahara, "A monomeric G protein-coupled receptor isolated in a high-density lipoprotein particle efficiently activates its G protein", *Proceedings of the National Academy of Sciences of the United States of America* **2007**, *104*, 7682–7687.

[42] R. Franco, A. Cordomí, C. L. del Torrent, A. Lillo, J. Serrano-Marín, G. Navarro, L. Pardo, "Structure and function of adenosine receptor heteromers", *Cellular and Molecular Life Sciences* **2021**, *78*, 3957–3968.

[43] J. H. Felce, S. J. Davis, D. Klenerman, "Single-Molecule Analysis of G Protein-Coupled Receptor Stoichiometry: Approaches and Limitations", *Trends in Pharmacological Sciences* **2018**, *39*, 96–108.

[44] G. Navarro, A. Cordomí, M. Zelman-Femiak, M. Brugarolas, E. Moreno, D. Aguinaga, L. Perez-Benito, A. Cortés, V. Casadó, J. Mallol, E. I. Canela, C. Lluís, L. Pardo, A. J. García-Sáez, P. J. McCormick, R. Franco, "Quaternary structure of a G-protein-coupled receptor heterotetramer in complex with Gi and Gs", *BMC Biology* **2016**, *14*, 1–12.

[45] P. M. Dijkman, O. K. Castell, A. D. Goddard, J. C. Munoz-Garcia, C. D. Graaf, M. I. Wallace, A. Watts, "Dynamic tuneable G protein-coupled receptor monomer-dimer populations", *Nature Communications* **2018**, *9*, 1710.

[46] J. Möller, A. Isbilir, T. Sungkaworn, B. Osberg, C. Karathanasis, V. Sunkara, E. O. Grushevskyi, A. Bock, P. Annibale, M. Heilemann, C. Schütte, M. J. Lohse, "Single-molecule analysis reveals agonist-specific dimer formation of μ-opioid receptors", *Nature Chemical Biology* **2020**, *16*, 946–954.

[47] P. A. D. Oliveira, E. Moreno, N. Casajuana-Martin, V. Casadó-Anguera, N. S. Cai, G. A. Camacho-Hernandez, H. Zhu, A. Bonifazi, M. D. Hall, D. Weinshenker, A. H. Newman, D. E. Logothetis, V. Casadó, L. D. Plant, L. Pardo, S. Ferré, "Preferential Gs protein coupling of the galanin Gal1 receptor in the μ-opioid-Gal1 receptor heterotetramer", *Pharmacological Research* **2022**, *182*, 106322.

[48] I. Raïch, J. B. Rebassa, J. Lillo, A. Cordomi, R. Rivas-Santisteban, A. Lillo, I. Reyes-Resina, R. Franco, G. Navarro, "Antagonization of OX1 Receptor Potentiates CB2 Receptor Function in Microglia from APPSw/Ind Mice Model", *International Journal of Molecular Sciences* **2022**, *23*, 1–19.

[49] J. Lillo, I. Raïch, L. Silva, D. A. Zafra, A. Lillo, C. Ferreiro-Vera, V. S. de Medina, J. Martínez-Orgado, R. Franco, G. Navarro, "Regulation of Expression of Cannabinoid CB2 and Serotonin 5HT1A Receptor Complexes by Cannabinoids in Animal Models of Hypoxia and in Oxygen/Glucose-Deprived Neurons", *International Journal of Molecular Sciences* **2022**, *23*.

[50] A. Lillo, J. Lillo, I. Raïch, C. Miralpeix, F. Dosrius, R. Franco, G. Navarro, "Ghrelin and Cannabinoid Functional Interactions Mediated by Ghrelin/CB1 Receptor Heteromers That Are Upregulated in the Striatum From Offspring of Mice Under a High-Fat Diet", *Frontiers in Cellular Neuroscience* **2021**, *15*, 1–12.

[51] E. Martínez-Pinilla, A. J. Rico, R. Rivas-Santisteban, J. Lillo, E. Roda, G. Navarro, J. L. Lanciego, R. Franco, "Expression of GPR55 and either cannabinoid CB1 or CB2 heteroreceptor complexes in the caudate, putamen, and accumbens nuclei of control, parkinsonian, and dyskinetic non-human primates", *Brain Structure and Function* **2020**, *225*, 2153–2164.

[52] I. Reyes-Resina, G. Navarro, D. Aguinaga, E. I. Canela, C. T. Schoeder, M. Załuski, K. Kieć-Kononowicz, C. A. Saura, C. E. Müller, R. Franco, "Molecular and functional interaction between GPR18 and cannabinoid CB2G-protein-coupled receptors. Relevance in neurodegenerative diseases", *Biochemical Pharmacology* **2018**.

[53] G. Navarro, J. Jiménez, J. Martínez-Orgado, M. Villa, A. Gutiérrez-Rodríguez, R. Franco, N. Jagerovic, P. Morales, I. Reyes-Resina, "Increased expression of cannabinoid CB2 and serotonin 5-HT1A heteroreceptor complexes in a model of newborn hypoxic-ischemic brain damage", *Neuropharmacology* **2019**, *152*, 58–66.

[54] J. Liu, H. Tang, C. Xu, S. Zhou, X. Zhu, Y. Li, L. Prézeau, T. Xu, J. P. Pin, P. Rondard, W. Ji, J. Liu, "Biased signaling due to oligomerization of the G protein-coupled platelet-activating factor receptor", *Nature Communications* **2022**, *13*.

[55] T. Ullmann, M. Gienger, J. Budzinski, J. Hellmann, H. Hübner, P. Gmeiner, D. Weikert, "Homobivalent Dopamine D2Receptor Ligands Modulate the Dynamic Equilibrium of D2Monomers and Homo- And Heterodimers", *ACS Chemical Biology* **2021**, *16*, 371–379.

[56] D. Pulido, V. Casadó-Anguera, M. Gómez-Autet, N. Llopart, E. Moreno, N. Casajuana-Martin, S. Ferré, L. Pardo, V. Casadó, M. Royo, "Heterobivalent Ligand for the Adenosine A2A-Dopamine D2Receptor Heteromer", *Journal of Medicinal Chemistry* **2022**, *65*, 616–632.

[57] K. K. Kumar, M. J. Robertson, E. Thadhani, H. Wang, C. M. Suomivuori, A. S. Powers, L. Ji, S. P. Nikas, R. O. Dror, A. Inoue, A. Makriyannis, G. Skiniotis, B. Kobilka, "Structural basis for activation of CB1 by an endocannabinoid analog", *Nature Communications* **2023**, *14*, 1–11.

[58] C. D. Torrent, I. Raïch, A. Gonzalez, J. Lillo, N. Casajuana-Martin, R. Franco, L. Pardo, G. Navarro, "Allosterism in the adenosine A2A and cannabinoid CB2 heteromer", *British Journal of Pharmacology* **in press**.

[59] C. L. del Torrent, I. Raïch, A. Gonzalez, N. Casajuana-Martin, J. Lillo, J. B. Rebassa, C. Ferreiro-Vera, V. S. de Medina, R. Franco, G. Navarro, L. Pardo, "The Leu/Val6.51 Side Chain of Cannabinoid Receptors Regulates the Binding Mode of the Alkyl Chain of Δ9-Tetrahydrocannabinol", *Journal of Chemical Information and Modeling* **2023**, *63*, 5927–5935.

[60] J. C. Gómez-Tamayo, A. Cordomí, M. Olivella, E. Mayol, D. Fourmy, L. Pardo, "Analysis of the interactions of sulfur-containing amino acids in membrane proteins", *Protein Science* **2016**, *25*, 1517–1524.

[61] M. A. Lomize, I. D. Pogozheva, H. Joo, H. I. Mosberg, A. L. Lomize, "OPM database and PPM web server: resources for positioning of proteins in membranes.", *Nucleic acids research* **2012**, *40*, D370–6.

[62] Y. Y. Liao, H. Zhang, Q. Shen, C. Cai, Y. Ding, D. D. Shen, J. Guo, J. Qin, Y. Dong, Y. Zhang, X. M. Li, "Snapshot of the cannabinoid receptor 1-arrestin complex unravels the biased signaling mechanism", *Cell* **2023**, *186*, 5784–5797.e17.

[63] J. Granzin, U. Wilden, H. W. Choe, J. Labahn, B. Krafft, G. Buldt, "X-ray crystal structure of arrestin from bovine rod outer segments", *Nature* **1998**, *391*, 918–921.

[64] Y. Wang, L. Wu, T. Wang, J. Liu, F. Li, L. Jiang, Z. Fan, Y. Yu, N. Chen, Q. Sun, Q. Tan, T. Hua, Z. J. Liu, "Cryo-EM structure of cannabinoid receptor CB1-β-arrestin complex", *Protein & cell* **2024**, *15*, 230–234.

[65] C. C. Lally, B. Bauer, J. Selent, M. E. Sommer, "C-edge loops of arrestin function as a membrane anchor", *Nature communications* **2017**, *8*.

[66] A. H. Newman, F. O. Battiti, A. Bonifazi, "2016 Philip S. Portoghese Medicinal Chemistry Lectureship: Designing Bivalent or Bitopic Molecules for G-Protein Coupled Receptors. The Whole Is Greater Than the Sum of Its Parts", *Journal of Medicinal Chemistry* **2020**, *63*, 1779–1797.

[67] D. Piomelli, A. M. Tagne, "Endocannabinoid-Based Therapies", *Annual Review of Pharmacology and Toxicology* **2022**, *62*, 483–507.

[68] M. Maccarrone, V. D. Marzo, J. Gertsch, U. Grether, A. C. Howlett, T. Hua, A. Makriyannis, D. Piomelli, N. Ueda, M. van der Stelt, *Goods and Bads of the Endocannabinoid System as a Therapeutic Target: Lessons Learned after 30 Years*, *Vol. 75*, **2023**, pp. 885–958.

[69] V. Gasperi, T. Guzzo, A. Topai, N. Gambacorta, F. Ciriaco, O. Nicolotti, M. Maccarrone, "Recent Advances on Type-2 Cannabinoid (CB2) Receptor Agonists and their Therapeutic Potential", *Current Medicinal Chemistry* **2023**, *30*, 1420–1457.

Chapter 5

Designing heterobivalent ligands for the dopamine D_1-histamine H_3 heteromer

Both the dopamine D_1-receptor (D_1R) and the histamine H_3-receptor (H_3R) are class A GPCRs [1, 2]. The D_1R is one of five dopamine receptors and part of the subfamily of the D_1-like receptors [3, 4]. It's widely expressed in the central nervous system (CNS) and is coupled to a $G\alpha_s$ protein and therefore activates the adenylyl cyclase [2, 5]. The dopamine receptors are involved in a variety of physiological processes such as voluntary movement, feeding, affect, reward, sleep, attention, working memory, and learning and therefore drug targets for diseases such as schizophrenia, Parkinson's disease (PD), bipolar disorder, and others [2, 4, 6–9]. The H_3R is one of four histamine receptors coupled to $G\alpha_{i/o}$ proteins and almost exclusively expressed in the CNS [10, 11]. Despite being related to different diseases such as Parkinson's, Huntington's and Alzheimers disease (AD), the only FDA approved drug targeting the H_3R on the market is pitolisant for the treatment of narcolepsy [12–16].

In the recent decades the existence of numerous homo- and heteromeric GPCR dimers and oligomers have been proven using a variety of biochemical and biophysical methods including co-immunoprecipitation, fluorescence-based techniques, proximity-

ligation assays, and functional complementation studies [17–19]. Signaling, ligand-binding, and trafficking properties of a receptor can change dramatically due to dimerization, indicating that the receptor complexes have to be considered as a distinct pharmacological entity [17, 20].

The D_1R and H_3R were reported to form heteromers *in vitro* and *in vivo*. Moreover, it forms a macromolecular complex with NMDA-receptor subunits, which presented neuroprotective effects upon inhibition. Interest in the D_1R-H_3R heteromer has risen as a potential drug target for Alzheimer's disease and Huntington's disease. We herein report the synthesis of a set of novel bivalent ligands targeting this heteromer, containing different pharmacophores and spacers.

5.1. Case study 3. High affinity bivalent ligands targeting the dopamine D_1-histamine H_3 heteromer reduce β-amyloid-induced neuronal cell death

To be submitted as

Niklas Rosier, Denise Mönnich, Marc Gómez-Autet, Lisa Forster, Martin Nagl, Lukas Grätz, Iu Raich, Jaume Lillo, Irene Reyes-Resina, Gemma Navarro, Leonardo Pardo, Rafael Franco, Steffen Pockes. **High Affinity Bivalent Ligands Targeting the Dopamine D_1-Histamine H_3 Heteromer Reduce β-Amyloid-Induced Neuronal Cell Death.** In preparation.

5.1.1. Introduction

The existence of a D_1R-H_3R heteromeric complex was first published by the group of Franco [21, 22]. Due to dimerization, the signaling properties of the heteromer change in comparison to the individual receptor protomers. For instance, both D_1R and H_3R antagonists can block the effect of either D_1R or H_3R agonists (cross-antagonism), or the effect of a D_1R agonist was significantly counteracted by a H_3R agonist. Follow-up work could prove the existence of the D_1R-H_3R heteromer in GABAergic neurons of the direct striatal pathway and the formation of a macromolecular complex with NMDA-receptor subunits [13]. Inhibition of this complex with H_3R antagonists could reduce NMDA-, β-amyloid peptide (Aβ)- or D_1R agonist-induced cell death making this complex a potential drug target for Alzheimer's

disease [13, 22]. The study of Moreno-Delgado et al. recently showed the therapeutic potential of the D_1R-H_3R heteromer for the treatment of Huntington's disease [14].

The development of heteromer-specific drugs is more challenging than the development of compounds binding on orthosteric sites of monomeric GPCRs. One of the most widespread options to target heteromers is the design of single chemical entities composed of two pharmacophores for the biological targets of interest, which can be accomplished by linking pharmacophores with stable spacers, by fusing pharmacophores, or by merging pharmacophores [23] (see *Chapter 1 Introduction*). In recent years numerous bivalent ligands targeting different homo- and heteromeric GPCR dimers have been published, which are summarized in various reviews [17, 24–27]. In this case study, we present a series of novel bivalent ligands targeting the D_1R-H_3R heteromer with exceptional affinity for both receptors and their pharmacological characterization in co-expressing systems.

5.1.2. Results and discussion

Molecular design

The design of heterobivalent ligands for the D_1R-H_3R heteromer requires the choice of several key building blocks. First, we need to select lead compounds that bind the orthosteric binding site of D_1R and H_3R with high affinity (pharmacophore units). Because we aim to design bivalent ligands that act as antagonists, we have therefore selected pharmacophores that are antagonists for D_1R (SCH-23390) and H_3R [28] (JNJ-5207852) (Figure 5.1). Second, a derivatization point in the pharmacophore, or an attachment point, that faces the extracellular side, is chemically accessible, and maintains the affinity, selectivity and biological activity of the pharmacophore to introduce a linker (see *Chapter 1 Introduction*). Figure 5.1 shows structural models of SCH-23390 and JNJ-5207852 in the orthosteric binding site of D_1R and H_3R, respectively, and the channels towards the extracellular environment. This channel is wide and therefore less restrictive in

D_1R and narrow and more restrictive in H_3R. These models, together with structure-activity relationships (SAR), showed the 4'-position of SCH-23390 as a suitable attachment point because it is oriented towards the extracellular side and introduction of amide or sulfonamide groups at this point, as a linker, seemed to be beneficial for receptor binding [29, 30] (Figure 5.1). The insertion of a sulfonamide moiety instead of an amide group at the 4'-position of the 1-phenyl-2,3,4,5-tetrahydro-1H-benzazepines was reported to increase affinity at the D_1R [30]. Similarly, an amide group can be also attached to the para-position of the benzylic piperidine moiety of JNJ-5207852 because it points outside (Figure 5.1) and by the successful development of an H_3R fluorescent ligand with similar modifications of the same pharmacophore. [31, 32] Finally, small aliphatic groups with terminal C-C triple bonds were added to connect the pharmacophore-linker moieties of D_1R and H_3R with the rest of the bivalent system (Figure 5.1). And third, a spacer with an appropriate length to cover the distance between both pharmacophore-linker moieties. We selected polyethylene glycol (PEG) moieties, often used to increase water solubility, as a spacer or other spacers based on aliphatic carbons. All spacers were terminally functionalized with azide groups, to permit a final connection with the pharmacophore-linker moieties of D_1R and H_3R, by a copper catalyzed azide alkyne click (CuAAC) reaction. This permits easy synthesis of a variety of bivalent ligands by using different pharmacophore-linker moieties of D_1R and H_3R and spacers.

The spacer length is a key factor and depends on the heterodimer interface, the surface of the extracellular domains of the heterodimer, and the position and orientation of the attachment points of the pharmacophore moiety. It was shown that cross-antagonism, as previously described for the D_1R-H_3R heteromer [21, 22], is due to the formation of a high surface complementarity between TMs 5 and 6 of the two protomers, via a four-helix bundle [33], which blocks the opening of the intracellular cavity for G protein binding at the other protomer [34]. Thus, we assume, as a working hypothesis, the TM5/6 interface for the D_1R-H_3R heteromer (see *Chapter 3 Methods*). Notably, this interface requires a smaller number of atoms in the spacer than other interfaces because of the shorter distance between the two orthosteric

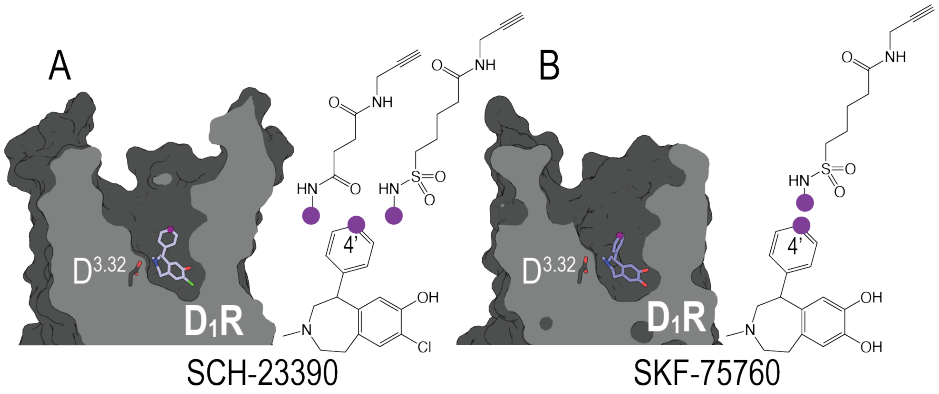

Figure 5.1: Structures and docking models of the SCH-23390 antagonist bound to D_1R and the JNJ-5207852 antagonist bound to H_3R. Attachement points in the docking models and structures, to introduce the depicted linkers, are shown as purple spheres. D_1R: modelled from PDB ID 7JOZ and 4BVN (see *Chapter 3 Methods* and (Moreno et al. 2022)), H_3R: PDB ID 7F61.

sites [35]. We calculated the preferred spacer length by adjusting different spacer moieties to the van der Waals surface of the heteromer, using a computational tool developed for the MOE software (Chemical Computing Group Inc., Montreal, Quebec, Canada) [35] (see *Chapter 3 Methods*), as previously performed for other bivalent ligands [36, 37]. The calculation was performed for PEG-based spacers of different lengths $(\text{-OCH2CH2-})_{n=10\text{-}15}$. The predicted minimum length of energetically favorable spacers is between 33 (n=11) and 36 (n=12) atoms, calculated between attachment atoms shown in purple in Figure 5.1. Because amide groups and the 1,2,3 triazole ring, used as part of the spacer in the synthesis of the bivalent ligands, are more rigid that the flexible PEG spacer, used in the calculation, we set our focus on spacers with a length of 39 to 47 atoms between both attachment points. Moreover, we synthesized other spacers with longer lengths up to 57 atoms in case the D_1R-H_3R heteromer exhibits other TM interface for dimerization with longer distance between orthosteric sites.

Figure 5.2 shows molecular dynamics (MD) simulations of designed compounds with spacer lengths of 41 (**44**) and 47 (**45**) atoms,

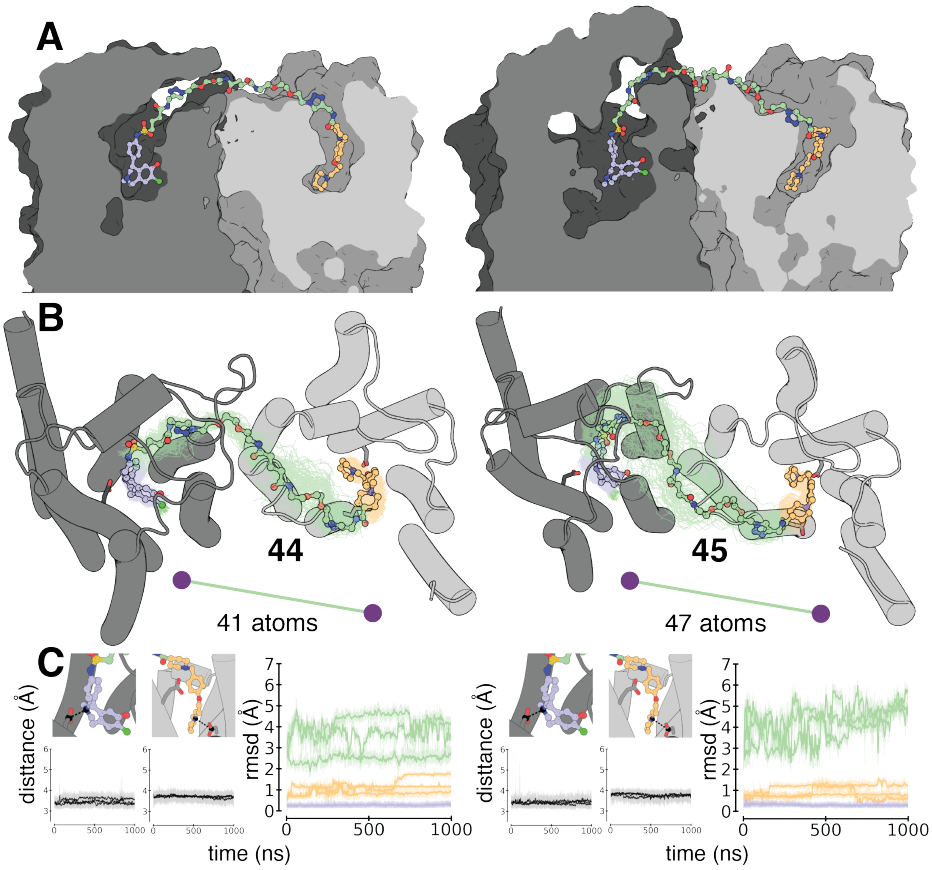

Figure 5.2: Evolution of bivalent ligands **44** and **45** in the D_1R-H_3R heteromer, constructed via the TM5/6 interface, as devised from molecular dynamic (MD) simulations. (A) Molecular models of bivalent ligands **44** (spacer length of 41 atoms between attachment points in purple spheres, see Scheme 5) and **45** (spacer length of 47 atoms) bound to the D_1R-H_3R heteromer. (B) Representative structures (opaque ball and spheres) and 100 structures collected every 10 ns (translucent lines) of **44** and **45**, extracted from one of the simulations, whereas the structure of the D_1R-H_3R heterodimer corresponds to the initial model. (C) Distances (dashed black line between black spheres in the inset panel) between the protonated amines of SCH-23390 and JNJ-5207852 and the C_γ atom of $Asp_{3.32}$ of D_1R and H_3R, respectively. Root-mean-square deviations (rmsds) of the heavy atoms of 44 and 45 (light blue and orange for the pharmacophore moieties of D_1R and H_3R, respectively, and green for the spacer moiety. Three replicas of 1 µs of each complex were run. See Figure 5.1 for the PDB IDs and *Chapter 3 Methods* for the modelling details of the dimer.

in the computational model of the D_1R-H_3R heteromer, to evaluate their stability (see *Chapter 3 Methods*). The stabilities were analyzed via root-mean square deviations (rmsds) (Figure 5.2C). Clearly, rmsd values of the pharmacophore units remains low (<2 Å) during the simulation time. Accordingly, the salt bridge distances between the protonated amines of the SCH-23390 and JNJ-5207852 pharmacophores and $Asp^{3.32}$ of D_1R and H_3R, respectively, remained stable across three replicas of a 1 µs unbiased MD simulation, suggesting that the designed spacers facilitate simultaneous binding of the pharmacophoric units to the orthosteric binding sites of the D_1R-H_3R heteromer constructed via the TM5/6 interface. As expected, rmsd values of the spacer group are larger than those of the pharmacophore moiety due to its flexibility. However, these values are larger for compound **45**, with a spacer length of 47 atoms, than for **44**, with a length of 41 atoms. This suggests that the shorter compound fits better onto the van der Waals surface of the heteromer, restricting its movement, while the longer compound is likely more exposed to the less restrictive extracellular aqueous environment.

Chemical synthesis

The different pharmacophores and the spacers were synthesized separately and connected in the end by a CuAAC reaction by Niklas Rosier and Steffen Pockes at the Institute of Pharmacy, University of Regensburg, Regensburg (Germany). Figure 5.3 shows the structures of bivalent ligands **40-47**, and Figure 5.4 shows the structures of end-capped (monovalent) ligands **59** and **61** that lack one of the pharmacophores.

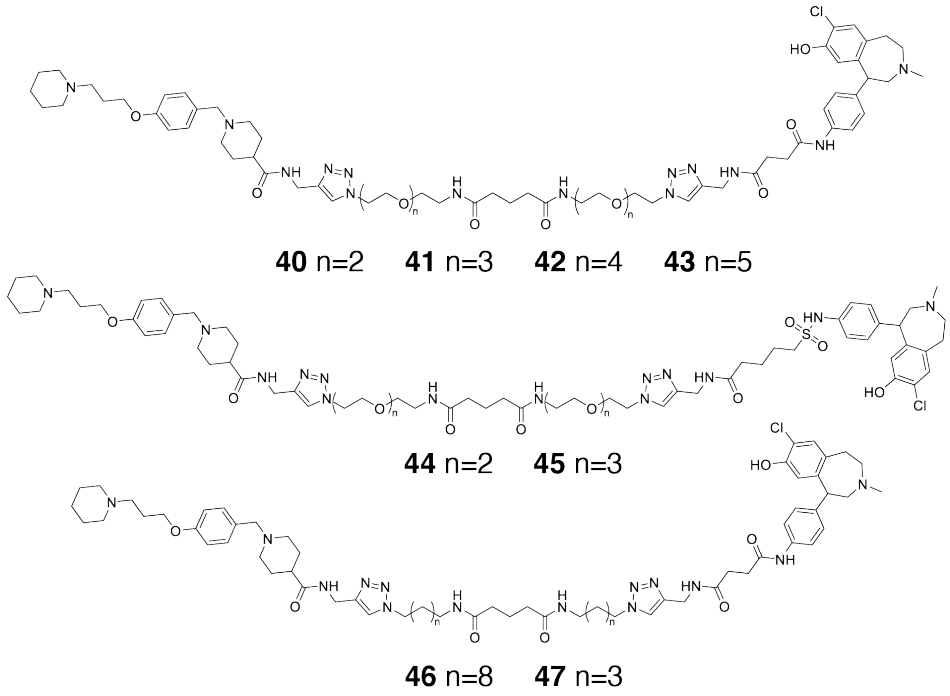

Figure 5.3: Bivalent ligands **40-47**.

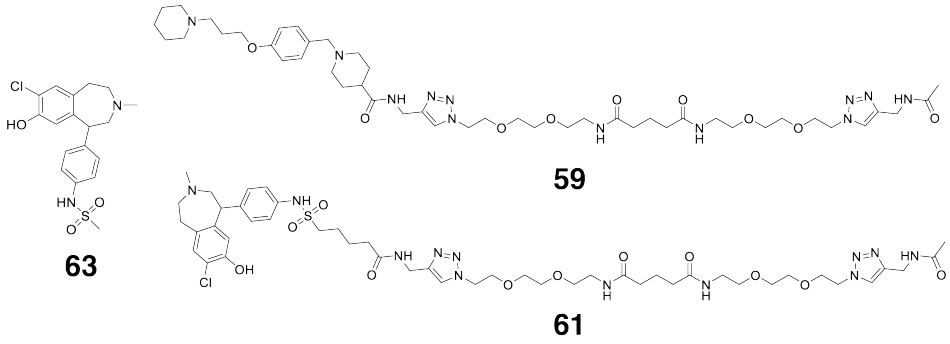

Figure 5.4: End-capped ligands **59** and **61** and D_1R reference compound **63**.

compd	D_1R linker[a]	H_3R linker[a]	linker length (atoms)[b]	pK_i (± SEM)		
				D_1R (RLB)[c]	H_3R (Nano BRET)[d]	H_3R (RLB)[e]
40	amide	amide	39	8.10 ± 0.08	10.08 ± 0.05	10.16 ± 0.01
41	amide	amide	45	7.77 ± 0.07	9.97 ± 0.15	9.87 ± 0.15
42	amide	amide	51	7.69 ± 0.11	9.84 ± 0.03	9.98 ± 0.08
43	amide	amide	57	7.39 ± 0.02	9.71 ± 0.08	9.67 ± 0.11
44	sulfona.	amide	41	8.88 ± 0.09	10.21 ± 0.10	nd
45	sulfona.	amide	47	8.67 ± 0.14	10.00 ± 0.04	10.11 ± 0.15
46	amide	amide	43 (al.)	8.41 ± 0.09	10.09 ± 0.04	10.03 ± 0.03
47	amide	amide	47 (al.)	6.59 ± 0.03	7.16 ± 0.23	7.74 ± 0.08
59	e-c	amide	-	<5	9.99 ± 0.05	nd
61	sulfona.	e-c	-	7.91 ± 0.11	6.30 ± 0.07	nd
63	sulfona.	D_1R ref	-	8.99 ± 0.13	5.54 ± 0.06	nd

Table 5.1: [a]Structure of the linker used to connect the pharmacophore with the spacer. [b]Number of atoms between attachment points of both pharmacophores. [c]Competition binding experiments at HEK-293T cell homogenates stably expressing the hD_1R [38]; displacement of 0.2 nM, 0.4 nM or 1 nM [^{3}H]N-Methyl-SCH-23390 (K_d = 0.4 nM). [d]Competition binding experiments at HEK-293T cells stably expressing NLuc-hH_3R [39]; displacement of 0.5 nM UR-NR266 [31] (K_d = 0.16 nM). [e]Competition binding assays at HEK293T-SP-FLAG-hH_3R cells [31]; displacement of [^{3}H]UR-PI294 [40] (K_d = 3 nM). Data shown are mean values ± SEM of N independent experiments, each performed in triplicate. N was 3 for D_1R RLB and H_3R NanoBRET, and 2 for H_3R RLB. Data were analyzed by nonlinear regression and were best fitted to sigmoidal concentration-response curves. sulfona.: sulfonamide, nd: no determined, al.: alkyl., e-c: end-capped.

Pharmacological characterization

The first step of the pharmacological characterization of the novel bivalent ligands was the determination of their binding affinity towards their primary targets, the D_1R and H_3R, using competitive NanoBRET binding assays (H_3R) [31] by Gemma Navarro and Rafael Franco at the Department of Biochemistry and Physiology, Faculty of Pharmacy and Food Sciences, Universitat de Barcelona, Barcelona (Spain) and competitive radioligand binding assays (D_1R) by D. Mönnich at the Institute of Pharmacy, University of Regensburg, Regensburg (Germany) (see *Chapter 3 Methods*). The results of these assays as well as the composition of the bivalent ligands are presented in Table 5.1. Compounds **40-43** and **45-47** were tested in both radioligand and NanoBRET binding assays (H_3R). Notably, the values of pK_i obtained with both assays show a remarkably good agreement, confirming that addition of NLuc to the receptor does not interfere with the binding of ligands.

The first set of bivalent ligands (**40-43**) possesses a common SCH-23390 as D_1R and JNJ-5207852 as H_3R pharmacophores and amide groups as linkers but contain an increasing number of PEG units (n=2-5) in the spacer (spacer lengths between attachment points of 39, 45, 51, 57 atoms, respectively) (Figure 5.3). Therefore, this set of compounds is well suited for the analysis of the influence of the spacer length on the receptor binding. Notably an increasing spacer length decreases the affinity of the bivalent ligand towards both receptors [pK_i (D_1R) = 8.1, 7.8, 7.7, 7.4; pK_i (H_3R) = 10.1, 10.0, 9.8, 9.7 for **40-43**, respectively]. Therefore, these results experimentally support the D_1R-H_3R heteromer interaction through the TM5/6 interface, which requires bivalent ligands with shorter spacers than other interfaces [35, 37], and validate our design strategy.

Compounds **46-47** are like **40-43** but replace the more polar PEG-based spacers by hydrophobic aliphatic carbons (Figure 5.3). The binding affinity of **46** [pK_i (D_1R) = 8.4; pK_i (H_3R) = 10.1], with a spacer length of 43 atoms, is in the same range as **40** [pK_i (D_1R) = 8.1; pK_i (H_3R) = 10.1], with 39 atoms as a spacer, and **41** [pK_i (D_1R) = 7.8; pK_i (H_3R) = 10.0], with 45 atoms. Surprisingly, **47** [pK_i (D_1R)

= 6.6; pK_i (H_3R) = 7.2], with a spacer length of 47 atoms (it only has four more methylene units than **46**), and comparable in length to **41** with 45 atoms, loses up to 100-fold affinity at both receptors compared with **41** or **46**. This huge loss of affinity is not fully understood, however, it is easy to speculate that the shorter spacer can form stable hydrophobic interactions with the amino acids forming the extracellular surface of the heteromer, while the longer chain is forced to be more exposed to the unfavorable aqueous environment (see above). Nevertheless, no further experiments were conducted to determine the reasons of this phenomenon, because the other bivalent ligands showed more promising binding data. Moreover, the PEG-based bivalent ligands are better water-soluble, making them more suitable for *in vitro* and *in vivo* assays.

Comparing the binding data at the D_1R of **40** [pK_i (D_1R) = 8.1; pK_i (H_3R) = 10.1] and **41** [pK_i (D_1R) = 7.8; pK_i (H_3R) = 10.0] to those of **44** [pK_i (D_1R) = 8.9; pK_i (H_3R) = 10.2] and **45** [pK_i (D_1R) = 8.7; pK_i (H_3R) = 10.0], it can be noted that replacement of a more restrictive planar amide group by a more flexible tetrahedral sulfonamide group, as a linker to the D_1R pharmacophore, led to an increase in D_1R affinity. Despite their size, **44** with 41 atoms, and **45** with 47 atoms, show exceptional K_i-values in the one-digit nanomolar range for the D_1R and subnanomolar range at the H_3R. Comparing the pK_i-values to those of the pharmacophore units SCH-23390 modified with a sulfonamide group (**63**) [pK_i (D_1R) = 9.0] and JNJ-5207852 (pK_i (H_3R) = 10.2) [31], there is only a small loss in affinity towards both receptors, despite the addition of the large spacers and the second pharmacophore.

Notably, the end-capped ligand with the SCH-23390 pharmacophore **61** [pK_i (D_1R) = 7.91] showed lower affinity towards its receptor than its bivalent counterpart **44** [pK_i (D_1R) = 8.88]. The end-capped ligand with the JNJ-5207852 pharmacophore **59** possesses pK_i values in the same range as the bivalent ligands.

β-amyloid-induced neuronal cell death

The D_1R-H_3R heteromer was reported to have a neuroprotective properties and its inhibition by H_3R antagonists leads to a reduction of excitotoxic cell death [13]. Based on these results, the antagonistic bivalent ligands should be able to reduce the Aβ-induced cell death in neurons. To test this hypothesis, cortex cells from mice embryos were extracted and cultivated. After seven days Aβ (c = 500 nM) and the respective compounds were added. After an additional seven days the cells were detached and the percentage of live cells versus total cells was determined. The results are depicted in Figure 5.5. Comparing the end-capped ligands **59** and **61** with the bivalent ligand **45**, a more pronounced neuroprotective effect for **45** was observed, due to a possible higher affinity towards the receptor dimer.

All three compounds were able to reduce the Aβ-induced cell death, with **45** showing the most pronounced effect at concentrations of 10 and 100 nM (Figure 5.5A). Focusing on **45**, a concentration-dependent neuroprotective effect was observed with a significant reduction in cell death at concentrations of 10 and 100 nM compared to the addition of Aβalone (Figure 5.5B). The strongest neuroprotective effect was observed at 100 nM, significantly higher compared to the lower concentrations of 10 and 100 pM. An increase of the concentration up to 1 µM, led to a lower percentage of live cells. This is probably caused by an overdose effect, a neurotoxic effect of the compound itself at high concentrations. This was observed for all three compounds and confirmed by the fact, that the addition of 1 µM of the compounds alone without Aβ had a neurotoxic effect compared to the blank control. Comparing the three compounds at the concentration of 100 nM, a stronger neuroprotective effect of **45** was observed, although only compared to **59** the difference was statistically significant (Figure 5.5C).

Overall, this data supports the hypothesis of a neuroprotective potential for the D_1R-H_3R heteromer and indicates a higher binding affinity and stronger neuroprotective effect of the bivalent ligands compared to the end-capped controls.

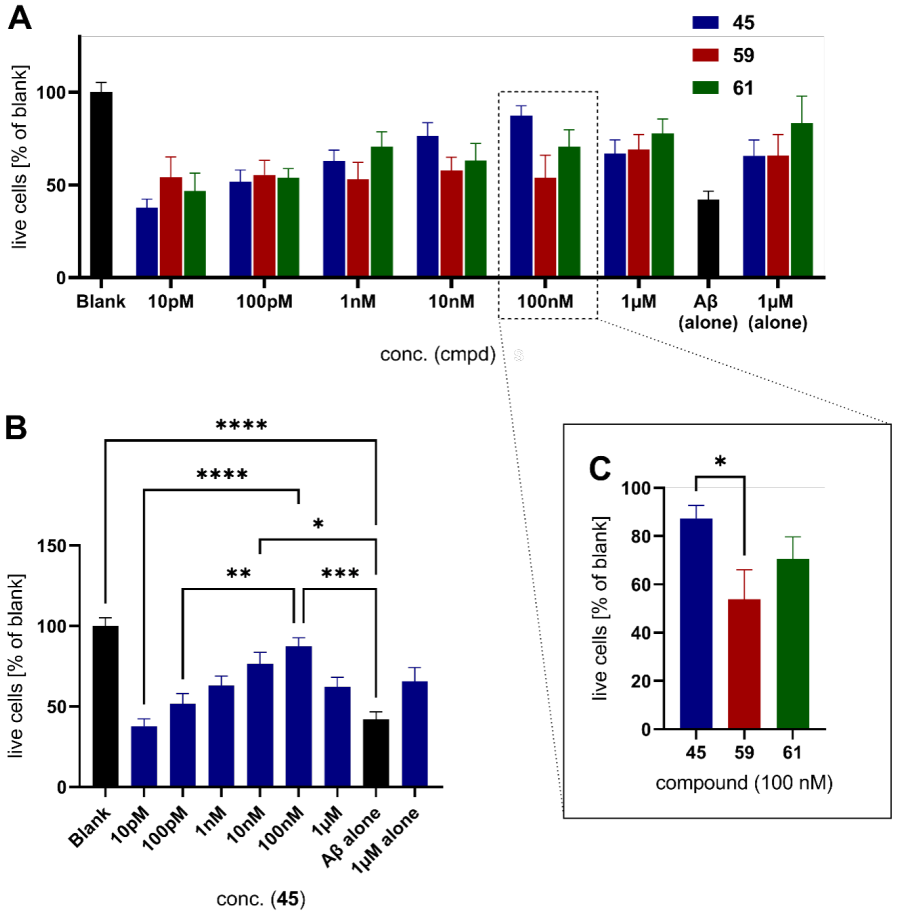

Figure 5.5: Cell death assay at mouse embryonal cortex cells. (A) Results of compounds **45**, **59** and **61**. (B) Isolated results of **45**. (C) Comparison of the three compounds at a concentration of 100 nM. Data represent mean values ± SEM of 2 (**59** and **61**) or 4 (**45**) different experiments on two different days, each performed in triplicate or quadruplicate. One-way ANOVA followed by Bonferroni's post hoc test showed significant effects between different concentrations (* $p < 0.05$; ** $p < 0.01$; *** $p < 0.001$; **** $p < 0.0001$).

5.1.3. Conclusions

Bivalent ligands for the D_1R-H_3R heteromer were designed based on docking studies and SAR of different lead structures. The attachment points of the pharmacophores for the linker were chosen appropriately and they retained a high affinity and selectivity towards the receptor. The addition of a C-C triple bond to all pharmacophores and terminal azide groups to all spacers, allowed the connection of pharmacophores and spacers by the CuAAC reaction. The synthetic approach of connecting all parts at the end allowed a synthesis of multiple bivalent and end-capped ligands without the need for an individual pharmacophore for each target structure. Bivalent ligands with the same pharmacophores, but different spacer lengths were synthesized because the needed length for a bivalent binding mode was not known.

All final compounds were tested in competitive binding assays for their affinity towards the D_1R and H_3R. Especially, compounds **44** and **45** showed exceptional high affinity at both receptors in the low nanomolar and sub-nanomolar range, which is remarkable for ligands of this size.

Finally, **45**, based on the previous results, the most promising compound, was tested in an *in vitro* neuroprotection assay using primary cortex cells of mice embryos. A significant reduction in Aβ-induced cell death was observed, which was higher than the effect of the end-capped ligands **59** and **61**. These results highlight the neuroprotective properties of the D_1R-H_3R heteromer and the potential of bivalent ligands to target this receptor complex with a higher affinity than monovalent ligands.

Bibliography

[1] J. M. Arrang, M. Garbarg, J. C. Schwartz, "Auto-inhibition of brain histamine release mediated by a novel class (H3) of histamine receptor", *Nature* **1983**, *302*, 832–837.

[2] J. M. Beaulieu, R. R. Gainetdinov, "The physiology, signaling, and pharmacology of dopamine receptors", *Pharmacological reviews* **2011**, *63*, 182–217.

[3] C. Missale, S. R. Nash, S. W. Robinson, M. Jaber, M. G. Caron, "Dopamine receptors: from structure to function", *Physiological reviews* **1998**, *78*, 189–225.

[4] J. M. Beaulieu, S. Espinoza, R. R. Gainetdinov, "Dopamine receptors - IUPHAR Review 13", *British journal of pharmacology* **2015**, *172*, 1–23.

[5] N. E. Andén, A. Carlsson, A. Dahlström, K. Fuxe, N. Å. Hillarp, K. Larsson, "Demonstration and mapping out of nigro-neostriatal dopamine neurons", *Life sciences (1962)* **1964**, *3*, 523–530.

[6] A. Carlsson, "A paradigm shift in brain research", *Science* **2001**, *294*, 1021–1024.

[7] P. Sokoloff, M. Andrieux, R. Besançon, C. Pilon, M. P. Martres, B. Giros, J. C. Schwartz, "Pharmacology of human dopamine D3 receptor expressed in a mammalian cell line: comparison with D2 receptor", *European journal of pharmacology* **1992**, *225*, 331–337.

[8] P. Seeman, J. Schwarz, J. F. Chen, H. Szechtman, M. Perreault, G. S. McKnight, J. C. Roder, R. Quirion, P. Boksa, L. K. Srivastava, K. Yanai, D. Weinshenker, T. Sumiyoshi, "Psychosis pathways converge via D2high dopamine receptors", *Synapse* **2006**, *60*, 319–346.

[9] D. Vallone, R. Picetti, E. Borrelli, "Structure and function of dopamine receptors", *Neuroscience and biobehavioral reviews* **2000**, *24*, 125–132.

[10] E. A. Clark, S. J. Hill, "Sensitivity of histamine H3 receptor agonist-stimulated [35S]GTPγ[S]binding to pertussis toxin", *European Journal of Pharmacology* **1996**, *296*, 223–225.

[11] Y. Takeshita, T. Watanabe, T. Sakata, M. Munakata, H. Ishibashi, N. Akaike, "Histamine modulates high-voltage-activated calcium channels in neurons dissociated from the rat tuberomammillary nucleus", *Neuroscience* **1998**, *87*, 797–805.

[12] Y. Y. Syed, "Pitolisant: First Global Approval", *Drugs* **2016**, *76*, 1313–1318.

[13] M. Rodríguez-Ruiz, E. Moreno, D. Moreno-Delgado, G. Navarro, J. Mallol, A. Cortés, C. Lluís, E. I. Canela, V. Casadó, P. J. McCormick, R. Franco, "Heteroreceptor Complexes Formed by Dopamine D1, Histamine H3, and N-Methyl-D-Aspartate Glutamate Receptors as Targets to Prevent Neuronal Death in Alzheimer's Disease", *Molecular neurobiology* **2017**, *54*, 4537–4550.

[14] D. Moreno-Delgado, M. Puigdellívol, E. Moreno, M. Rodríguez-Ruiz, J. Botta, P. Gasperini, A. Chiarlone, L. A. Howell, M. Scarselli, V. Casadó, A. Cortés, S. Ferré, M. Guzmán, C. Lluís, J. Alberch, E. I. Canela, S. Ginés, P. J. McCormick, "Modulation of dopamine D1 receptors via histamine H3 receptors is a novel therapeutic target for Huntington's disease", *eLife* **2020**, *9*, 1–31.

[15] G. RE, C. JA, H. I, P. MA, P. RH, I. P, J. E, P. EK, "Distribution of histamine H3-receptor binding in the normal human basal ganglia: comparison with Huntington's and Parkinson's disease cases", *The European journal of neuroscience* **1999**, *11*, 449–456.

[16] C. Ferrada, S. Ferré, V. Casadó, A. Cortés, Z. Justinova, C. Barnes, E. I. Canela, S. R. Goldberg, R. Leurs, C. Lluis, R. Franco, "Interactions between histamine H3 and dopamine D2 receptors and the implications for striatal function", *Neuropharmacology* **2008**, *55*, 190–197.

[17] C. Hiller, J. Kühhorn, P. Gmeiner, "Class A G-protein-coupled receptor (GPCR) dimers and bivalent ligands", *Journal of medicinal chemistry* **2013**, *56*, 6542–6559.

[18] A. Faron-Górecka, M. Szlachta, M. Kolasa, J. Solich, A. Górecki, M. Kuśmider, D. Żurawek, M. Dziedzicka-Wasylewska, "Understanding GPCR dimerization", *Methods in cell biology* **2019**, *149*, 155–178.

[19] B. Huang, C. M. S. Onge, H. Ma, Y. Zhang, "Design of bivalent ligands targeting putative GPCR dimers", *Drug discovery today* **2021**, *26*, 189–199.

[20] M. J. Lohse, "Dimerization in GPCR mobility and signaling", *Current opinion in pharmacology* **2010**, *10*, 53–58.

[21] C. Ferrada, E. Moreno, V. Casadó, G. Bongers, A. Cortés, J. Mallol, E. I. Canela, R. Leurs, S. Ferré, C. Lluís, R. Franco, "Marked changes in signal transduction upon heteromerization of dopamine D1 and histamine H3 receptors", *British journal of pharmacology* **2009**, *157*, 64–75.

[22] E. Moreno, H. Hoffmann, M. Gonzalez-Sepúlveda, G. Navarro, V. Casadó, A. Cortés, J. Mallol, M. Vignes, P. J. McCormick, E. I. Canela, C. Lluís, R. Moratalla, S. Ferré, J. Ortiz, R. Franco, "Dopamine D1-histamine H3 receptor heteromers provide a selective link to MAPK signaling in GABAergic neurons of the direct striatal pathway", *The Journal of biological chemistry* **2011**, *286*, 5846–5854.

[23] E. Proschak, H. Stark, D. Merk, "Polypharmacology by Design: A Medicinal Chemist's Perspective on Multitargeting Compounds", *Journal of medicinal chemistry* **2019**, *62*, 420–444.

[24] J. William Messer, "Bivalent ligands for G protein-coupled receptors", *Current pharmaceutical design* **2004**, *10*, 2015–2020.

[25] A. H. Newman, F. O. Battiti, A. Bonifazi, "2016 Philip S. Portoghese Medicinal Chemistry Lectureship: Designing Bivalent or Bitopic Molecules for G-Protein Coupled Receptors. The Whole Is Greater Than the Sum of Its Parts", *Journal of medicinal chemistry* **2020**, *63*, 1779–1797.

[26] J. Shonberg, P. J. Scammells, B. Capuano, "Design strategies for bivalent ligands targeting GPCRs", *ChemMedChem* **2011**, *6*, 963–974.

[27] J. Botta, J. Appelhans, P. J. McCormick, "Continuing challenges in targeting oligomeric GPCR-based drugs", *Progress in molecular biology and translational science* **2020**, *169*, 213–245.

[28] R. Apodaca, C. A. Dvorak, W. Xiao, A. J. Barbier, J. D. Boggs, S. J. Wilson, T. W. Lovenberg, N. I. Carruthers, "A new class of diamine-based human histamine H3 receptor antagonists: 4-(aminoalkoxy)benzylamines", *Journal of medicinal chemistry* **2003**, *46*, 3938–3944.

[29] J. Zhang, B. Xiong, X. Zhen, A. Zhang, "Dopamine D1 receptor ligands: where are we now and where are we going", *Medicinal research reviews* **2009**, *29*, 272–294.

[30] D. A. Burnett, W. J. Greenlee, B. Mckirtrick, J. Su, Z. Zhu, T. K. Sasikumar, R. Mazzola, L. Qiang, Y. Ye, B. Mckittrick, "Selective D1/D5 receptor antagonists for the treatment of obesity and CNS disorders", US20040850530 20040520.

[31] N. Rosier, L. Grätz, H. Schihada, J. Möller, A. Işbilir, L. J. Humphrys, M. Nagl, U. Seibel, M. J. Lohse, S. Pockes, "A Versatile Sub-Nanomolar Fluorescent Ligand Enables NanoBRET Binding Studies and Single-Molecule Microscopy at the Histamine H3 Receptor", *Journal of medicinal chemistry* **2021**, *64*, 11695–11708.

[32] K. Wingen, J. S. Schwed, K. Isensee, L. Weizel, A. Živković, D. Odazic, H. Stark, "Benzylpiperidine variations on histamine H3 receptor ligands for improved drug-likeness", *Bioorganic & medicinal chemistry letters* **2014**, *24*, 2236–2239.

[33] A. Manglik, A. C. Kruse, T. S. Kobilka, F. S. Thian, J. M. Mathiesen, R. K. Sunahara, L. Pardo, W. I. Weis, B. K. Kobilka, S. Granier, "Crystal structure of the μ-opioid receptor bound to a morphinan antagonist", *Nature* **2012**, *485*, 321–326.

[34] S. Ferré, F. Ciruela, C. W. Dessauer, J. González-Maeso, T. E. Hébert, R. Jockers, D. E. Logothetis, L. Pardo, "G protein-coupled receptor-effector macromolecular membrane assemblies (GEMMAs)", *Pharmacology & therapeutics* **2022**, *231*.

[35] L. Pérez-Benito, A. Henry, M. T. Matsoukas, L. Lopez, D. Pulido, M. Royo, A. Cordomí, G. Tresadern, L. Pardo, "The size matters? A computational tool to design bivalent ligands", *Bioinformatics* **2018**, *34*, 3857–3863.

[36] D. Pulido, V. Casadó-Anguera, L. Pérez-Benito, E. Moreno, A. Cordomí, L. López, A. Cortés, S. Ferré, L. Pardo, V. Casadó, M. Royo, "Design of a True Bivalent Ligand with Picomolar Binding Affinity for a G Protein-Coupled Receptor Homodimer", *Journal of medicinal chemistry* **2018**, *61*, 9335–9346.

[37] D. Pulido, V. Casadó-Anguera, M. Gómez-Autet, N. Llopart, E. Moreno, N. Casajuana-Martin, S. Ferré, L. Pardo, V. Casadó, M. Royo, "Heterobivalent Ligand for the Adenosine A2A-Dopamine D2 Receptor Heteromer", *Journal of medicinal chemistry* **2022**, *65*, 616–632.

[38] L. Forster, L. Grätz, D. Mönnich, G. Bernhardt, S. Pockes, "A Split Luciferase Complementation Assay for the Quantification of β-Arrestin2 Recruitment to Dopamine D2-Like Receptors", *International journal of molecular sciences* **2020**, *21*, 1–20.

[39] E. Bartole, L. Grätz, T. Littmann, D. Wifling, U. Seibel, A. Buschauer, G. Bernhardt, "UR-DEBa242: A Py-5-Labeled Fluorescent Multipurpose Probe for Investigations on the Histamine H3 and H4 Receptors", *Journal of medicinal chemistry* **2020**, *63*, 5297–5311.

[40] P. Igel, D. Schnell, G. Bernhardt, R. Seifert, A. Buschauer, "Tritium-labeled N(1)-[3-(1H-imidazol-4-yl)propyl]-N(2)-propionylguanidine ([(3)H]UR-PI294), a high-affinity histamine H(3) and H(4) receptor radioligand", *ChemMedChem* **2009**, *4*, 225–231.

Chapter 6

Designing homo- and heterobivalent and tetravalent ligands for the adenosine A_{2A}-dopamine D_2 receptor heteromer

The concept of polypharmacology denotes the ability of one drug to interact with multiple (two or more) targets simultaneously for a greater therapeutic effect [1]. This "one drug-multiple targets" idea contrasts with the more traditional drug discovery programs of "one drug-one target", aimed at minimizing adverse effects. However, "one drug–one target–one disease" approaches in drug discovery have become increasingly inefficient because many human diseases are multifactorial [2, 3], such as neurodegenerative and psychiatric disorders, infectious and cardiovascular diseases, and cancer, among others [4]. For instance, schizophrenia has multifactorial etiology and complex polygenic architecture [5, 6]. The dopamine system is hyperresponsive in schizophrenia, and all clinically used antipsychotic drugs block dopamine D_2 receptors (D_2Rs) [7]. In the brain, D_2R is highly expressed in the striatum and to a somewhat lower extent in the midbrain, cortex, hypothalamus, amygdala, and hippocampus [8]. There

is significant evidence that a main population of striatal D_2R forms heteromers with the adenosine A_{2A} receptor ($A_{2A}R$) [9, 10]. $A_{2A}R$-D_2R heteromers have been found in transfected cells [11], in native tissue [9], and in human post-mortem brains in which the amount of heteromer differs from healthy and diseased, increasing in Parkinson's disease [12] and decreasing in schizophrenia [13]. Remarkably, an increase in $A_{2A}R$-D_2R heteromerization has been proposed to be involved in the extrapyramidal side effects of antipsychotics [12], and the selective $A_{2A}R$ antagonist istradefylline (marketed as Nouriast™ in Japan in 2013 and as Nourianz™ in the United States in 2019) is used as an adjunctive treatment to the dopamine precursor L-DOPA in patients with Parkinson's disease experiencing "off" episodes [14]. Thus, the $A_{2A}R$-D_2R heteromer is an attractive multitarget. Other published approaches to target the $A_{2A}R$-D_2R heteromer have consisted in the development of dual-target bitopic ligands [15] and bivalent ligands [16].

In the following two case studies, we have used our previous knowledge to design and synthesize homobivalent, hetereobivalent and heterotetravalent ligands for the $A_{2A}R$-D_2R heterotetramer.

6.1. Case study 4. Heterobivalent ligand for the adenosine A_{2A}-dopamine D_2 receptor heteromer

Published as co-first author in

Daniel Pulido[1], Verònica Casadó-Anguera[1], Marc Gómez-Autet[1], Natàlia Llopart, Estefanía Moreno, Nil Casajuana-Martin, Sergi Ferré, Leonardo Pardo[*], Vicent Casadó[*], Miriam Royo[*]. **Heterobivalent ligand for the adenosine A_{2A}-dopamine D_2 receptor heteromer.** Journal of Medicinal Chemistry 2022, 65(1), 616–632.

[1]These authors contributed equally.

6.1.1. Introduction

Despite the initial skepticism and discussion [17, 18] and the fact that some monomeric GPCRs can efficiently activate G proteins [19], it is now increasingly accepted that GPCRs form homomers and heteromers [20]. These oligomers are in some cases the predominant species [21] and constitute primary functional signaling units [22]. However, some of this evidence has been obtained in artificial systems, but recent *in vivo* studies also support the functional importance of GPCR oligomerization [23–26]. As introduced, a GPCR heteromer which has become an attractive drug target [27, 28] is the complex formed by the adenosine A_{2A} receptor ($A_{2A}R$) and the dopamine D_2 receptor (D_2R).

A major focus has been on the generation of heteromer-selective tools that recognize oligomers in native tissues [29]. These include

antibodies that selectively recognize an epitope in the heteromer [30] or/and the development of high-affinity bivalent ligands (fluorophore-coupled or not) that selectively target the heteromer. Moreover, heterobivalent ligands would be the paradigm of heteromer-selective drugs [31] able to modulate receptor function within a particular heteromer with lesser secondary effects, key to design a new generation of GPCR drugs. Compared to the monomeric, the oligomeric approach would be more disease-specific because heteromers are likely to have a restricted tissue distribution and/or to be up- or down-regulated in specific tissues under pathological conditions [20, 29, 32]. Here, we have used the previous experience of our group in obtaining a homobivalent ligand with picomolar binding affinity for the D_2R homodimer [33], using a combination of computational, chemical, and biochemical tools, to design and synthesize heterobivalent ligands for the $A_{2A}R$-D_2R heteromer.

6.1.2. Results and discussion

Molecular design

The design of the heterobivalent ligand for the $A_{2A}R$-D_2R heteromer (Figure 6.1) follows similar trends as in the reported homobivalent ligand for the D_2R homomer [33]. (i) The main scaffold is the nitrilotriacetic acid-based scaffold (NTA) that contains three symmetric carboxylic acids, permitting the attachment of two different pharmacophore-containing chains and, if desired, an additional pharmacophore-containing chain to study higher-order oligomers or a reporter molecule for imaging studies, via a controlled desymmetrization of each of these functional groups [34]. (ii) The D_2R pharmacophore is a derivative of the antagonist spiperone, namely the *N*-(*p*-aminophenethyl)spiperone (NAPS), which was functionalized through the amine group with an extra succinic acid linker to facilitate its incorporation to the bivalent system, as in the previous study [33]. The selected $A_{2A}R$ pharmacophore is a derivative of the selective antagonist SCH-442,416,

2-(4-(3-(5-amino-2-(furan-2-yl)-7*H*-pyrazolo[4,3-*e*][1,2,4]triazolo[1,5-*c*]pyrimidin-7-yl)propyl)phenoxy)acetic acid, which includes in its structure a phenoxyacetic acid moiety that allows its integration into the bivalent system. In both pharmacophores the derivatization points to introduce the linkers were selected considering their orientation to the extracellular side and chemical accessibility (see *Chapter 3 Methods*). (iii) The spacer length of the bivalent ligand is a key factor and depends on the dimer interface, the surface of the extracellular domains of the dimer, and the position and orientation of the attachment points of the pharmacophore-linker moieties [35]. It was previously determined the interface of the $A_{2A}R$-D_2R heteromer by bimolecular fluorescence complementation (BiFC) experiments in cells expressing $A_{2A}R$-nYFP and D_2R-cYFP in the presence of synthetic peptides with the sequence of different TM domains of $A_{2A}R$ and D_2R (fused to the cell-penetrating HIV transactivator of transcription (TAT) peptide) [36] *Chapter 3 Methods*). Disruption of fluorescence complementation was only significantly observed in the presence of peptides with the amino acid sequence of TM4 and TM5 of both A_{2A} and D_2R, suggesting a TM4/5 interface for the $A_{2A}R$-D_2R heteromer [10]. Notably, this interface requires a larger number of atoms in the spacer between the attachment points than other interfaces (i.e. TM5/6 interface), because of a longer distance between the two different orthosteric sites [33, 35]. To calculate the optimal size of the spacer, we docked the pharmacophore-linker derivatives **7** for $A_{2A}R$ and **11** for D_2R (Figure 6.2A) to the previously published computational model of the $A_{2A}R$-D_2R heteromer [10] built from the TM4/5 dimeric interface observed in the oligomeric structure of the β_1-adrenergic receptor (see *Chapter 3 Methods*). We calculated the preferred spacer length by adjusting different spacer moieties to the van der Waals surface of the heteromer, using a computational tool developed for the MOE software (Chemical Computing Group Inc., Montreal, Quebec, Canada) [35] (see *Chapter 3 Methods*). The selected spacers were oligoethylene glycol (OEG) moieties, with the aim to increase water solubility of the final bivalent ligands, of different lengths $(\text{-}OCH_2CH_2\text{-})_{n=1\text{-}4}$. The tool predicts the favorable conformation of the linker/spacer/scaffold/spacer/linker

moieties with the molecular surface and calculates the interaction energy between the bivalent ligand and the rest of the heteromer system after a stepped energy minimization protocol. The predicted lengths of energetically favorable spacer/scaffold/spacer groups are between 35 and 43 atoms, calculated between attachment atoms shown in purple in Figure 6.1.

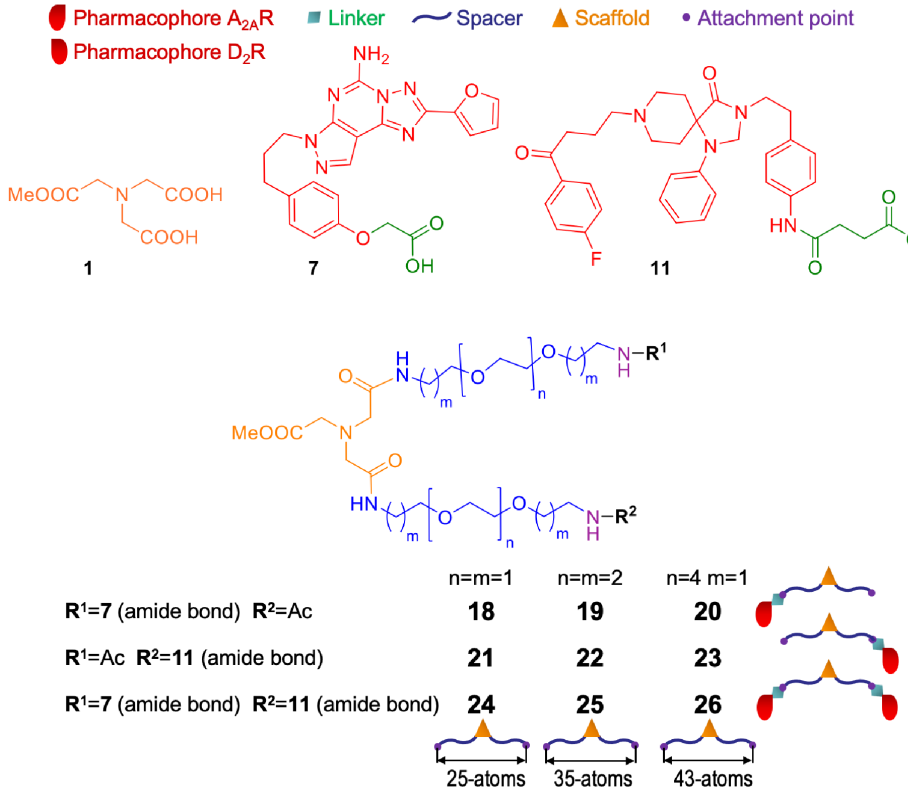

Figure 6.1: The heterobivalent ligand contains (i) a scaffold that can be properly derivatized (in orange), (ii) pharmacophore units (in red) that bind the orthosteric binding site of $A_{2A}R$ (**7**) and D_2R (**11**) with high affinity, (iii) a spacer to cover the distance between both protomers of the heteromer (in blue), and (iv) a linker (in green) between the pharmacophore units and the spacer, adequate for the chemistry used for conjugation.

Compounds **25** and **26** with spacer lengths of 35 (n=m=2) and 43 (n=4, m=1) atoms were used for molecular dynamic (MD) sim-

ulations (see *Chapter 3 Methods*) to evaluate their stability in the computational model of the $A_{2A}R$-D_2R heteromer (Figure 6.2B). The stabilities of the ligand-heteromer complexes were analyzed via root mean-square deviations (rmsd) (Figure 6.2C). As expected, rmsd values of the spacer/scaffold/spacer group are larger than those of the pharmacophore-linker moiety due to its flexibility. The binding of the pharmacophore units to the two different orthosteric sites was monitored by the salt bridge distance between the protonated amine of the NAPS pharmacophore and $Asp^{3.32}$ of D_2R and the hydrogen bond distance between the adenine moiety of the SCH-442,416 pharmacophore and $Asn^{6.55}$ of $A_{2A}R$ (Figure 6.2C). These interactions remain stable throughout three replicas of 1 µs unbiased MD simulation, suggesting that compounds **25** and **26** can fulfill the simultaneous binding of the pharmacophoric units to the orthosteric binding sites. Thus, these spacer lengths were used as recommendations for synthesis. As a negative control, we have also synthesized bivalent compound **24** with a spacer length of 25-atoms (n=m=1) that is not capable of interacting simultaneously with the two different orthosteric sites due to the shorter spacer length.

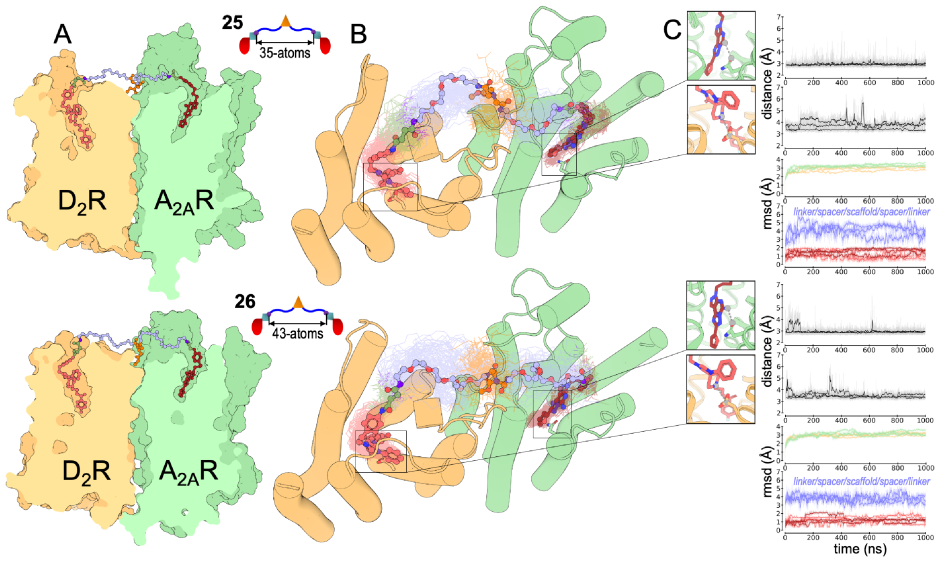

Figure 6.2: Evolution of bivalent ligands **25** and **26** in the $A_{2A}R$-D_2R heteromer, constructed via the TM 4/5 interface, as devised from MD simulations. (A) Molecular models of bivalent ligands 25 (spacer length of 35, n=m=2, see Figure 6.1) and **26** (spacer length of 43, n=4, m=1) bound to the $A_{2A}R$-D_2R heteromer. A MOE-based computational tool [35] was used to model these ligands into the heteromer. (B) Representative structures (opaque sticks) and 100 structures collected every 10 ns (translucent lines) of **25** and **26** (the color code of the atoms is as in Figure 6.1), extracted from the simulations, whereas the structure of the $A_{2A}R$-D_2R heterodimer corresponds to the initial model. (C) The simultaneous binding of the pharmacophore units of **25** and **26** to both orthosteric sites was monitored by the salt bridge distance between the protonated amine of the NAPS pharmacophore and the C_γ atom of $Asp^{3.32}$ of D_2R and the hydrogen bond distance between the -NH_2 group of the adenine moiety of the SCH-442,416 pharmacophore and the $O_{\delta 1}$ atom of $Asn^{6.55}$ of $A_{2A}R$ (dashed gray line between gray spheres in the inset panel). The stability of the ligand-heteromer complex was analyzed via root mean-square deviations (rmsd) of the heavy atoms of **25** and **26** (red for the pharmacophore moieties and blue for linker/spacer/scaffold/spacer/linker moities) and the stability of the $A_{2A}R$-D_2R heteromer was also analyzed by rmsd of $A_{2A}R$ (green) and D_2R (orange). Three replicas of 1 μs of each complex were run.

Chemical synthesis

The synthesis of both monovalent (**18-23**) and bivalent (**24-26**) ligands was performed by Daniel Pulido and Miriam Royo at the Department of Surfactants and Nanobiotechnology, Institute for Advanced Chemistry of Catalonia (IQAC-CSIC), Barcelona (Spain).

Binding affinity assays

In vitro binding affinities of the suggested $A_{2A}R$-D_2R heterobivalent ligands **24-26**, and the corresponding monovalent counterparts **18-20** for $A_{2A}R$ and **21-23** for D_2R, were obtained from [^{3}H]ZM 241 385 or [^{3}H]YM-09151-2 radioligand competition-binding assays (see *Chapter 3 Methods*), performed by Verònica Casadó-Anguera and Vicent Casadó at the Department of Biochemistry and Molecular Biomedicine, Faculty of Biology, Universitat de Barcelona, Barcelona (Spain), using membranes from sheep brain striatum that naturally express $A_{2A}R$ and D_2R (Table 6.1). Data were analyzed according to a "receptor dimer model" [37], which assumes GPCR dimers as a main functional unit and provides the affinity of the competing ligand for the first protomer in the unoccupied dimer (K_{DB1}) and the affinity for the second protomer when the first protomer is already occupied by the competing ligand (K_{DB2}). Except for pharmacophore derivative **7** (Figure 6.3A), all studied ligands showed monophasic noncooperative curves, as expected for an antagonist ligand, and in these conditions, K_{DB1} is enough to characterize the binding of these compounds (Table 6.1, Figure 6.3).

The D_2R pharmacophore derivative **11** has high affinity for D_2R (K_{DB1} = 0.70 nM) and the introduction of the OEG-based platform (scaffold + OEG spacers), to generate monovalent compounds **21** (25-atoms, K_{DB1} = 0.77 nM), **22** (35-atoms, K_{DB1} = 1.5 nM) and **23** (43-atoms, K_{DB1} = 0.50 nM), does not have a negative impact in the binding affinities. Heterobivalent ligands **24** (25-atoms, K_{DB1} = 0.6 nM), **25** (35-atoms, K_{DB1} = 1.2 nM) and **26** (43-atoms, K_{DB1} = 0.13 nM), that also contain the $A_{2A}R$ pharmacophore, show binding affinities for D_2R in the low nanomolar to subnanomolar range. Only compound **26** has a significantly enhanced binding affinity compared

Compound	K_{DB1} $A_{2A}R$ (nM)	K_{DB2} $A_{2A}R$ (nM)	K_{DB1} D_2R (nM)	K_{DB1} $A_{2A}R$ + TM3 $A_{2A}R$	K_{DB1} $A_{2A}R$ + TM5 $A_{2A}R$
11	-	-	0.70 ± 0.06[a]	-	-
21	-	-	0.77 ± 0.04[a]	-	-
22	-	-	1.5 ± 0.6[a]	-	-
23	-	-	0.50 ± 0.04	-	-
7	8 ± 1	430 ± 130	-	-	-
18	50 ± 10	-	-	-	-
19	160 ± 40	-	-	-	-
20	50 ± 11	-	-	-	-
24	6 ± 1###	-	0.6 ± 0.1	-	-
25	1.9 ± 0.3### **	-	1.2 ± 0.3	1.3 ± 0.6	1.1 ± 0.3
26	2.1 ± 0.4## **	-	0.13 ± 0.04## **	1.7 ± 0.3	36 ± 12^^^

Table 6.1: Affinity constants (K_{DB1}, K_{DB2}) of the $A_{2A}R$ and D_2R ligands **7**, **11**, **18-26** with or without TM3-TAT and TM5-TAT $A_{2A}R$ peptides. Values are mean ± SEM (nM) from 3-7 determinations. Statistical significance was calculated by one-way ANOVA followed by Bonferroni's post hoc test. $^{\#\#}p<0.01$, $^{\#\#\#}p<0.001$ compared with the corresponding monovalent ligand; $^{**}p<0.01$ compared with the pharmacophore derivative **7** or **11**; $^{\wedge\wedge\wedge}p<0.001$ compared with the respective control without TM-TAT peptides. [a]Results previously reported [33].

to that of the corresponding monovalent counterpart **23** (43-atoms, 4-fold, $p<0.01$) and the pharmacophore 11 (5-fold, $p<0.01$) (Table 6.1).

The results are totally different for $A_{2A}R$. The incorporation of the OEG-based platforms to the $A_{2A}R$ pharmacophore derivative **7** (K_{DB1} = 8 nM) to generate monovalent compounds **18** (25-atoms, K_{DB1} = 50 nM), **19** (35-atoms, K_{DB1} = 160 nM) and **20** (43-atoms, K_{DB1} = 50 nM) decreases the binding affinity for $A_{2A}R$ by 6-, 20- and 6-fold, respectively (Table 6.1) as compared to **7**. These results reveal the impact of the OEG-based platform of the monovalent ligands on the negative cooperativity of **7**, already reported for the parent antagonist SCH-442,416 [38]. Remarkably, heterobivalent ligands **24** (25-atoms, K_{DB1} = 6 nM), **25** (35-atoms, K_{DB1} = 1.9 nM) and **26** (43-atoms, K_{DB1} = 2.1 nM) show statistically significant increase of binding affinity relative to the monovalent counterparts (8-fold, $p<0.001$; 84-fold, $p<0.001$; and 24-fold, $p<0.01$; respectively) and relative to the $A_{2A}R$ pharmacophore **7** in the case of **25** (35-atoms, 4-fold, $p<0.01$) and **26** (43-atoms, 4-fold, $p<0.01$) (Table 6.1). A plausible explanation for these results might be the presence of the spiperone moiety as D_2R pharmacophore that contains a protonated amine that forms a strong ionic interaction with $Asp^{3.32}$ of D_2R (Figure 6.2). Thus, this moiety might act as a conductor of the interaction between the heterobiva-

lent ligand and the heteromer due to its high affinity for the receptor. We suggest that following the initial binding of the D_2R pharmacophore within the heterobivalent construct, subsequent binding of the $A_{2A}R$ pharmacophore to the heteromer is more favorable because it is present at a much higher local concentration once tethered in a close radius above the dimer [39] and thanks to decreased loss of entropy [40].

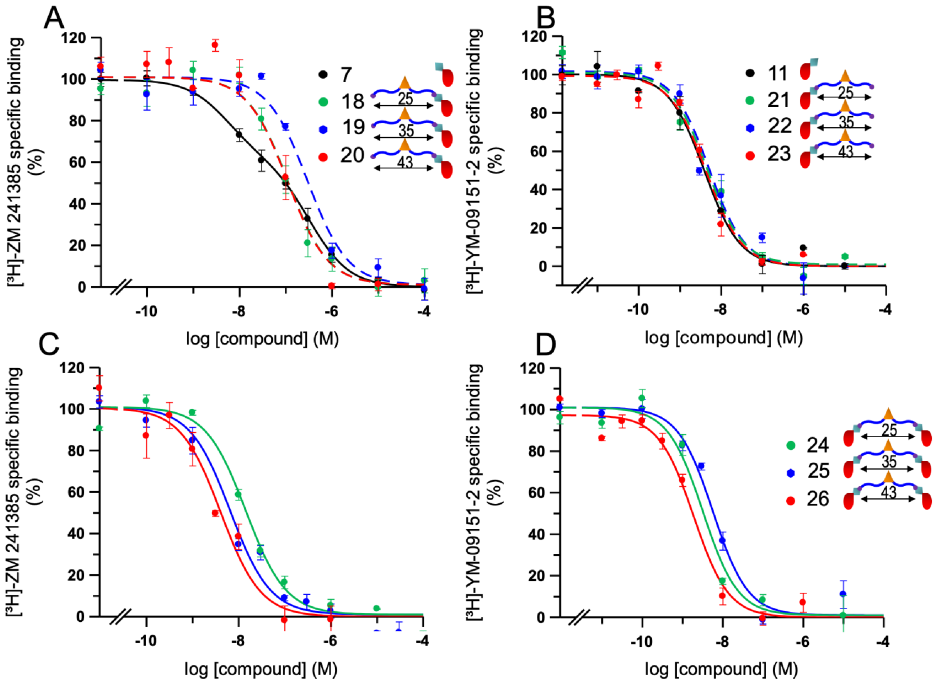

Figure 6.3: Competition experiments of the $A_{2A}R$ and D_2R ligands **7**, **11**, **18-26**. Competition experiments (see *Chapter 3 Methods*) of [^{3}H]ZM 241 385 for $A_{2A}R$ (A,C) or [^{3}H]YM-09151-2 for D_2R (B,D) vs increasing concentrations of $A_{2A}R$ and D_2R pharmacophores (**7** and **11**, respectively), $A_{2A}R$ and D_2R monovalent compounds (**18-20** and **21-23**, respectively) (A,B), and heterobivalent ligands **24-26** (C,D), using membranes from sheep brain striatum that naturally express $A_{2A}R$ and D_2R. Experimental data were fitted to the dimer receptor model. Data are mean ± SEM from a representative competitive experiment (n=3-7) performed in triplicate. 100% corresponds to 0.14±0.02 (A,C) or 0.15±0.01 (B,D) pmol/mg of protein. For statistical significance analysis, see Table 6.1.

Because it was previously shown that TAT-TM4 and TM5-TAT

peptides disrupt the $A_{2A}R$-D_2R heteromer [10, 41], we tested the binding affinity of heterobivalent ligands **25** (35-atoms) and **26** (43-atoms) in the presence of TM5-TAT and TM3-TAT (negative control) of $A_{2A}R$ in native tissues (Table 6.1 and Figure 6.4). The main idea behind this approach is that a disrupting peptide would alter the $A_{2A}R$-D_2R heteromer interface, increasing the distance between orthosteric sites of the two protomers [10] (see *Chapter 3 Methods*). Therefore, disrupting TM5-TAT peptide, but not the negative control TM3-TAT, should decrease the binding affinity of only those compounds that certainly act in a bivalent mode. We have focused on the $A_{2A}R$ because the binding affinity differences between bivalent ligands (**25** and **26**) and the corresponding monovalent counterparts (**19**, **20**, **22** and **23**) were more remarkable for this receptor (see Table 6.1). Neither TM5-TAT nor TM3-TAT influenced the binding of compound **25** [K_{DB1} (**25**) = 1.9 nM vs K_{DB1} (**25**+TM5) = 1.1 nM and K_{DB1} (**25**+TM3) = 1.3 nM] (Figure 6.4A). In contrast, the $A_{2A}R$ binding affinity of compound **26** significantly decreased in the presence of TM5-TAT peptide [K_{DB1} (**26**) = 2.1 nM vs K_{DB1} (**26**+TM5) = 36 nM] and remains practically unaltered in the presence of TM3-TAT peptide [(K_{DB1} (**26**) = 2.1 nM vs K_{DB1} (**26**+TM3) = 1.7 nM] (Figure 6.4B). Furthermore, bivalent ligand **26** in the presence of the disrupting peptide TM5-TAT of $A_{2A}R$ performed similarly to the corresponding monovalent $A_{2A}R$ counterpart **20** [K_{DB1} (**26**+TM5) = 36 nM vs K_{DB1} (**20**) = 50 nM]. All these data suggest that only compound **26** with a 43-atoms spacer acts as a "true bivalent" ligand of the $A_{2A}R$-D_2R heteromer, which implies a simultaneous binding of the two pharmacophore units at the two different orthosteric sites of this heteromer. Remarkably, this agrees with our binding affinity experiments (see Table 6.1) in which we showed that only compound **26** was able to increase the binding affinity relative to the $A_{2A}R$ (**7**, 4-fold) and D_2R (**11**, 5-fold) pharmacophores. The fact that **25** does not behave as a bivalent ligand, but increases the binding affinity for the $A_{2A}R$ relative to the monovalent counterpart (**19**, 84-fold), suggests the binding of the second pharmacophore unit at an extracellular site of the second protomer different than the orthosteric.

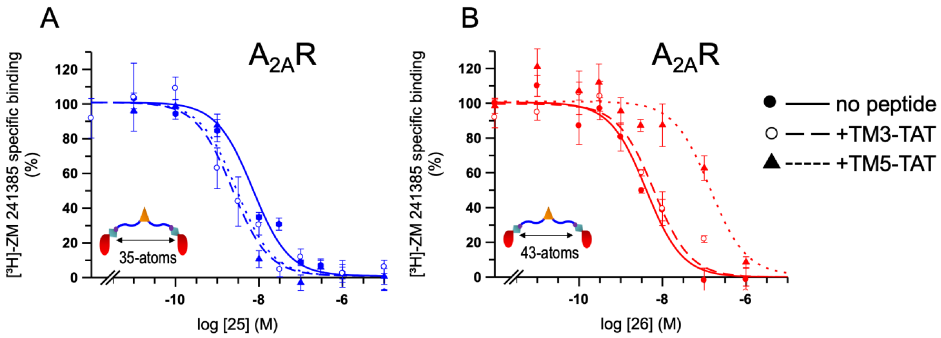

Figure 6.4: Effect of TM3-TAT and TM5-TAT peptide of $A_{2A}R$ in the binding affinity of heterobivalent ligands **25** and **26** for $A_{2A}R$. Competition experiments (see *Chapter 3 Methods*) of [^{3}H]ZM 241 385 vs increasing concentrations of heterobivalent ligands. **25** (A) or **26** (B) in the absence (solid line) or the presence of TM5-TAT (dash-dotted line) or of TM3-TAT (dashed line) peptides of $A_{2A}R$, using membranes from sheep brain striatum. Experimental data were fitted to the dimer receptor model. Data are mean ± SEM from a representative competitive experiment (n=3-6) performed in triplicate. 100% corresponds to 0.14±0.02 pmol/mg protein. For statistical significance analysis, see Table 6.1.

Bioluminescence resonance energy transfer assays

We also tested the ability of these compounds to modulate the dynamics of oligomerization, as it has been suggested for other bivalent compounds [42]. With this aim, we compared the bioluminescence resonance energy transfer (BRET) obtained in untreated and treated HEK-293T cells transiently transfected with $A_{2A}R$-Rluc and D_2R-YFP (Figure 6.5) (see *Chapter 3 Methods*). Cotreatment with monovalent compounds **20**+**23** does not increase BRET relative to untreated cells. To our surprise, all bivalent compounds **24** (25-atoms, $p<0.05$), **25** (35-atoms, $p<0.001$), and **26** (43-atoms, $p<0.001$) increase BRET relative to untreated cells in a statistically significant manner. Importantly, **26**, but not **25** (no statistical differences), increases BRET more than **24** ($p<0.01$). We also analyzed the BRET signal obtained in cells treated with a negative control, a picomolar D_2R homobivalent ligand (homo-D_2R), previously reported by our

group [33], which contains two D_2R pharmacophores. Clearly, this compound does not increase the BRET signal relative to untreated cells despite containing two pharmacophores. Thus, our findings that compounds **24** and **25** with shorter spacer lengths increase BRET, in contrast to monovalent compounds or homo-D_2R, suggest the interaction of these compounds with the second protomer at the extracellular site, to stabilize dimer formation. In conclusion, the "true bivalent" ligand **26** favors heteromer stabilization by altering the monomer-dimer balance towards dimer formation. This is of interest in the pharmaceutical context as changes in $A_{2A}R$-D_2R heteromer population has been observed in pathological conditions such as Parkinson's disease [12] and schizophrenia [13].

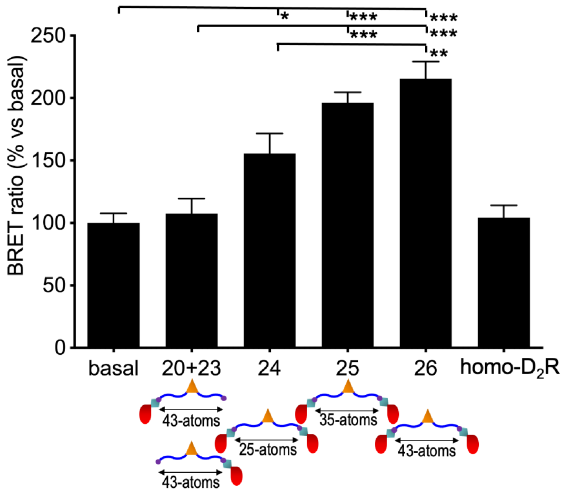

Figure 6.5: Influence of bivalent ligands on $A_{2A}R$-D_2R heterodimerization. BRET experiments were performed using HEK-293T cells transiently transfected with $A_{2A}R$-Rluc and D_2R-YFP treated or not with 100 nM of the corresponding ligands. Data show mean ± SEM in % vs basal of 8-10 different experiments. Statistical significance was calculated by one-way ANOVA followed by Bonferroni's multiple comparison post hoc test. $^*p < 0.05$, $^{**}p < 0.01$, $^{***}p < 0.001$.

6.1.3. Conclusions

We have designed, synthesized, and evaluated a set of potential heterobivalent ligands applying the strategy previously developed [33] that allows to (a) estimate potential distances between pharmacophores of bivalent ligands by computational tools that consider the different TM interfaces; (b) build the potential bivalent ligands by a modular chemical synthesis; and (c) precisely determine the binding mode of the potential bivalent ligands by radioligand competition-binding assays in the absence and presence of TAT-fused TM peptides that disrupt the receptor oligomer. As a result of this strategy, we have identified compound **26** [K_{DB1} ($A_{2A}R$) = 2.1 nM, K_{DB1} (D_2R) = 0.13 nM], with a spacer length of 43 atoms, as a "true bivalent" ligand that simultaneously binds both orthosteric sites of the $A_{2A}R$-D_2R heteromer.

We define **26** as a "true bivalent" ligand because (i) it enhances the binding affinity relative to the $A_{2A}R$ (4-fold) and D_2R (5-fold) pharmacophores, (ii) its binding affinity decreases in the presence of the TM5-TAT peptide (17-fold), (iii) it favors dimer stabilization, and (iv) it remains stable at the orthosteric binding cavities during three replicas of 1 µs unbiased MD simulation. We do not define compounds **24** (25-atoms) and **25** (35-atoms), with shorter spacer lengths, as "true bivalent" ligands because (i) they do not enhance the binding affinity relative to the D_2R and $A_{2A}R$ pharmacophores, and (ii) TM5-TAT does not decrease the binding affinity. However, (iii) **24** and **25** favor dimer stabilization but in a less efficient manner than **26**, and (iv) **25**, but not **24** (not shown), remains stable in MD simulations. These data show the importance of performing different experimental test to determine whether a bivalent ligand is capable of simultaneous binding to the orthosteric sites of the dimer. However, the influence of TAT-fused peptides in ligand binding affinities is, in our opinion, the most conclusive test.

We suggest that **26** with longer spacer length (43-atoms) simultaneously binds at the two orthosteric binding sites, whereas ligands with short spacers **24** (25-atoms) and **25** (35-atoms) might bind the orthosteric pocket of one protomer and a complementary extracellu-

lar site, different than the orthosteric site, of the second protomer, probably interacting through an alternating movement (see *Chapter 4*). This complementary cavity is often located at the entrance of the orthosteric binding site, as identified in ligand binding pathway simulations [43, 44], which has been named extracellular vestibule [44] or secondary [43, 45] or metastable [46] binding site, or exosite [47]. In particular, two meta-binding sites have been described for the human A_{2A} adenosine receptor, located in extracellular loops 2 and 3, which participate in the ligand recognition process [48, 49]. The importance of the dimer interface in the size of the spacer can be illustrated by the comparison between our previously reported homobivalent ligand for the D_2R homomer [33] (homo-D_2R) and **26**. Homo-D_2R requires an optimal spacer length of 25-atoms for the TM6 interface of the D_2R homomer, whereas **26** requires an optimal spacer length of 43-atoms for the TM4/5 interface of the $A_{2A}R$-D_2R heteromer.

Drugs targeting a specific receptor heteromer can potentially be more efficiently in a particular cell type, cellular domain, or disease [29, 31, 32, 50, 51]. Heterobivalent compound **26** would be useful, for instance, for the treatment of schizophrenia, but some issues as compound capacity to cross the blood-brain barrier among others should be considered.

6.2. Case study 5. A heterotetravalent ligand for a G protein-coupled receptor heterotetramer

To be submitted as

Daniel Pulido[1], Verònica Casadó-Anguera[1], Marc Gómez-Autet[1], Natàlia Llopart, Estefanía Moreno, Laura Pérez-Benito, Nil Casajuana-Martin, Sergi Ferré, Leonardo Pardo[*], Vicent Casadó[*], Miriam Royo[*]. **A heterotetravalent ligand for a G protein-coupled receptor heterotetramer.** In preparation.

[1]These authors contributed equally.

6.2.1. Introduction

Single-molecule microscopy techniques [52] have shown that GPCRs are present in a dynamic equilibrium between monomers, dimers, and tetramers [53–56]. Thus, the preferential number and composition of protomers in the heteromer is a key factor in the design of multitarget compounds. Of special functional significance are those heteromers constituted by one homodimer coupled to a G_s protein and another different homodimer coupled to a G_i protein, a GPCR heterotetramer [57–59]. Examples of GPCR heterotetramers, in which one of its constituents is the adenosine A_{2A} receptor ($A_{2A}R$), are the A_1R-$A_{2A}R$ [60], $A_{2A}R$-$A_{2B}R$ [61], $A_{2A}R$-CB_1R [62], and $A_{2A}R$-D_2R [60], among others, in all cases with a cell surface 2:2 receptor stoichiometry (dimer of dimers).

Knowledge of the stoichiometry is fundamental, but the knowledge of the molecular interfaces by which the protomers interact is key to understand the quaternary arrangement of the protomers in the heterotetramer. The use of synthetic peptides with the sequence of the transmembrane (TM) domains of the receptor fused to the cell-penetrating HIV transactivator of transcription (TAT) peptide (YGRKKRRQRRR) [36, 63], to disrupt bimolecular fluorescence complementation (BiFC) signals attained by receptors fused to two complementary halves of YFP (cYFP and nYFP), has been very valuable to predict contacts among TM domains of interacting GPCRs (see *Chapter 3 Methods*) [10, 56, 60–62, 64]. Using this approach, we had previously identified the TM interfaces involved in $A_{2A}R$-D_2R heterodimerization (TM4/5) and $A_{2A}R$ and D_2R homodimerization (TM6) [60]. This structural information about TM interfaces were used to design a homobivalent ligand for the D_2R homodimer [33], and a heterobivalent ligand for the $A_{2A}R$-D_2R heteromer (see section 6.1) [65]. Here, using this experience and a combination of computational, chemical, and biochemical tools, we have designed and synthesized heterotetravalent ligands for the $A_{2A}R$-D_2R heterotetramer.

6.2.2. Results

Molecular design of homobivalent ligands for the $A_{2A}R$ homodimer

As noted in the introduction, the $A_{2A}R$-D_2R heterotetramer is formed by one homodimer of $A_{2A}R$ and one homodimer of D_2R [10]. It has been previously obtained a homobivalent ligand for the D_2R homodimer [33], therefore, with the ultimate objective of obtaining heterotetravalent ligands for the the $A_{2A}R$-D_2R heterotetramer, we first need to obtain a homobivalent ligand for the $A_{2A}R$ homodimer. The design followed similar trends as in our reported heterobivalent ligand for the $A_{2A}R$-D_2R heteromer (see section 6.1) [65]. (i) The main scaffold is the nitrilotriacetic acid (NTA) that contains three symmetric carboxylic acids [34], permitting the attachment of

two pharmacophore-containing chains, for the $A_{2A}R$ homobivalent ligand, and an additional chain capable of linking to the other NTA scaffold of the D_2R homobivalent ligand [33], to ultimately form the tetravalent ligand (see below). (ii) The selected $A_{2A}R$ pharmacophore is a derivative of the selective antagonist SCH-442,416, 2-(4-(3-(5-amino-2-(furan-2-yl)-7H-pyrazolo[4,3-e][1,2,4]triazolo[1,5-c]pyrimidin-7-yl)propyl)phenoxy)acetic acid, which includes in its structure a phenoxyacetic acid moiety that allows its integration into the bivalent system, as in our previous study (see section 6.1) [65]. (iii) The spacer length of the $A_{2A}R$ homobivalent ligand was calculated for the TM6 interface of the $A_{2A}R$ homodimer, as previously determined [10], using a computational tool developed for the Molecular Operating Environment (MOE) software (Chemical Computing Group Inc., Montreal, Quebec, Canada) (see *Chapter 3 Methods*) [35]. The selected spacers were oligoethylene glycol (OEG) moieties, with the aim to increase water solubility of the final bivalent ligands, of different lengths $(\text{-OCH2CH2-})_{n=1\text{-}4}$. The predicted lengths of energetically favorable spacer/scaffold/spacer groups are between 25 (n=2) and 35 (n=3) atoms, calculated between attachment atoms shown in purple in Figure 6.6. Figure 6.7A shows molecular dynamic (MD) simulations (see *Chapter 3 Methods*) of compound **18** (n=3) in the previously obtained computational model of the $A_{2A}R$ homodimer [10]. The binding of the pharmacophore units to the two orthosteric sites of the homodimer was monitored by the hydrogen bond distance between the adenine moiety of the SCH-442,416 pharmacophore and $Asn^{6.55}$ of $A_{2A}R$ (Figure 6.7B). These interactions remain stable throughout three replicas of 1 µs unbiased MD simulation, suggesting that compound **18** can fulfill the simultaneous binding of the pharmacophoric units to the orthosteric binding sites. Importantly, the pharmacophore units of compound **17** with a spacer length of 25 atoms (n=2) also remain stable in the orthosteric binding sites during similar MD simulations (not shown). Thus, spacer lengths of 25 (n=2) and 35 (n=3) atoms were used as recommendations for synthesis. The synthesis of these compounds was performed by Daniel Pulido and Miriam Royo at the Department of Surfactants and Nanobiotechnology, Institute for

Advanced Chemistry of Catalonia (IQAC-CSIC), Barcelona (Spain). *In vitro* binding affinities of the suggested $A_{2A}R$ homodimer ligands **17** (25-atoms, K_{DB1} = 1.5 nM) and **18** (35-atoms, K_{DB1} = 1.1 nM) were obtained from [^{3}H]ZM 241385 radioligand competition-binding assays (see *Chapter 3 Methods*), by Verònica Casadó-Anguera and Vicent Casadó at the Department of Biochemistry and Molecular Biomedicine, Faculty of Biology, Universitat de Barcelona, Barcelona (Spain), using membranes from sheep brain striatum that naturally express $A_{2A}R$.

Molecular design of heterotetravalent ligands for the $A_{2A}R$-D_2R heterotetramer

Due to their best experimental binding affinities, we have selected compound **14** with a spacer length of 25 atoms (n=2) as a homobivalent ligand for the D_2R homodimer, previously reported [10], and compound **18** with a spacer length of 35 atoms (n=3) as a homobivalent ligand for the $A_{2A}R$ homodimer, reported in this thesis, to build heterotetravalent ligands for the $A_{2A}R$-D_2R heterotetramer (Figure 6.6). Figure 6.7A shows MD simulations of these compounds in the D_2R and the $A_{2A}R$ tetramer. These simulations, within the constructed $A_{2A}R$-D_2R heterotetramer via the TM6 interface in homo- and TM4/5 interface in hetero-dimerization [10], were used to calculate the optimal distance between NTA scaffolds of the D_2R and $A_{2A}R$ homobivalent ligands. Figure 6.7A (right) shows the histogram distribution of the distance between nitrogen atoms of the NTA scaffolds. This analysis illustrates optimal distances between ≈50-60 Å. We calculated the preferred spacer length by adjusting different spacer moieties to the van der Waals surface of the heterotetramer, using a computational tool developed for the MOE software (Chemical Computing Group Inc., Montreal, Quebec, Canada) [35] (see *Chapter 3 Methods*), as done before in this thesis. The predicted lengths of energetically favorable lengths are 31 (m=n=2, o=3), 34 (m=n=2, o=4), and 41 (m=1, n=6, o=3) atoms, calculated between the nitrogen atoms of the NTA scaffolds (Figure 6.6). Figure 6.7C shows molecular dynamic (MD) simulations (see *Chapter 3 Methods*) of compound

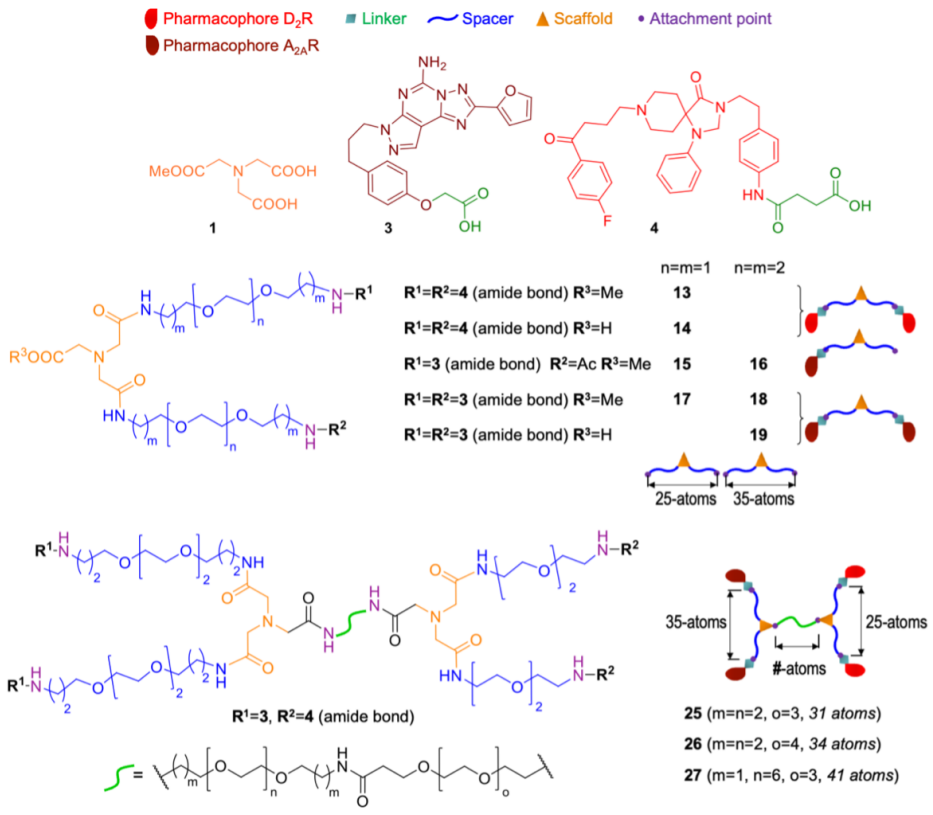

Figure 6.6: The $A_{2A}R$ homobivalent ligand contains (i) a scaffold that can be properly derivatized (in orange), (ii) pharmacophore units (in red) that bind the orthosteric binding site of $A_{2A}R$ (**4**) with high affinity, (iii) a spacer to cover the distance between both protomers of the heteromer (in blue), and (iv) a linker (in green) between the pharmacophore units and the spacer, adequate for the chemistry used for conjugation. The $A_{2A}R$-D_2R heterotetravalent ligand consists of an $A_{2A}R$ homobivalent ligand and a D_2R homobivalent ligand linked by a spacer of specific length (lime green).

26 (m=n=2, o=4) with a spacer length of 34 atoms. The interactions of the pharmacophoric units within the orthosteric binding sites of the four receptors remain stable throughout three replicas of 1 µs unbiased MD simulations (Figure 6.7D). With this, spacer lengths between the NTA scaffolds of 31 (**25**), 34 (**26**) and 41 (**27**) atoms were suggested for synthesis (dashed red lines in Figure 6.7A (right)). The synthesis of these compounds was performed by Daniel Pulido and Miriam Royo at the Department of Surfactants and Nanobiotechnology, Institute for Advanced Chemistry of Catalonia (IQAC-CSIC), Barcelona (Spain). *In vitro* binding affinities of compound **26** [(K_{DB1} ($A_{2A}R$) = 0.3 nM; K_{DB1} (D_2R) = 0.1 nM] were obtained from from [^{3}H]ZM 241 385 or [^{3}H]YM-09151-2 radioligand competition-binding assays (see *Chapter 3 Methods*) by Verònica Casadó-Anguera and Vicent Casadó at the Department of Biochemistry and Molecular Biomedicine, Faculty of Biology, Universitat de Barcelona, Barcelona (Spain).

6.2.3. Conclusions

This work, not yet finished, has permitted to identify a heterotetravalent ligand for the $A_{2A}R$-D_2R heterotetramer, with exceptional high affinity in the sub-nanomolar range for both receptors, which is remarkable for ligands of this size and complexity. However, the precise binding mode of this compound to the heterotetramer remains to be determined. The influence of TAT-fused peptides in ligand binding affinities is an ongoing task to accomplish this objective.

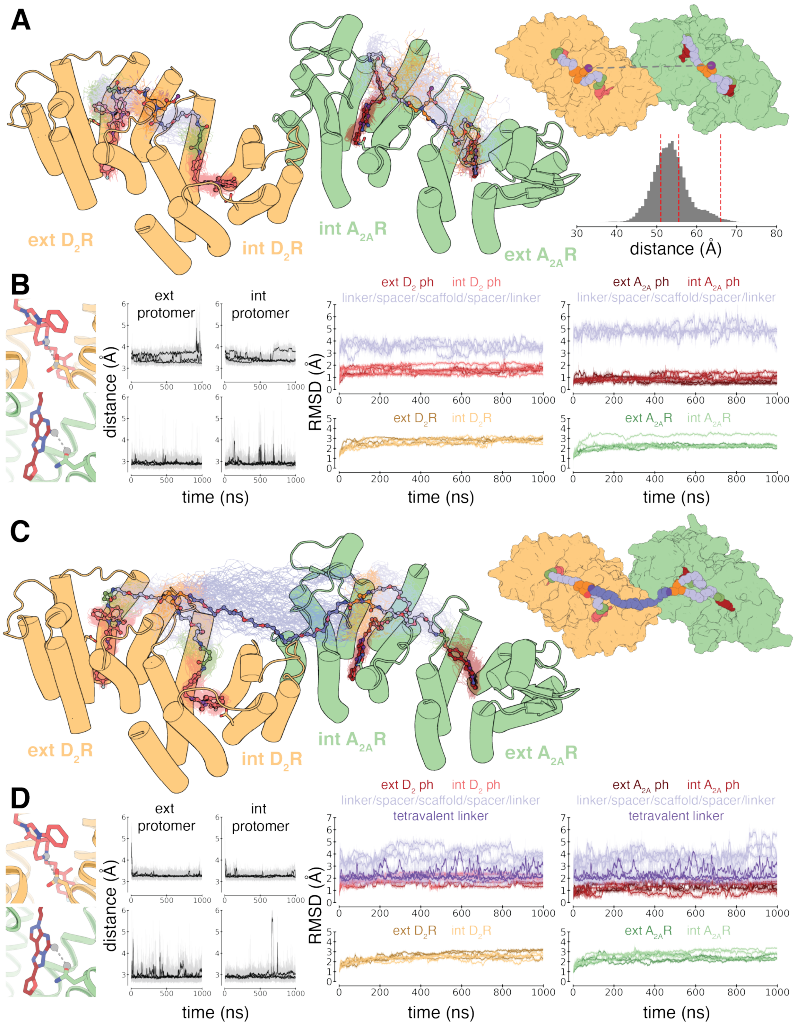

Figure 6.7: (A) MD simulations of homobivalent compunds **14** and **18** in the A^{2A}-D_2R tetramer (left) and the histogram distribution of the distance between nitrogen atoms of the NTA scaffolds during the simulation. (B) Binding of the pharmacophore units of **14** and **18** monitored by the salt bridge distance between the protonated amine of the NAPS pharmacophore and the Cγatom of $Asp^{3.32}$ of D_2R and the hydrogen bond distance between the -NH2 group of the adenine moiety of the SCH-442,416 pharmacophore and the $O_{\delta 1}$ atom of $Asn^{6.55}$ of $A_{2A}R$ (dashed gray line between gray spheres). The stability of the ligand-heteromer complex was analyzed via root-mean-square deviations (rmsds). (C,D) MD simulations and analysis of the heterotetravalent compound **18**(see above). ext: external, int: internal, ph: pharmacophore.

Bibliography

[1] A. Kabir, A. Muth, "Polypharmacology: The science of multi-targeting molecules", *Pharmacological research* **2022**, *176*.

[2] P. M. Sexton, A. Christopoulos, "To Bind or Not to Bind: Unravelling GPCR Polypharmacology", *Cell* **2018**, *172*, 636–638.

[3] A. I. Casas, A. A. Hassan, S. J. Larsen, V. Gomez-Rangel, M. Elbatreek, P. W. Kleikers, E. Guney, J. Egea, M. G. López, J. Baumbach, H. H. Schmidt, "From single drug targets to synergistic network pharmacology in ischemic stroke", *Proceedings of the National Academy of Sciences of the United States of America* **2019**, *116*, 7129–7136.

[4] C. Nogales, Z. M. Mamdouh, M. List, C. Kiel, A. I. Casas, H. H. Schmidt, "Network pharmacology: curing causal mechanisms instead of treating symptoms", *Trends in pharmacological sciences* **2022**, *43*, 136–150.

[5] O. B. Smeland, O. Frei, A. M. Dale, O. A. Andreassen, "The polygenic architecture of schizophrenia - rethinking pathogenesis and nosology", *Nature reviews. Neurology* **2020**, *16*, 366–379.

[6] A. K. Merikangas, M. Shelly, A. Knighton, N. Kotler, N. Tanenbaum, L. Almasy, "What genes are differentially expressed in individuals with schizophrenia? A systematic review", *Molecular psychiatry* **2022**, *27*, 1373–1383.

[7] A. A. Grace, "Dysregulation of the dopamine system in the pathophysiology of schizophrenia and depression", *Nature reviews. Neuroscience* **2016**, *17*, 524–532.

[8] J. M. Beaulieu, R. R. Gainetdinov, "The physiology, signaling, and pharmacology of dopamine receptors", *Pharmacological reviews* **2011**, *63*, 182–217.

[9] P. Trifilieff, M. L. Rives, E. Urizar, R. A. Piskorowski, H. D. Vishwasrao, J. Castrillon, C. Schmauss, M. Slättman, M. Gullberg, J. A. Javitch, "Detection of antigen interactions ex vivo by proximity ligation assay: Endogenous dopamine D2-adenosine A2A receptor complexes in the striatum", *BioTechniques* **2011**, *51*, 111–118.

[10] G. Navarro, A. Cordomí, V. Casadó-Anguera, E. Moreno, N. S. Cai, A. Cortés, E. I. Canela, C. W. Dessauer, V. Casadó, L. Pardo, C. Lluís, S. Ferré, "Evidence for functional pre-coupled complexes of receptor heteromers and adenylyl cyclase", *Nature Communications 2018 9:1* **2018**, *9*, 1–12.

[11] M. Canals, D. Marcellino, F. Fanelli, F. Ciruela, P. D. Benedetti, S. R. Goldberg, K. Neve, K. Fuxe, L. F. Agnati, A. S. Woods, S. Ferré, C. Lluis, M. Bouvier, R. Franco, "Adenosine A2A-dopamine D2 receptor-receptor heteromerization: Qualitative and quantitative assessment by fluorescence and bioluminescence energy transfer", *Journal of Biological Chemistry* **2003**, *278*, 46741–46749.

[12] V. Fernández-Dueñas, M. Gómez-Soler, M. Valle-León, M. Watanabe, I. Ferrer, F. Ciruela, "Revealing Adenosine A2A-Dopamine D2 Receptor Heteromers in Parkinson's Disease Post-Mortem Brain through a New AlphaScreen-Based Assay", *International Journal of Molecular Sciences 2019 Vol. 20 Page 3600* **2019**, *20*, 3600.

[13] M. Valle-León, L. F. Callado, E. Aso, M. M. Cajiao-Manrique, K. Sahlholm, M. López-Cano, C. Soler, X. Altafaj, M. Watanabe, S. Ferré, V. Fernández-Dueñas, J. M. Menchón, F. Ciruela, "Decreased striatal adenosine A2A-dopamine D2 receptor heteromerization in schizophrenia", *Neuropsychopharmacology* **2020**, *46*, 665–672.

[14] M. Valle-León, L. F. Callado, E. Aso, M. M. Cajiao-Manrique, K. Sahlholm, M. López-Cano, C. Soler, X. Altafaj, M. Watanabe, S. Ferré, V. Fernández-Dueñas, J. M. Menchón, F. Ciruela, "Decreased striatal adenosine A2A-dopamine D2 receptor heteromerization in schizophrenia", *Neuropsychopharmacology* **2021**, *46*, 665–672.

[15] S. Kampen, D. D. Vo, X. Zhang, N. Panel, Y. Yang, M. Jaiteh, P. Matricon, P. Svenningsson, J. Brea, M. I. Loza, J. Kihlberg, J. Carlsson, "Structure-Guided Design of G-Protein-Coupled Receptor Polypharmacology", *Angewandte Chemie International Edition* **2021**, *60*, 18022–18030.

[16] A. Soriano, R. Ventura, A. Molero, R. Hoen, V. Casado, A. Corte, F. Fanelli, F. Albericio, C. Lluís, R. Franco, M. Royo, "Adenosine A2A receptor-antagonist/dopamine D2 receptor-agonist bivalent ligands as pharmacological tools to detect A 2A-D2 receptor heteromers", *Journal of Medicinal Chemistry* **2009**, *52*, 5590–5602.

[17] M. Bouvier, T. E. Hébert, "CrossTalk proposal: Weighing the evidence for Class A GPCR dimers, the evidence favours dimers", *The Journal of Physiology* **2014**, *592*, 2439–2441.

[18] N. A. Lambert, J. A. Javitch, "CrossTalk opposing view: Weighing the evidence for class A GPCR dimers, the jury is still out", *The Journal of Physiology* **2014**, *592*, 2443–2445.

[19] M. R. Whorton, M. P. Bokoch, S. G. Rasmussen, B. Huang, R. N. Zare, B. Kobilka, R. K. Sunahara, "A monomeric G protein-coupled receptor isolated in a high-density lipoprotein particle efficiently activates its G protein", *Proceedings of the National Academy of Sciences of the United States of America* **2007**, *104*, 7682–7687.

[20] S. Ferré, V. Casadó, L. A. Devi, M. Filizola, R. Jockers, M. J. Lohse, G. Milligan, J. P. Pin, X. Guitart, "G Protein–Coupled Receptor Oligomerization Revisited: Functional and Pharmacological Perspectives", *Pharmacological Reviews* **2014**, *66*, 413–434.

[21] K. Herrick-Davis, E. Grinde, A. Cowan, J. E. Mazurkiewicz, "Fluorescence Correlation Spectroscopy Analysis of Serotonin, Adrenergic, Muscarinic, and Dopamine Receptor Dimerization: The Oligomer Number Puzzle", *Molecular Pharmacology* **2013**, *84*, 630–642.

[22] S. Ferré, R. Baler, M. Bouvier, M. G. Caron, L. A. Devi, T. Durroux, K. Fuxe, S. R. George, J. A. Javitch, M. J. Lohse, K. Mackie, G. Milligan, K. D. Pfleger, J. P. Pin, N. D. Volkow, M. Waldhoer, A. S. Woods, R. Franco, "Building a new conceptual framework for receptor heteromers", *Nature Chemical Biology 2009 5:3* **2009**, *5*, 131–134.

[23] M. Fribourg, J. L. Moreno, T. Holloway, D. Provasi, L. Baki, R. Mahajan, G. Park, S. K. Adney, C. Hatcher, J. M. Eltit, J. D. Ruta, L. Albizu, Z. Li, A. Umali, J. Shim, A. Fabiato, A. D. MacKerell, V. Brezina, S. C. Sealfon, M. Filizola, J. González-Maeso, D. E. Logothetis, "Decoding the signaling of a GPCR heteromeric complex reveals a unifying mechanism of action of antipsychotic drugs", *Cell* **2011**, *147*, 1011–1023.

[24] K. Baba, A. Benleulmi-Chaachoua, A. S. Journé, M. Kamal, J. L. Guillaume, S. Dussaud, F. Gbahou, K. Yettou, C. Liu, S. Contreras-Alcantara, R. Jockers, G. Tosini, "Heteromeric MT1/MT2 melatonin receptors modulate photoreceptor function", *Science Signaling* **2013**, *6*.

[25] N. S. Cai, C. Quiroz, J. Bonaventura, A. Bonifazi, T. O. Cole, J. Purks, A. S. Billing, E. Massey, M. Wagner, E. D. Wish, X. Guitart, W. Rea, S. Lam, E. Moreno, V. Casadó-Anguera, A. D. Greenblatt, A. E. Jacobson, K. C. Rice, V. Casadó, A. H. Newman, J. W. Winkelman, M. Michaelides, E. Weintraub, N. D. Volkow, A. M. Belcher, S. Ferré, "Opioid–galanin receptor

heteromers mediate the dopaminergic effects of opioids", *The Journal of Clinical Investigation* **2019**, *129*, 2730–2744.

[26] D. Guinart, E. Moreno, L. Galindo, A. Cuenca-Royo, M. Barrera-Conde, E. J. Pérez, C. Fernández-Avilés, C. U. Correll, E. I. Canela, V. Casadó, A. Cordomi, L. Pardo, R. D. L. Torre, V. Pérez, P. Robledo, "Altered Signaling in CB1R-5-HT2AR Heteromers in Olfactory Neuroepithelium Cells of Schizophrenia Patients is Modulated by Cannabis Use", *Schizophrenia Bulletin* **2020**, *46*, 1547–1557.

[27] V. Casadó, A. Cortés, J. Mallol, K. Pérez-Capote, S. Ferré, C. Lluis, R. Franco, E. I. Canela, "GPCR homomers and heteromers: A better choice as targets for drug development than GPCR monomers?", *Pharmacology & Therapeutics* **2009**, *124*, 248–257.

[28] R. Rozenfeld, L. A. Devi, "Receptor heteromerization and drug discovery", *Trends in Pharmacological Sciences* **2010**, *31*, 124–130.

[29] I. Gomes, M. A. Ayoub, W. Fujita, W. C. Jaeger, K. D. Pfleger, L. A. Devi, "G Protein–Coupled Receptor Heteromers", *Annual Review of Pharmacology and Toxicology* **2016**, *56*, 403–425.

[30] A. Gupta, J. Mulder, I. Gomes, R. Rozenfeld, I. Bushlin, E. Ong, M. Lim, E. Maillet, M. Junek, C. M. Cahill, T. Harkany, L. A. Devi, "Increased abundance of opioid receptor heteromers after chronic morphine administration", *Science Signaling* **2010**, *3*.

[31] V. Casadó-Anguera, A. Cortés, V. Casadó, E. Moreno, "Targeting the receptor-based interactome of the dopamine D1 receptor: looking for heteromer-selective drugs", *Expert Opinion on Drug Discovery* **2019**, *14*, 1297–1312.

[32] A. Cortés, E. Moreno, M. Rodríguez-Ruiz, E. I. Canela, V. Casadó, "Targeting the dopamine D3 receptor: an overview of drug design strategies", *Expert Opinion on Drug Discovery* **2016**, *11*, 641–664.

[33] D. Pulido, V. Casadó-Anguera, L. Pérez-Benito, E. Moreno, A. Cordomí, L. López, A. Cortés, S. Ferré, L. Pardo, V. Casadó, M. Royo, "Design of a True Bivalent Ligand with Picomolar Binding Affinity for a G Protein-Coupled Receptor Homodimer", *Journal of Medicinal Chemistry* **2018**, *61*, 9335–9346.

[34] D. Pulido, F. Albericio, M. Royo, "Controlling multivalency and multimodality: Up to pentamodal dendritic platforms based on diethylenetriaminepentaacetic acid cores", *Organic Letters* **2014**, *16*, 1318–1321.

[35] L. Pérez-Benito, A. Henry, M. T. Matsoukas, L. Lopez, D. Pulido, M. Royo, A. Cordomí, G. Tresadern, L. Pardo, "The size matters? A computational tool to design bivalent ligands", *Bioinformatics* **2018**, *34*, 3857–3863.

[36] S. R. Schwarze, A. Ho, A. Vocero-Akbani, S. F. Dowdy, "In vivo protein transduction: delivery of a biologically active protein into the mouse", *Science* **1999**, *285*, 1569–1572.

[37] V. Casadó, A. Cortés, F. Ciruela, J. Mallol, S. Ferré, C. Lluis, E. I. Canela, R. Franco, "Old and new ways to calculate the affinity of agonists and antagonists interacting with G-protein-coupled monomeric and dimeric receptors: The receptor–dimer cooperativity index", *Pharmacology & Therapeutics* **2007**, *116*, 343–354.

[38] M. Orru, J. Bakešová, M. Brugarolas, C. Quiroz, V. Beaumont, S. R. Goldberg, C. Lluís, A. Cortés, R. Franco, V. Casadó, E. I. Canela, S. Ferré, "Striatal Pre- and Postsynaptic Profile of Adenosine A2A Receptor Antagonists", *PloS one* **2011**, *6*, e16088.

[39] J. Numata, A. Juneja, D. J. Diestler, E. W. Knapp, "Influence of spacer-receptor interactions on the stability of bivalent ligand-receptor complexes", *Journal of Physical Chemistry B* **2012**, *116*, 2595–2604.

[40] L. L. Kiessling, J. E. Gestwicki, L. E. Strong, "Synthetic Multivalent Ligands as Probes of Signal Transduction", *Angewandte Chemie International Edition* **2006**, *45*, 2348–2368.

[41] J. Bonaventura, G. Navarro, V. Casadó-Anguera, K. Azdad, W. Rea, E. Moreno, M. Brugarolas, J. Mallol, E. I. Canela, C. Lluís, A. Cortés, N. D. Volkowd, S. N. Schiffmann, S. Ferré, V. Casadó, "Allosteric interactions between agonists and antagonists within the adenosine A2A receptordopamine D2 receptor heterotetramer", *Proceedings of the National Academy of Sciences of the United States of America* **2015**, *112*, E3609–E3618.

[42] T. Ullmann, M. Gienger, J. Budzinski, J. Hellmann, H. Hübner, P. Gmeiner, D. Weikert, "Homobivalent Dopamine D2Receptor Ligands Modulate the Dynamic Equilibrium of D2Monomers and Homo- And Heterodimers", *ACS Chemical Biology* **2021**, *16*, 371–379.

[43] A. González, T. Perez-Acle, L. Pardo, X. Deupi, "Molecular Basis of Ligand Dissociation in β-Adrenergic Receptors", *PloS one* **2011**, *6*, e23815.

[44] R. O. Dror, A. C. Pan, D. H. Arlow, D. W. Borhani, P. Maragakis, Y. Shan, H. Xu, D. E. Shaw, "Pathway and mechanism of drug binding to G-protein-coupled receptors", *Proceedings of the National Academy of Sciences of the United States of America* **2011**, *108*, 13118–13123.

[45] A. H. Newman, F. O. Battiti, A. Bonifazi, "2016 Philip S. Portoghese Medicinal Chemistry Lectureship: Designing Bivalent or Bitopic Molecules for G-Protein Coupled Receptors. The Whole Is Greater Than the Sum of Its Parts", *Journal of medicinal chemistry* **2020**, *63*, 1779–1797.

[46] P. Fronik, B. I. Gaiser, D. S. Pedersen, "Bitopic Ligands and Metastable Binding Sites: Opportunities for G Protein-Coupled Receptor (GPCR) Medicinal Chemistry", *Journal of Medicinal Chemistry* **2017**, *60*, 4126–4134.

[47] M. Masureel, Y. Zou, L. P. Picard, E. van der Westhuizen, J. P. Mahoney, J. P. Rodrigues, T. J. Mildorf, R. O. Dror, D. E. Shaw, M. Bouvier, E. Pardon, J. Steyaert, R. K. Sunahara, W. I. Weis, C. Zhang, B. K. Kobilka, "Structural insights into binding specificity, efficacy and bias of a β2AR partial agonist", *Nature Chemical Biology* **2018**, *14*, 1059–1066.

[48] D. Sabbadin, S. Moro, "Supervised molecular dynamics (SuMD) as a helpful tool to depict GPCR-ligand recognition pathway in a nanosecond time scale", *Journal of Chemical Information and Modeling* **2014**, *54*, 372–376.

[49] D. Sabbadin, A. Ciancetta, G. Deganutti, A. Cuzzolin, S. Moro, "Exploring the recognition pathway at the human A2A adenosine receptor of the endogenous agonist adenosine using supervised molecular dynamics simulations", *MedChemComm* **2015**, *6*, 1081–1085.

[50] M. Rivera-Oliver, E. Moreno, Y. Álvarez-Bagnarol, C. Ayala-Santiago, N. Cruz-Reyes, G. C. Molina-Castro, S. Clemens, E. I. Canela, S. Ferré, V. Casadó, M. Díaz-Ríos, "Adenosine A 1 -Dopamine D 1 Receptor Heteromers Control the Excitability of the Spinal Motoneuron", *Molecular Neurobiology* **2019**, *56*, 797–811.

[51] V. Casadó, C. Ferrada, J. Bonaventura, E. Gracia, J. Mallol, E. I. Canela, C. Lluís, A. Cortés, R. Franco, "Useful pharmacological parameters for G-protein-coupled receptor homodimers obtained from competition experiments. Agonist–antagonist binding modulation", *Biochemical Pharmacology* **2009**, *78*, 1456–1463.

[52] J. H. Felce, S. J. Davis, D. Klenerman, "Single-Molecule Analysis of G Protein-Coupled Receptor Stoichiometry: Approaches and Limitations", *Trends in pharmacological sciences* **2018**, *39*, 96–108.

[53] G. Navarro, A. Cordomí, M. Zelman-Femiak, M. Brugarolas, E. Moreno, D. Aguinaga, L. Perez-Benito, A. Cortés, V. Casadó, J. Mallol, E. I. Canela, C. Lluís, L. Pardo, A. J. García-Sáez, P. J. McCormick, R. Franco, "Quaternary structure of a G-protein-coupled receptor heterotetramer in complex with Gi and Gs", *BMC biology* **2016**, *14*.

[54] P. M. Dijkman, O. K. Castell, A. D. Goddard, J. C. Munoz-Garcia, C. D. Graaf, M. I. Wallace, A. Watts, "Dynamic tuneable G protein-coupled receptor monomer-dimer populations", *Nature communications* **2018**, *9*.

[55] J. Möller, A. Isbilir, T. Sungkaworn, B. Osberg, C. Karathanasis, V. Sunkara, E. O. Grushevskyi, A. Bock, P. Annibale, M. Heilemann, C. Schütte, M. J. Lohse, "Single-molecule analysis reveals agonist-specific dimer formation of μ-opioid receptors", *Nature chemical biology* **2020**, *16*, 946–954.

[56] P. A. D. Oliveira, E. Moreno, N. Casajuana-Martin, V. Casadó-Anguera, N. S. Cai, G. A. Camacho-Hernandez, H. Zhu, A. Bonifazi, M. D. Hall, D. Weinshenker, A. H. Newman, D. E. Logothetis, V. Casadó, L. D. Plant, L. Pardo, S. Ferré, "Preferential Gs protein coupling of the galanin Gal1 receptor in the μ-opioid-Gal1 receptor heterotetramer", *Pharmacological research* **2022**, *182*.

[57] S. Ferré, "The GPCR heterotetramer: challenging classical pharmacology", *Trends in pharmacological sciences* **2015**, *36*, 145–152.

[58] R. Franco, A. Cordomí, C. L. del Torrent, A. Lillo, J. Serrano-Marín, G. Navarro, L. Pardo, "Structure and function of adenosine receptor heteromers", *Cellular and molecular life sciences : CMLS* **2021**, *78*, 3957–3968.

[59] S. Ferré, F. Ciruela, C. W. Dessauer, J. González-Maeso, T. E. Hébert, R. Jockers, D. E. Logothetis, L. Pardo, "G protein-coupled receptor-effector macromolecular membrane assemblies (GEMMAs)", *Pharmacology & therapeutics* **2022**, *231*.

[60] G. Navarro, A. Cordomí, M. Brugarolas, E. Moreno, D. Aguinaga, L. Pérez-Benito, S. Ferre, A. Cortés, V. Casadó, J. Mallol, E. I. Canela, C. Lluís, L. Pardo, P. J. McCormick, R. Franco, "Cross-communication between Gi and Gs in a G-protein-coupled receptor heterotetramer guided by a receptor C-terminal domain", *BMC biology* **2018**, *16*.

[61] T. Gnad, G. Navarro, M. Lahesmaa, L. Reverte-Salisa, F. Copperi, A. Cordomi, J. Naumann, A. Hochhäuser, S. Haufs-Brusberg, D. Wenzel, F. Suhr, N. Z. Jespersen, C. Scheele, V. Tsvilovskyy, C. Brinkmann, J. Rittweger, C. Dani, M. Kranz, W. Deuther-Conrad, H. K. Eltzschig, T. Niemi, M. Taittonen, P. Brust, P. Nuutila, L. Pardo, B. K. Fleischmann, M. Blüher, R. Franco, W. Bloch, K. A. Virtanen, A. Pfeifer, "Adenosine/A2B Receptor Signaling Ameliorates the Effects of Aging and Counteracts Obesity", *Cell metabolism* **2020**, *32*, 56–70.e7.

[62] A. Köfalvi, E. Moreno, A. Cordomí, N. S. Cai, V. Fernández-Dueñas, S. G. Ferreira, R. Guixà-González, M. Sánchez-Soto, H. Yano, V. Casadó-Anguera, R. A. Cunha, A. M. Sebastião, F. Ciruela, L. Pardo, V. Casadó, S. Ferré, "Control of glutamate release by complexes of adenosine and cannabinoid receptors", *BMC biology* **2020**, *18*.

[63] S. Q. He, Z. N. Zhang, J. S. Guan, H. R. Liu, B. Zhao, H. B. Wang, Q. Li, H. Yang, J. Luo, Z. Y. Li, Q. Wang, Y. J. Lu, L. Bao, X. Zhang, "Facilitation of μ-Opioid Receptor Activity by Preventing δ-Opioid Receptor-Mediated Codegradation", *Neuron* **2011**, *69*, 120–131.

[64] E. Moreno, N. Casajuana-Martin, M. Coyle, B. C. Campos, E. Galaj, C. L. del Torrent, A. Seyedian, W. Rea, N. S. Cai, A. Bonifazi, B. Florán, Z. X. Xi, X. Guitart, V. Casadó, A. H. Newman, C. Bishop, L. Pardo, S. Ferré, "Pharmacological targeting of G protein-coupled receptor heteromers", *Pharmacological research* **2022**, *185*.

[65] D. Pulido, V. Casadó-Anguera, M. Gómez-Autet, N. Llopart, E. Moreno, N. Casajuana-Martin, S. Ferré, L. Pardo, V. Casadó, M. Royo, "Heterobivalent Ligand for the Adenosine A2A-Dopamine D2 Receptor Heteromer", *Journal of medicinal chemistry* **2022**, *65*, 616–632.

Chapter 7

General discussion

GPCRs regulate a vast number of cellular processes [1], and their malfunction, with 435 disease-associated mutations [2], commonly translates into pathological outcomes [3]. Thus, they form one of the most important pharmaceutical drug-target class (475 drugs in the market that represent ≈34% of all drugs approved by the US Food and Drug Administration) [4]. However, these drugs target only 108 unique GPCRs, which represent <10% of all known GPCRs (or ≈30% of the ≈360 non-olfactory GPCRs), but account for ≈27% of the global market share of therapeutic drugs, with aggregated sales for 2011–2015 of ≈US$890 billion [5]. Thus, the GPCR family is globally underused regarding its potential in drug discovery.

Traditional drug design programs for GPCRs have been dominated by efforts to develop compounds that act as agonists, partial agonists, antagonists, or inverse agonists by binding to the orthosteric site of the receptor, a conserved pocket that optimally accommodates the electrostatic and steric properties of the endogenous ligand. However, this approach is often unfavorable because orthosteric binding sites are highly conserved, making it difficult to achieve high selectivity for specific GPCR subtypes.

The recent analysis of the pocketome of GPCRs has shown multitude non-conserved pockets in addition to the orthosteric pocket [6]. These are located at the membrane-facing part of the receptor, at the entrance (vestibule, secondary, or metastable site or exosite) of the or-

thosteric site, as previously suggested by molecular dynamics (MD) simulations [7, 8], and others. Pharmacophoric moieties that bind at the orthosteric site exhibit high-affinity for the receptor, whereas pharmacophores that bind at these non-conserved pockets exhibit receptor selectivity [9–11]. The bivalent approach [12] bridges these two pharmacophores covalently by a spacer for selectivity, off-rates, and signaling bias [13–15].

GPCRs can also engage protein-protein allosteric interactions among them, by forming complexes constituted by the same (homo) or different (hetero) receptor protomers [16]. Drugs targeting a specific heteromer can potentially be more efficient in a particular cell type, cellular domain, or disease [17]. One proposed approach to target these GPCR heteromers is based on the use of bivalent ligands [18], i.e. ligands composed of two covalently linked (through a spacer) pharmacophores that can simultaneously bind both orthosteric sites of the (homo/hetero) dimer.

In this thesis, we have presented a computational framework that guides the design, synthesis, and evaluation of these ligands. As presented through the different chapters, for the design of these compounds, is paramount to: (i) computationally model the system and estimate potential distances between pharmacophores; (ii) build the potential bivalent ligands by a modular chemical synthesis considering the structural restrains (anchoring points) and chemical properties; and (iii) precisely determine the binding mode with the combination of computational and experimental methods. This requires complementary expertise in various aspects of early drug development. Thus, in addition to ligand- and structure-based drug design techniques, performed by me, chemical synthesis, chemical biology, and in vitro evaluation have been performed by others listed at the beginning of each case study.

Specific discussions for each of the chapters can be summarized as follows:

Chapter 4. CB_2Rs are capable to recognize orthosteric ligands at the membrane-facing vestibule, subsequently moving to the orthosteric binding site through the channel between TMs 1 and 7. Our de-

signed CB_2R homobivalent bitopic ligands link two equal orthosteric pharmacophores with a methylene spacer that allows simultaneous binding of the orthosteric binding site and the vestibule. The binding of this secondary binding cavity in the same protomer provides them with the ability to selectively activate CB_2R versus CB_1R. Also, one of the homobivalent ligands with a longer methylene spacer binds the vestibule of a inactive second CB_2R protomer instead. This binding mode triggers the formation of the CB_2R-CB_2R homodimer via the TM 1/7 interface, which provides increased potency in Gi binding and increased recruitment of β-arrestin.

Chapter 5. Despite initial skepticism and discussion regarding GPCR oligomers, GCPR dimers are in some cases the predominant species and constitute primary functional signaling units. Our designed D_1R-H_3R heterobivalent ligands have high affinity at both receptors and high selectivity inside their respective families, except for the D_5R (since the used D_1R pharmacophore is not selective inside the D_1-like receptor family). The reduction in Aβ-induced cell death observed when testing the most promising compound highlights the neuroprotective properties of the D_1R-H_3R heteromer and the potential of our bivalent ligands to selectively target this complex with a higher affinity than monovalent ligands.

Chapter 6. GPCRs are present in a dynamic equilibrium between monomers, dimers and tetramers. Our designed $A_{2A}R$-D_2R heterobivalent ligand and $A_{2A}R$ homobivalent ligands simultaneously bind the two orthosteric sites of the $A_{2A}R$-D_2R heteromer and $A_{2A}R$ homodimer, respectively. Our designed $A_{2A}R$-D_2R heterotetravalent ligands link the higher affinity $A_{2A}R$ and D_2R (previously published by our group) homobivalent ligands with a spacer that allows simultaneously binding of the four orthosteric binding sides of the $A_{2A}R$-D_2R heterotetramer.

Bibliography

[1] D. Wootten, A. Christopoulos, M. Marti-Solano, M. M. Babu, P. M. Sexton, "Mechanisms of signalling and biased agonism in G protein-coupled receptors", *Nature reviews. Molecular cell biology* **2018**, *19*, 638–653.

[2] Q. Zhou, D. Yang, M. Wu, Y. Guo, W. Guo, L. Zhong, X. Cai, A. Dai, W. Jang, E. Shakhnovich, Z. J. Liu, R. C. Stevens, N. A. Lambert, M. M. Babu, M. W. Wang, S. Zhao, "Common activation mechanism of class A GPCRs", *eLife* **2019**, *8*.

[3] T. Schöneberg, I. Liebscher, "Mutations in G Protein-Coupled Receptors: Mechanisms, Pathophysiology and Potential Therapeutic Approaches", *Pharmacological reviews* **2021**, *73*, 89–119.

[4] A. S. Hauser, M. M. Attwood, M. Rask-Andersen, H. B. Schiöth, D. E. Gloriam, "Trends in GPCR drug discovery: new agents, targets and indications", *Nature reviews. Drug discovery* **2017**, *16*, 829–842.

[5] T. I. Oprea, C. G. Bologa, S. Brunak, A. Campbell, G. N. Gan, A. Gaulton, S. M. Gomez, R. Guha, A. Hersey, J. Holmes, A. Jadhav, L. J. Jensen, G. L. Johnson, A. Karlson, A. R. Leach, A. Ma'ayan, A. Malovannaya, S. Mani, S. L. Mathias, M. T. McManus, T. F. Meehan, C. V. Mering, D. Muthas, D. T. Nguyen, J. P. Overington, G. Papadatos, J. Qin, C. Reich, B. L. Roth, S. C. Schürer, A. Simeonov, L. A. Sklar, N. Southall, S. Tomita, I. Tudose, O. Ursu, D. Vidović, A. Waller, D. Westergaard, J. J. Yang, G. Zahoránszky-Köhalmi, "Unexplored therapeutic opportunities in the human genome", *Nature reviews. Drug discovery* **2018**, *17*, 317–332.

[6] J. B. Hedderich, M. Persechino, K. Becker, F. M. Heydenreich, T. Gutermuth, M. Bouvier, M. Bünemann, P. Kolb, "The pocketome of G-protein-coupled receptors reveals previously untargeted allosteric sites", *Nature communications* **2022**, *13*.

[7] R. O. Dror, A. C. Pan, D. H. Arlow, D. W. Borhani, P. Maragakis, Y. Shan, H. Xu, D. E. Shaw, "Pathway and mechanism of drug binding to G-protein-coupled receptors", *Proceedings of the National Academy of Sciences of the United States of America* **2011**, *108*, 13118–13123.

[8] N. Casajuana-Martin, G. Navarro, A. Gonzalez, C. L. D. Torrent, M. Gómez-Autet, A. Q. García, R. Franco, L. Pardo, "A Single Point Mutation Blocks the Entrance of Ligands to the Cannabinoid CB2Receptor via the Lipid Bilayer", *Journal of Chemical Information and Modeling* **2022**, *62*, 5771–5779.

[9] P. Fronik, B. I. Gaiser, D. S. Pedersen, "Bitopic Ligands and Metastable Binding Sites: Opportunities for G Protein-Coupled Receptor (GPCR) Medicinal Chemistry", *Journal of medicinal chemistry* **2017**, *60*, 4126–4134.

[10] A. H. Newman, F. O. Battiti, A. Bonifazi, "2016 Philip S. Portoghese Medicinal Chemistry Lectureship: Designing Bivalent or Bitopic Molecules for G-Protein Coupled Receptors. The Whole Is Greater Than the Sum of Its Parts", *Journal of medicinal chemistry* **2020**, *63*, 1779–1797.

[11] J. Zha, J. He, C. Wu, M. Zhang, X. Liu, J. Zhang, "Designing drugs and chemical probes with the dualsteric approach", *Chemical Society reviews* **2023**, *52*, 8651–8677.

[12] P. S. Portoghese, "Bivalent ligands and the message-address concept in the design of selective opioid receptor antagonists", *Trends in pharmacological sciences* **1989**, *10*, 230–235.

[13] R. A. Medina, H. Vázquez-Villa, J. C. Gómez-Tamayo, B. Benhamú, M. Martín-Fontecha, T. D. L. Fuente, G. Caltabiano, P. B. Hedlund, L. Pardo, M. L. López-Rodríguez, "The extracellular entrance provides selectivity to serotonin 5-HT7 receptor antagonists with antidepressant-like behavior in vivo", *Journal of medicinal chemistry* **2014**, *57*, 6879–6884.

[14] M. Masureel, Y. Zou, L. P. Picard, E. van der Westhuizen, J. P. Mahoney, J. P. Rodrigues, T. J. Mildorf, R. O. Dror, D. E. Shaw, M. Bouvier, E. Pardon, J. Steyaert, R. K. Sunahara, W. I. Weis, C. Zhang, B. K. Kobilka, "Structural insights into binding specificity, efficacy and bias of a β2AR partial agonist", *Nature chemical biology* **2018**, *14*, 1059–1066.

[15] A. Bock, M. Bermudez, "Allosteric coupling and biased agonism in G protein-coupled receptors", *The FEBS journal* **2021**, *288*, 2513–2528.

[16] S. Ferré, R. Baler, M. Bouvier, M. G. Caron, L. A. Devi, T. Durroux, K. Fuxe, S. R. George, J. A. Javitch, M. J. Lohse, K. Mackie, G. Milligan, K. D. Pfleger, J. P. Pin, N. D. Volkow, M. Waldhoer, A. S. Woods, R. Franco, "Building a new conceptual framework for receptor heteromers", *Nature chemical biology* **2009**, *5*, 131–134.

[17] V. Casadó, A. Cortés, J. Mallol, K. Pérez-Capote, S. Ferré, C. Lluis, R. Franco, E. I. Canela, "GPCR homomers and heteromers: a better choice as targets for drug development than GPCR monomers", *Pharmacology & therapeutics* **2009**, *124*, 248–257.

[18] C. Hiller, J. Kühhorn, P. Gmeiner, "Class A G-protein-coupled receptor (GPCR) dimers and bivalent ligands", *Journal of medicinal chemistry* **2013**, *56*, 6542–6559.

Chapter 8

Conclusions

The discovery of multivalent ligands which simultaneously bind multiple binding sites has been shown to be a promising approach to understand basic biology of GPCRs. The rational design of these compounds is aided by the increase in structural knowledge derived from target GPCR structures. On one side, the identification of subtype specific secondary binding sites can be exploited with bitopic ligands to increase selectivity for a GPCR subtype. On the other side, multivalent ligands that bind multiple GPCR protomers are useful tools to interrogate GPCR oligomerization. Also, the unique way in which these molecules engage the receptor allows the optimization of efficacies and/or signaling bias.

The conclusions can be summarized as follows:

1. We have developed a series of homobivalent ligands with selectivity for CB_2R over CB_1R. One of these bivalent ligands modulate the dynamics of CB_2R homodimerization, which gives unique pharmacological properties.

2. We have developed a series of heterobivalent ligands for the D_1R-H_3R heteromer that contain antagonist moieties as pharmacophores.

3. We have developed a series of homobivalent ligands for the $A_{2A}R$

homodimer that contain an antagonist moiety as a pharmacophore.

4. We have developed a series of heterobivalent ligands for the $A_{2A}R$-D_2R heteromer that contain antagonist moieties as pharmacophores.

5. We have developed a series of tetravalent ligands for the $A_{2A}R$-D_2R heterotetramer that contain antagonist moieties as pharmacophores.

6. We have designed a series of heterobivalent ligands for the $A_{2A}R$-D_2R heterotetramer that contain an antagonist moiety as $A_{2A}R$ pharmacophore and an agonist moiety as D_2R pharmacophore (not shown).

7. We have designed a series of heterobivalent ligands for the $A_{2A}R$-$A_{2B}R$ heterotetramer that contain agonist moieties as pharmacophores (not shown).

Finally, this thesis has shown the benefits of integrating computational studies in experimental research to increase understanding of observed phenomena and guide future experiments.

8.1. List of publications.

Included in the thesis.

Morales, P.[1], Navarro, G.[1], Gómez-Autet, M.[1], Redondo, L., Fernández-Ruiz, J., Pérez-Benito, L., Cordomí, A., Pardo, L., Franco, R., & Jagerovic, N. (2020). **Discovery of Homobivalent Bitopic Ligands of the Cannabinoid CB_2 Receptor**. Chemistry – A European Journal, 26(68), 15839–15842. https://doi.org/10.1002/CHEM.202003389

Pulido, D.[1], Casadó-Anguera, V.[1], Gómez-Autet, M.[1], Llopart, N., Moreno, E., Casajuana-Martin, N., Ferré, S., Pardo, L., Casadó, V., & Royo, M. (2022). **Heterobivalent Ligand for the Adenosine A_{2A}–Dopamine D_2 Receptor Heteromer**. Journal of Medicinal Chemistry, 65(1), 616–632. https://doi.org/10.1021/acs.jmedchem.1c01763

Brugal, G.[1], Gómez-Autet, M.[1], Morales, P.[1], Biel Rebassa, J., Llinas del Torrent, C., Jagerovic, N., Pardo, L., & Franco, R. (2024). **Homodimerization of CB_2 cannabinoid receptor triggered by a bivalent ligand enhances cellular signaling.** Pharmacological Research. *Submitted.*

Rosier, N., Mönnich, D., Gómez-Autet, M., Forster, L., Nagl, M., Grätz, L., Raich, I., Lillo, J., Reyes-Resina, I., Navarro, G., Pardo, L., Franco, R., & Pockes, S. (2024). **High Affinity Bivalent Ligands Targeting the Dopamine D_1-Histamine H_3 Heteromer Reduce β-Amyloid-Induced Neuronal Cell Death.** *To be submitted.*

[1]These authors contributed equally to this work.

Pulido, D.[1], Casadó-Anguera, V.[1], Gómez-Autet, M.[1], Llopart, N., Moreno, E., Pérez-Benito, L., Casajuana-Martin, N., Ferré, S., Pardo, L., Casadó, V., & Royo, M. **A heterotetravalent ligand for a G protein-coupled receptor heterotetramer.** *To be submitted.*

Others.

Casajuana-Martin, N., Navarro, G., Gonzalez, A., Llinas Del Torrent, C., Gómez-Autet, M., Quintana García, A., Franco, R., & Pardo, L. (2022). A Single Point Mutation Blocks the Entrance of Ligands to the Cannabinoid CB_2 Receptor via the Lipid Bilayer. Journal of Chemical Information and Modeling, 62(22), 5771–5779. https://doi.org/10.1021/acs.jcim.2c00865